C.P. No. 1271

C.P. No. 1271

MINISTRY OF DEFENCE (PROCUREMENT EXECUTIVE)

AERONAUTICAL RESEARCH COUNCIL

CURRENT PAPERS

A Parametric Study of the Use of Nose Blunting to Reduce the Supersonic Wave Drag of Forebodies

By

P. G. Pugh and L. C. Ward

LONDON· HER MAJESTY'S STATIONERY OFFICE

1974

PRICE £1 25 NET

C.P. No.1271*
August, 1970

A PARAMETRIC STUDY OF THE USE OF NOSE BLUNTING TO REDUCE THE SUPERSONIC WAVE DRAG OF FOREBODIES

- by -
P. G. Pugh and L. C. Ward

SUMMARY

This parametric study examines the application of nose blunting to axisymmetric forebodies at supersonic speeds to reduce pressure drag and stagnation-point heat-transfer rate and to increase their volume. Sufficient information is given to enable the magnitude of these benefits to be estimated for most practical applications.

Nomenclature (see also Fig (1))

C_V	specific heat of air at constant volume
C_D	drag coefficient based on maximum cross-sectional area and free-stream dynamic pressure
C_{D_N}	drag coefficient of blunting in isolation (based on maximum cross-sectional area of blunting and free-stream dynamic pressure)
C_p	pressure coefficient - difference between surface pressure and free-stream static pressure normalised by the free-stream dynamic pressure
a	sonic velocity
d	body diameter at junction between blunting and conical portion of body (single cones only)
k	a constant (used in section 5.3)
k_1	a constant (used in section 5.8)
f	fineness ratio - ratio of length to diameter of forebody
$\dot{q}$	stagnation-point heat-transfer rate

s/

---

*Replaces NPL Aero Special Report 043 - A.R.C.32 284

s	distance measured along surface of body from stagnation point
y'	radial distance from axis of symmetry normalised by maximum diameter of body
D	maximum (base) diameter of forebody (single cones only)
D_1	body diameter at downstream end of blunting (double cones only)
D_2	body diameter at junction between two conical portions of body (double cones only)
D_3	base diameter of body (double cones only - normally taken as unity)
F_1, F_2, F_3, F_4	functions (section 5.6)
L	length of forebody
Me	Mach number just external to boundary layer
M	free-stream Mach number
N	a constant (section 5.3)
Q	stagnation-point heat-transfer rate normalised by $\dot{q}$ for a hemisphere of base diameter equal to that of forebody (i.e. equal to D or D_3 for single or double cones respectively)
R_s	Y co-ordinate of shock-wave in base-plane of forebody.
ΔS	increase in entropy of unit mass of air on passing through bow shock-wave
U	velocity just external to boundary layer
V	total internal volume of forebody, normalised by the cube of the base diameter (D^3 or D_3^3)
X, x	streamwise distance (i.e. measured parallel to axis of symmetry)
Y	radial distance from axis of symmetry
β	shock angle
ε	semi-apex angle of conical portion of body
τ	thickness ratio ($\tau = 1/f$)

θ_b/

θ_b	semi-apex angle of (conical) blunting
μ	Mach angle

Subscripts

MIN	minimum value
s.c.	value appropriate to sharp cone
=	conditions such that C_D is equal to that for a sharp cone having the same value of f
OPT.	conditions such that C_D is a minimum for a given value of f
b	spherical blunting
s	conditions at stagnation point
t	truncated
ref	reference conditions (defined in text)

Superscripts

^{1}	transformed values (section 5.3)
*	conditions at sonic point

---

1. Introduction

The recent past has seen a revival of interest in the use of nose blunting to reduce forebody drag. Initially, existing data were reanalysed to obtain some general guide lines (or "ground rules")[1,2]. Most of these data were for spherically-blunted cones. Although this class of body is only one of many in common use and is definitely non-optimum, this analysis served to delineate the circumstances in which the use of nose blunting was advantageous. In particular, the use of blunting can give substantial gains in both drag and volume when the fineness ratio of the forebody is constrained to be a fixed value. This is in conformity with results obtained using approximate analytical expressions for surface pressure together with either the calculus of variations, or numerical optimisation techniques[3,4,5].

These/

These facts generate a need for a prediction method which is powerful enough to be capable of dealing with blunted bodies yet is sufficiently simple to allow of its repetitive use in optimisation studies. Few such methods are available[6], and a novel approach has been developed by the present authors[7]. This method has been checked as far as is practicable at present and gives satisfactory agreement with experiment, so that it is appropriate to use it in parametric studies to elucidate further the potential of nose bluntness. Having then derived at least semi-quantitative ground-rules for applying nose blunting, two vital things can be done. Firstly, new experiments can be devised with the specific aim of further validating the proposed uses of nose blunting. Secondly, full optimisation studies can be conducted in order to derive minimum-drag forebody shapes appropriate to practical constraints under which nose blunting is likely to be advantageous.

This report takes a few steps along this road. It describes a parametric study of the type mentioned above and draws some conclusions as to the uses of nose blunting which appear most likely to be profitable. The majority of the calculations were performed for a Mach number of 3.05 but some consideration is given to the effect of varying the Mach number. The precise quantitative conclusions as to optimum forebody shapes naturally require experimental confirmation. However, the calculation method employed has been well enough validated already to allow reasonable confidence to be reposed in the results.

2. Forebody Geometry

A natural extension of earlier analyses of the drag of blunted single cones[1,2] is to consider blunted double cones of unit base diameter (Fig.1). By so doing it is possible to consider the effects of some shaping of the body downstream of the bluntness and, hence, to examine the influence of such shaping on the effectiveness of nose blunting. If the benefits of nose blunting were found to be much less for a double cone than for a single cone then grave doubt would be cast on the generality of the utility of blunting. If, however, blunting is no less beneficial for the double cone than for the single cone then this would tend to suggest that blunting was of widespread usefulness. Both single and double cones are considered in this report. To ensure unambiguity and to make clear which type of body is being considered a different nomenclature has been used for each (see Fig.1). In the case of double cones the base diameter D_3 is taken to be unity except where otherwise stated.

Although a blunt double cone is, of course, still well removed from the continuously curved shapes commonly adopted for low-drag forebodies, it has the merit of being completely described by three independent variables (L, D_1, D_2)*. As will be seen later, even as few as three independent variables pose considerable problems of presentation and analysis. To use more would run the risk of obscuring the central points in a mass of detail. While it would, of course, be possible to take the forebody shape between D_1 and the base as being derived from a family of curves, this is no more general than the study of double cones unless the family of curves used is described by more than one independent parameter.

---

*These being respectively the total length from the extreme rise rip to the base, the diameter of the body at the blunting, and the diameter of the body at the discontinuity of slope downstream end of which is assumed to be midway between D_1 and D_3.

Accordingly, the majority of the calculations analysed in this report were performed for blunted double-cone forebodies. A few additional calculations were done for continuously curved forebody shapes.

3. Constraints and Dependent Variables

An optimum forebody shape is only optimum in the sense that it is the shape that corresponds to the best value of some dependent variable that can be obtained given certain constraints. It is important, therefore, to specify at the outset of a study such as this which dependent variables are to be optimised and under what constraints the study is to be performed.

Two dependent variables are considered. These are the forebody pressure-drag coefficient C_D, and the volume of the forebody V. Since the drag of the forebody is usually a substantial fraction of the total drag of a practical vehicle, the importance of minimising C_D is self-evident. It is also often desirable to maximise the volume V since such volume is required for the stowage of equipment.

The most important constraint is that of a fixed fineness ratio.f. This frequently closely approximates constraints arising in practice and bars the simplest way of reducing C_D (to increase f). In addition, it is also necessary to consider the imposition of minimum values on either D_1 or D_2 thus simulating the requirements of particular items of equipment. On other occasions the minimisation of the heat-transfer rate at the stagnation point may also be of prime importance.

4. Derivation of Data Analysed

The data analysed were obtained using the method for predicting forebody drag described in Ref (7). Approximately 200 such calculations were made using about 75 mins of computer time on an ICL KDF9 computer. All the calculations were performed for M = 3.05, but a limited discussion of the effects of Mach number appears in section 5.6.

5. Analysis of Data

5.1 Blunted cones - optimisation

An analysis of the data obtained for the blunted (single) cone forms a most useful background to any discussion of more complex forebody shapes. Fig.2 illustrates the benefits to be obtained from nose blunting of single cones. The presentation employed in this figure is somewhat novel and follows that used by one of the authors on an earlier occasion when presenting results for blunted single-cone forebodies[8]. The variation of C_D with V is shown for two sets of forebodies, each set having a fixed fineness ratio and being generated by varying the bluntness ratio (d/D). It will be seen that a minimum drag coefficient is achieved for a forebody having considerable nose blunting and a substantially larger volume than the sharp cone (d = 0) of the same fineness ratio. Nose blunting is clearly useful in this case. Nose blunting is not beneficial in the application illustrated in Fig.3. Here a range of sharp cones, of varying

fineness/

fineness ratio, are compared with a series of blunted cones derived by keeping the cone apex angle constant and reducing the fineness ratio by increasing the blunting. Blunting then causes an increase in drag and a decrease in volume as compared to the sharp cone of the same apex angle. When compared to sharp cones of the same apex angle, the drag of the blunted cone is considerably greater than that of the sharp cone.

However, nose blunting can be an effective way or reducing the fineness ratio without a drag penalty since the drag invariably decreases with increasing fineness ratio and nose blunting can be used to decrease the drag at a fixed fineness ratio. This way of using nose blunting is illustrated in Fig.(4) which combines the information presented in the previous two figures. As well as reiterating the points made earlier, this figure shows that one blunted cone of fineness ratio 2 has the same drag and the same volume as a sharp cone of a different fineness ratio. This sharp cone has a larger volume (and, hence, greater length) than a sharp cone of fineness ratio 2. It follows that for fineness ratios around 2 (but not for fineness ratio around 1) it is possible, by the proper selection of nose blunting and apex angle, to obtain a modest reduction in fineness ratio without any penalty in either drag or volume.

Corresponding data for a fineness ratio of 3 are given in Fig.(5). This figure shows that, just as for a fineness ratio of 2, nose blunting may be used either to reduce the drag for a fixed fineness ratio or to reduce the fineness ratio without an increase in drag or loss of volume. There are interesting differences, however, in the results for fineness ratios of 1.0, 2.0 and 3.0. These are best shown, as in Fig.(6), by the variation of three significant bluntness ratios (d/D) with fineness ratio. These values of d/D are those that corresponding to (a) the minimum drag for a given fineness ratio, (b) that giving a reduction in fineness ratio without drag or volume penalties, and (c) the maximum value of (d/D) that can be used without resulting in a drag greater than that for a sharp cone of the same fineness ratio. The values of (d/D) for minimum drag for a given fineness ratio, and (d/D) for the drag not exceeding that of a sharp cone of the same fineness ratio, move in sympathy with each other. The values of (d/D) resulting in reduction of fineness ratio (without reduction in volume or increase in drag) do not move in sympathy with the other two. No such blunting appears to exist for a fineness ratio of 1. (Fig.4). One is found for a fineness ratio of 2 but its magnitude diminishes with increase in fineness ratio beyond 2. Thus, the use of blunting to reduce fineness ratio may have a somewhat limited range of applicability. However, this range includes many cases of practical interest so that this possible use of nose blunting should not be neglected.

The minimum values of C_D discussed above are presented in Fig.7. It will be seen that the use of nose blunting offers substantial gains in any of the basic variables without disadvantageous effects upon the others. It remains to be seen if these gains are maintained when an extra degree of freedom is introduced into the body shape.

5.2/

5.2 Blunted double cones - optimisation

Turning, therefore, to the blunted double cone configuration, the data are summarised in Figs.8a and 8b. In these figures the drag coefficient (C_D) is presented as a function of the volume (V) (as before). Lines of constant D_1 and D_2 are drawn on this figure as also are lines corresponding to the special cases of sharp nosed double cones ($D_1 = 0$) and single cones ($D_2 = (D_3 + D_1)/2$). These figures present the information that is available from the computed results in a condensed form. Interpretation of Figs.8a and 8b is made easier if it is recalled that increases in either D_1 or D_2 increases the volume in a regular fashion. If this is kept in mind it is not difficult to distinguish between that intersection of a pair of curves for given values of D_1 and D_2 which corresponds to a particular forebody shape and any other such intersections which are not significant and arise solely because of the difficulty of representing four-dimensional information on a two-dimensional plane.

We first seek an answer to the question as to whether the advantages of nose blunting are maintained when the forebody shape is allowed the extra degree of freedom. Figs.9 and 10 present the variation of drag with volume at fixed fineness ratios of 2 and 3 for:-

(a) sharp nosed double cones ($D_1 = 0$)

(b) blunted single cones ($D_2 = (D_3 + D_1)/2$)

(c) blunted double cones (the values of D_1 and D_2 being varied so as to give the minimum value of C_D for each value of V).

These figures demonstrate that adjustments of either of D_1 alone or D_2 alone can be made so as to give increased volume and reduced drag. However, adjustment of both D_1 and D_2 enables yet greater improvements in drag and volume to be effected.

At the lower fineness ratio the introduction of the extra degree of freedom on body shape, represented by the extension of the analysis to double cones, allows of improvements in both drag and volume. At the higher fineness ratio such improvements are mainly in increased volume. Indeed, an interesting feature of Figs.9 and 10 is that the variation of C_D with V for the blunted double cones is seen to have a very flat minima. This must not be interpreted as showing that C_D is insensitive to D_1 or D_2. Indeed, inspection of Figs.8a and 8b will reveal that C_D is normally sensitive to variations in either D_1 or D_2. However, within a region surrounding the drag minimum, the effects of deviations of D_2 from its optimum value can be almost completely compensated for by adjustment of D_1 (and vice versa). This point will be returned to in more detail in section 5.9.

5.3 More complex bodies - optimisation

Returning to the minimisation of drag, it is natural to enquire how the picture presented by Figs.9 and 10 would be modified by the introduction of further degrees of freedom in body shape. Consider,

however/

however, the effects of adding an extra degree of freedom upon the number of calculations required. If the "buckshot" or "latin square" method of finding an optimum implicit in Figs.9 and 10 is applied to bodies with greater degrees of freedom, unmanageable problems of presentation and analysis arise. Proper optimisation techniques must be employed and some future work will be directed towards this end. In the interim, some indications may be obtained by assuming that the body downstream of D_1 is derived from a family of shapes. For example, Fig.11 shows results obtained in this way for a 3/4 power-law body (i.e. the basic body shape being $y \sim x^{3/4}$) of fineness ratio 2, this type of profile being of interest because of the low drag of the basic body. The basic shape was first blunted so that the body diameter at the downstream end of the blunting (D_1) was one of a number of chosen values. The process decreased the fineness ratio of the body, which was then restored to its original value by the transformation $D^1 = D$, $x^1 = x(1 + kx^N)$ (k being chosen so that this transformation resulted in the fineness ratio being restored to 2). By varying N the restoration of the fineness ratio could be made to stretch the body either predominantly at the front ($N < 0$), evenly ($N = 0$), or predominantly at the rear ($N > 0$). The best results were obtained with $N = +2$ and (as shown in Fig.(11) a significant increase in volume accompanied by a slight reduction in drag was then obtained from the use of nose blunting. It is also interesting to note that virtually the same performance as regards C_D and V was obtained from the best blunted double-cone as from the basic three-quarter power-law body. This fact seems to suggest that the introduction *of additional degrees of freedom in body shape aft of the blunting proper* would not open the way to significant additional reductions in C_D, and would only allow of modest increases in V at a given value of C_D. Thus, at least for the present purpose of outlining trends and of obtaining a "feel" for the benefits to be obtained from nose blunting, the single degree of freedom (that of choosing D_2) seems to represent adequately the effects of variations in forebody shape aft of the blunting. In interpreting Fig.11 it must be remembered that the basic 3/4 power-law body is already blunted in the sense that the surface slope is infinite at the axis of symmetry. Therefore, it would have been surprising had the application of nose blunting had as marked an effect as it has when applied to a sharp-nosed body. However, Fig.11 clearly shows that there are still gains to be made from bolder use of blunting than that implicit in a 3/4 power-law profile.

5.4 The physical mechanism of drag reduction by nose blunting

Before proceeding further it is useful to discuss the physical mechanism underlying the reductions in C_D and increases in V described above. In addition, this discussion provides a measure of cross-checking, tending to confirm the validity of the conclusions reached so far, and to give confidence in later analyses.

The basic mechanism whereby benefits are obtained from the use of larger than average surface slopes over the most forward part of a forebody of fixed fineness ratio is, of course, well understood[1]. Because of the axisymmetry of the body, the increased pressures consequent upon such increased surface slopes act upon a relatively small forward-facing area. The disadvantageous effect of these increased pressures is more than offset by

the/

the influence of the lower pressures associated with reduced surface slopes further aft (which act upon a much larger area). Additionally, such a forebody clearly has a higher volume than a forebody whose surface slopes were more nearly constant. It should be noted that the lower pressures on the rearward portion of the forebody are not solely a direct consequence of the reduction in surface slope. In fact, the entropy layer, i.e. the gas which suffers a larger increase in entropy because it passes through the stronger bow shock-wave near the axis of symmetry, has a displacement effect analogous to that of a boundary layer[7]. However, unlike the boundary layer, the entropy layer has a constant displacement cross-sectional area. As the flow proceeds downstream this constant area is spread out over an increasing periphery. Thus, the effective surface slope (and the pressure) is further reduced.

It should be noted that these qualitative arguments are independent of the numerical value of the maximum surface slope. They are equally valid as an explanation of the benefits of adopting a convex shape for a sharp-nosed forebody as they are of describing why nose blunting can be used to reduce the drag of a circular cone. Indeed, too much should not be made of the differences between the use of nose blunting and other, longer-established, drag-reduction techniques. Nose blunting simply represents the logical conclusion of the classical approaches such as those based on linearised theory theory[9]. Virtually all previous attacks on the drag minimisation problems have resulted in "optimum" shapes in which the surface slope decreases with increasing distance downstream of the nose. A major difficulty inherent in these earlier works is that the methods used to compute the forebody drag have a limited valid range which may be expressed in terms of a maximum surface slope[6] and which is often violated, at least locally, by the derived "optimum" shape. Thus, the truly novel aspects of the results presented in this paper are:-

(a) they are derived using a theory which is not subject to a limitation on maximum surface slope and is, accordingly, more reliable;

(b) they suggest that earlier studies of drag minimisation have underestimated the advantages of high surface slopes near the nose. Indeed it seems clear that, for a fixed fineness ratio, the optimum body has a marked degree of nose blunting.

(c) because more confidence can be reposed in the computed values of C_D it is possible to study the benefits and penalties of nose blunting greater than that required for minimum drag. This information is of value since such increases in nose blunting may sometimes be desirable for non-aerodynamic reasons[18].

Returning to the examination of the physical mechanism underlying forebody optimisation, the benefits of high surface slopes near the nose may be thought of as arising in two ways:-

(a) by accepting higher pressures acting on a small forward-facing area of the body, lower pressures are produced downstream where they are acting over a larger forward-facing area of the body.

(b)/

(b) by accepting higher rates of entropy production over a small forward-facing area of the bow shock-wave, lower rates of entropy production are produced downstream and over large forward-facing areas of the shock-wave.

These two concepts are, of course, equivalent; the latter corresponds to the calculations embodied in the prediction method used in this report and the former corresponds to previous, more conventional, approaches to this problem. It is, accordingly, useful to demonstrate the equivalence of these two concepts. Indeed, by the use of an inverse, non-homeontropic*, characteristics calculation method due to Moore[10] it is possible to do this in such a way as to provide some check on the reliability of the data presented in other parts of this report.

Bow shock-wave shapes, predicted during the course of deriving some of the data presented earlier, were used as input to the inverse, non-homeontropic characteristics calculation mentioned above[10]. Thus, the shock shape predicted by one method was analysed by an independent method to yield streamline patterns and pressure distributions. The compatibility of these streamline patterns with the body geometries originally assumed give a measure of the accuracy with which the shock shape was predicted. An additional check can be obtained by comparing drag coefficients (C_D), computed using the basic prediction method (Ref 7), with corresponding drag coefficients obtained by integrating the derived surface pressure distributions. Unfortunately, the inverse characteristics method cannot be used to calculate pressures on a streamline if the flow velocity at any point on that streamline is subsonic. Therefore, this method cannot be used to calculate the flow over the surface of the body. However, a typical radial distance between the surface of the body and the innermost streamline along which the flow can be calculated is normally small compared to the radial distance between this streamline and the bow shock-wave. It is, thus, not unreasonable to estimate the surface pressures by extrapolating the variation of static pressure along each characteristic to the point at which that characteristic would cross the surface of the body.

These points are illustrated in Fig.12. Here the computed flow field about an optimum blunted double cone is shown. The relative magnitudes of the distances between the body and the innermost calculated streamline, and between that streamline and the shock can be clearly seen. The innermost streamline is evidently compatible with the body shape. This was found to be true for a number of forebody shapes for which such data were obtained. Indeed, if at the base of the body, the mass flux density of the flow between the body and the innermost calculated streamline is taken to be equal to the mass flux density on this streamline, then a fineness ratio for the body may be derived from the inverse calculations. This may be compared with the true fineness ratio. Good agreement is found as can be seen from the following table:-

BODY/

---

*i.e., full account being taken of differences in entropy production at different points on the bow shock wave.

BODY	TRUE FINENESS RATIO	FINENESS RATIO FROM INVERSE CALCULATIONS
Sharp cone	2.00	1.94
Sharp cone	3.00	2.93
Optimum blunted double cone	2.00	1.93
Optimum blunted double cone	3.00	2.99
3/4 power-law body	2.00	1.92

Furthermore, the estimated surface pressures may be integrated to yield a value for C_D which can be compared with the value of C_D derived from the prediction method used in this report. Comparisons of these two values of C_D are given in the tables of Figs.13, 14 and 15. Again, good agreement is found.

The direct method of Ref 7 comprises two main steps. These are the prediction of the shock shape from a known body shape, followed by the calculation of C_D from this shock shape. The first of these steps has been checked by taking shock shapes derived for various bodies by the direct method and analysing these using the inverse method[10] and noting that the body shapes thus derived agree well with those originally chosen. The second of these steps has been checked by performing a separate analysis of the shock shapes, again using the inverse method, and noting good agreement between the two independently derived values of C_D.

The main purpose of the preceding argument has been to demonstrate the physical mechanism underlying the use of nose blunting to reduce C_D, and to show that this is faithfully represented in the direct method[7] used to generate the data analysed in the main body of this report. It is reasonable to have confidence in these data and especially in the trends that they indicate. This is borne out by comparison with experiment. For example, the differences between calculated and measured forebody drag coefficients for a 20° semi-apex angle cone having $0 \leq d/D \leq 0.5$ have been analysed. The mean of these differences is 6.0% of the mean value of C_D (i.e. comparable to the differences in the two calculated values of C_D shown in

Figs./

Figs.13, 14 and 15). However, the standard deviation of these differences was only 1.8% of the mean value of C_D. Thus, not only is a useful accuracy achieved in the prediction of absolute values of C_D, but notably better accuracy is achieved in the prediction of trends. This point is also exemplified by the following table showing the values of (d/D) that were required to produce a given increment in C_D above that of the sharp cone (C_D = 0.28)

INCREMENT IN C_D	REQUIRED VALUES OF (d/D)	
	EXPERIMENTAL	CALCULATED
0.02	0.20	0.21
0.04	0.28	0.28
0.06	0.33	0.32
0.08	0.38	0.36

In Fig.13 the pressure distribution over the optimum blunted double cone for f = 3 is compared to that over a sharp cone of the same fineness ratio. The pressure distributions are plotted in the form $C_p.y'$ as a function of y' so that the ordinate represents the contribution of the surface pressure acting at a point on the body to the pressure drag. The area under the curve is thus proportional to the pressure drag of the forebody to which it relates. (The chain dotted portion of the curve for the optimum double cone is an interpolation between the first calculated point and $C_p.y'$ = 0 at y' = 0, which was drawn having regard to the known slope of this curve at y' = 0). It will be seen that the blunting leads to a local excess of drag of the optimum double cone over that of the sharp cone at y' < 0.15. However, between y' = 0.08 and y' = 0.15 the local drag contribution $C_p.y'$ falls rapidly because of the expansion in the vicinity of the downstream end of the blunting. For $0.15 \leq y' \leq 0.275$ the local drag contribution rises again because of the nearly constant value of C_p over the first conical segment. It is important to note, however, that, despite the surface slope of the optimum body being higher in this region than the surface slope of the sharp cone, the local drag contributions are virtually identical. That this is so is, of course, due to the effect of the entropy layer noted earlier. Between $0.275 \leq y' \leq 0.375$ the local drag contribution falls because of the expansion, and subsequent over-expansion, associated with the change in slope at $y' = D_2/2$. Thereafter the local drag contribution rises only very slowly and over the whole range $0.275 \leq y' \leq 0.5$ the local drag contribution for the optimum body is

substantially/

substantially less than the corresponding value for the sharp cone.

This particular figure has been discussed at some length because it clearly illustrates the physical mechanisms involved and the practical importance of the entropy layer. Similar behaviour is evident in Fig.14 which presents the pressure distributions for optimum blunted double cones and sharp cones for f = 2 in the same way as Fig.13. Fig.15 presents similar data for a 3/4 power-law body having f = 2. In this case $C_p.y'$ varies monotonically with y'. However, this figure again demonstrates how the concession of a small advantage in local drag contribution to the sharp cone for y' < 0.2 can be made to yield large benefits in local drag contribution at y' > 0.5.

Figs.16, 17 and 18 are similar to Figs.13, 14 and 15 except that instead of the local drag contributions being presented in terms of weighted values of C_p, the rate of entropy production at the bow shock-wave is used. It will be seen that the distribution of entropy production is similar to the distribution of surface pressure. In particular, although the optimum double blunted cones have high local rates of entropy production at small values of (y'), the rates of entropy production are low for high values of (y') resulting in a substantial net gain.

5.5 The optimisation process

In this section we offer some comments upon the problems of optimising a forebody - either by means of a series of calculations or via experimental tests on a systematic series of bodies. The problem of efficiently locating a set of values for a multiplicity of independent variables such that a single dependent variable has an optimum value (subject to constraints on the independent variables) is a complex study in itself. There would be obvious advantages in combining the prediction method[7] with a suitable optimisation algorithm. Some insight into the nature of this problem may be gained through an analysis of the present data. In Figs.19 and 20, the calculated drag coefficients of f = 2 and f = 3 blunted double cones are replotted so as to provide contours of C_D on the D_1, D_2 plane. The existence of a minimum value of C_D (and, hence, an optimum pair of values for D_1 and D_2) is evident. The relationship of this optimum shape to the minimum drag configurations of a blunted single cone or a sharp-nosed double cone, is of interest as this information may be valuable in deciding upon suitable starting points for optimisation processes for more complex shapes.

It will be seen that points representing all possible blunted single cones lie on the line $2.D_2 = D_3 + D_1$, while all possible sharp-nosed double cones are represented by points on the line $D_1 = 0$. By examining the intersections of the contours of C_D with these lines the conditions for minimum drag forebodies of these types can be seen. It is interesting to note that the optimum bodies have slightly larger values of both D_1 and D_2 than the best blunted single cone or sharp-nosed double cone. An attempt to establish the optimum value of D_1 by gradually increasing its value from

zero/

zero, and retaining the same value of D_2 as is best for a sharp nosed body, would underestimate the optimum value of D_1, and over-estimate the minimum value of C_D. These errors could be serious especially for f = 2. Similar, but less serious, errors would be incurred if D_1 was held fixed at the best value for a blunted single cone and D_2 varied in an effort to find the optimum.

Fortunately, however, C_D appears to be a well behaved function of D_1 and D_2. Thus, no fundamental difficulties would be expected if some efficient optimisation algorithm were employed, other than that the minimum is relatively flat. This is not a serious practical problem since it implies that a slight error in either D_1 or D_2 will not result in a serious over-estimate of the minimum value of C_D. Such optimisation algorithms are, however, not suitable for attempts to find optimum configurations via a series of experimental tests. This is because they use the results of one set of calculations to identify improved starting conditions for a subsequent set of calculations. Any attempt to conduct an experimental programme on this basis would involve bouts of model making interposed between series of tests. The whole programme would be very protracted.

It is, therefore, appropriate to enquire if there is any way in which a family of models may be designed a priori with some confidence that experimental data obtained using these models will reveal a best configuration which will, in turn, be close to the optimum shape. For economy such a family should be described by one disposable parameter (D_1, say). The simplest such family is that in which D_2 is a linear function of D_1. Geometrical considerations require that when $D_1 = 1$, $D_2 = D_1 = 1 (D_3 = 1)$. However the choice of D_2 when $D_1 = 0$ remains arbitrary. Fig.21 shows three such families, including one for which D_2 has, when $D_1 = 0$, the value pertaining to the minimum drag for a sharp-nosed double cone. Fig.22 shows the variation of C_D with D_1 for each of these three families of bodies. There are marked differences between both the minimum values of C_D and the corresponding values of D_1 for each family of forebodies and only one approximates to the true optimum condition. It is clear that attempts to find optimum configurations via a limited series of ad hoc experiments are of doubtful value. If no other recourse is available then a sensible approach would seem to be to adopt a one parameter family similar to those represented in Fig.21 and having the minimum drag for a sharp-nosed body when $D_1 = 0$. Even this is an unsatisfactory course in that it is necessary to know a priori what is the best shape when $D_1 = 0$ and because, given current understanding of the problem, there is still a considerable risk of missing the true optimum by a considerable amount. A far more preferable course is to conduct a programme of experimental tests incorporating systematic changes in each variable. Results from such tests can then be used to validate or modify appropriate prediction methods which can, in turn be used, together with suitable optimisation algorithms[19], to determine an optimum forebody shape.

5.6/

5.6 Generalisation of optimum conditions

The derivation of an optimum configuration, especially one involving a large number of independent variables, will, inevitably, absorb considerable effort despite the relative simplicity of the prediction method used in this report. It is, therefore, appropriate to enquire whether data obtained for one Mach number can be generalised in such a way as to give an approximate indication of optimum configurations at other Mach numbers. Such a generalisation would enable the designer to:-

(1) economise on the effort needed for full optimisation at additional Mach numbers by making available good initial estimates of the appropriate optimum configurations

(2) establish whether the optimum configuration for any particular set of constraints is sensitive to Mach number.

The latter aim is particularly important since this must be established if optimisation at a particular Mach number is to have any practical utility in many applications.

Unfortunately, adequate experimental data for a comprehensive treatment of this topic are not available. Indeed, for blunted configurations, data including systematic variation of both body shape and Mach number are available only for blunted single cones. Even for this class of body extensive interpolation of the available data is necessary. Such an interpolation has been performed by the Engineering Sciences Data Unit[2]. However, the quoted accuracy of their data sheets is such as to invalidate their use for optimisation studies except for high-drag bodies, for example, those having $f \leq 1.5$.

The original sources of data[1,2,12] used in such compilations and other, more limited analyses, are, of course, available and some are useful in providing particular examples of optimum, blunted single cones for larger fineness ratios.

The variation of C_D with both bluntness (d/D) and Mach number (M) for $f = 1$ blunted single cones (derived from Ref.2) is illustrated in Fig.23. The contours of C_D show the expected optimum values for each Mach number. Moreover, the optimum values of d/D vary little with Mach number, except near $M = 1$. Even then, the behaviour of C_D with M and D_1 is favourable in the sense that a body having the optimum value of D_1 for some supersonic speed will have a lower drag at transonic speeds than the sharp cone of the same fineness ratio (albeit not the minimum drag for the lower Mach number). Blunting also tends to decrease the maximum in the variation of drag coefficient with Mach number. These points were discussed in much greater detail in Ref.6 and it is not proposed to repeat that discussion except to say that the conclusions as to the favourable effect of blunting noted above are shown to be generally true for blunted single cones having $f \leq 1.5$. While there is every reason to believe that similar conclusions will also be valid for $f > 1.5$ no supporting experimental evidence is to hand.

The/

The method of generalising optimum configurations suggested in this report is based upon an interpretation of the conventional similarity parameters for supersonic and hypersonic flow.

The normal hypersonic similarity relationship[13] states that, for affinely-related bodies:-

$$C_D/\tau^2 = F_1 (M\tau)$$ or in more general supersonic/hypersonic form:-

$$C_D/\tau^2 = F_2 (\sqrt{M^2 - 1} \cdot \tau)$$

where $\tau = 1/f$, so:-

$$C_D f^2 = F_3 (f/\sqrt{M^2 - 1}) \qquad \ldots(1)$$

Although this relationship is general and is not invalidated by nose blunting, examinations of the requirement that the bodies considered should be affinely related shows that it cannot be applied directly to the type of bodies considered in this report. The above expressions relate, say, a spherically-blunted body at one Mach number to a body, at another Mach number, whose nose blunting takes the form of part of an ellipse. Thus, equation (1) does not allow one to relate, say, a spherically-blunted body at one Mach number to a second spherically-blunted body of related, but different, geometry at a second Mach number. To do this it is necessary to consider the physical significance of the right-hand side of equation (1) (which is, of course, entirely adequate for sharp-nosed bodies).

For sharp-nosed bodies the bow shock-wave is inclined to the free-stream direction at an angle which is everywhere closely related to the Mach angle. For slender bodies $(\beta-\mu) \ll \mu$, and if body length is taken as L, the shock radius at the base plane of the forebody is approximately given by

$$R_S \simeq L \tan \mu = L/\sqrt{M^2 - 1}$$

The body radius at the base plane is, of course, L/2f.

Thus, the ratio $\left(\frac{\text{shock radius}}{\text{body radius}}\right) = \frac{L}{\sqrt{M^2-1}} \cdot \frac{2.f}{(L)} = \frac{2.f}{\sqrt{M^2-1}}$

Accordingly, the term $\frac{f}{\sqrt{M^2-1}}$ may be interpreted as characterising the ratio of the shock radius to the body radius at the base plane of the forebody. Its square $\frac{f^2}{(M^2-1)}$ represents the ratio of the base area to the area of the flow "captured" by the bow shock wave upstream of the base plane, and thus, represents the area change which the fluid is forced to undergo.

It/

It is thus a index of the aerodynamic slenderness of a slender sharp-nosed body.

If attention is now turned to blunted forebodies, then examination of the predicted shock-wave shapes reveals that, for most such bodies, the shape of the bow shock-wave upstream of the base-plane of the forebody either derives completely from that region of the shock-wave which is determined by the blunting alone, or else such a large portion of it is thus derived that the blunting is the dominant influence on the radius of the shock-wave in the base plane. The bow shock-wave due to a blunt body at supersonic speeds is insensitive to Mach number and is given approximately by[14]:-

$$\frac{R_S}{d} \sim C_{D_N}^{\frac{1}{4}} \cdot \left(\frac{L}{d}\right)^{\frac{1}{2}}$$

where C_{D_N} is the drag coefficient of the blunting in isolation.

Thus, the ratio of base area to area of flow captured by the bow shock wave upstream of the base plane is proportional to:-

$$\left(\frac{D}{R_S}\right)^2 = \left(\frac{d}{R_S}\right)^2 \cdot \left(\frac{D}{d}\right)^2 \sim \left(\frac{d^{\frac{1}{2}}}{L^{\frac{1}{2}} C_{D_N}^{\frac{1}{4}}}\right)^8 \cdot \left(\frac{D}{d}\right)^2$$

i.e.
$$\left(\frac{D}{R_S}\right)^2 \sim \left(\frac{D}{d}\right) \cdot \left(\frac{1}{f C_{D_N}^{\frac{1}{2}}}\right)$$

Thus, by analogy with the well-established similarity rules for slender bodies, we hypothesize that:-

$$C_D \cdot f^2 = F_4 \left\{ \left(\frac{D}{d}\right) \cdot \frac{1}{(f\, C_{D_N}^{\frac{1}{2}})} \right\} \qquad \ldots(2)$$

We, therefore, seek relationships of the form of equation (2) for blunted bodies. In so doing it is reassuring to note that both the results of Chernyi's analysis of the hypersonic flow about slightly blunted cones[13] (based on blast-wave theory) and Erricson's scaling laws[15] (based on Sieff's embedded Newtonian flow theory) can be put into the form of equation (2).

If attention is initially concentrated upon those blunted single cones which have the minimum drag for a given Mach number and fineness ratio, then the correlation shown in Fig.24 may be derived. To a first approximation

the/

the data, which are derived from Refs.1,2 and 3 (and are for spherically-blunted cones and $1.24 \leq M \leq 5.0$ and $1.0 \leq f \leq 3.0$), are collapsed onto a single curve. The calculated optimum configurations, when plotted in this fashion, agree well with the experimental data, thus further confirming the validity of the calculation method of Ref.7.

Since the optimum bluntness ratios are correlated by plotting $1/(f\ C_{D_N}^{\frac{1}{2}})$, it is reasonable to expect that these same parameters would also correlate the ratio of minimum drag to the drag of the sharp cone of the same fineness ratio. Fig.25 shows that this is so. Additionally, Fig.26 demonstrates the particularly simple relationship between the optimum bluntness ratio and the bluntness ratio corresponding to C_D equal to that of a sharp cone of the same fineness ratio.

The fact that these three parameters $\left(\left(\frac{d}{D}\right)_{OPT}, \left(\frac{d}{D}\right)_{=}, \left(C_{D_{MIN}}/C_{D_{SC}}\right) \right)$, which broadly characterise the variation of C_D with bluntness ratio, can be approximately expressed as functions of $1/(f\ C_{D_N}^{\frac{1}{2}})$ alone, explains why the optimum configuration for a spherically blunted cone is insensitive to Mach number in the supersonic and hypersonic speed ranges. The drag coefficient of most blunt bodies varies little with increasing Mach number once the transonic speed range has been passed[11,13]. It is encouraging to note, however, that the correlation shown in Figs.24,25 and 26 covers a variation in C_{D_N} between $0.55 \leq C_{D_N} \leq 0.91$ and, hence, includes at least the upper part of the transonic speed range.

The drag savings shown in Fig.25 are possibly typical of those that can be achieved by nose blunting. Fig.27 compares the mean curve through the data of Fig.25 with the drag coefficients of two minimum-drag, spherically-blunted double-cones (normalised by the drag coefficients of both sharp single cones and optimum, sharp double cones of the same fineness ratio). Care is necessary to avoid reading too much into this sparse set of data, but it would appear that those reductions in drag which can only be realised by the use of nose blunting are similar for both single and double cones.

The available evidence appears to be insufficient to reach any firm answer to the question of a possible upper limit to the range of fineness ratios over which nose blunting can be used to reduce drag. Fig.24 would appear to indicate that the optimum bluntness ratio is very small for $fC_{D_N}^{\frac{1}{2}} \simeq 5$. However, Fig.25 appears to indicate some non zero asymptotic value for reduction in C_D. Nevertheless, it is clear that, properly applied, nose blunting may be expected to reduce forebody drag

for/

for values of $fC_{D_N}^{\frac{1}{2}}$ at least as high as 4. Thus, the usefulness of nose blunting for fineness ratios within the range shown in Fig.28 has been established. Further work is required to investigate the use of blunting at higher fineness ratios, and the boundary drawn in Fig.28 should be regarded as a pessimistic lower limit based on current knowledge.

5.7 Alternative forms of blunting

The entire preceding discussion has been confined to spherically-blunted bodies. While this is probably the case most commonly occuring in practice, there is no a priori reason why it should be the best form of blunting. For example, truncated (flat-faced) bodies are sometimes of practical importance and represent a considerable departure from spherical blunting. The variation of drag and volume with bluntness ratio has been examined for truncated single cones. The results of these calculations are presented in Figs.29,30, and 31. Each figure corresponds to a single, fixed, fineness ratio and, hence, may be compared with Figs.2 and 5, curves from which are also repeated in Figs.29, 30 and 31, in order to facilitate such comparisons.

Another form of blunting, often having a lower value of C_{D_N} than spherical blunting, is a cone of semi-apex angle substantially greater than that of the basic forebody. Results for single cones blunted by a 30° semi-apex angle conical cap are also shown in Figs.29, 30 and 31.

Comparison of the ways in which C_D varies with V for the different forms of blunting shows that, in general, those forms of blunting having high values of C_{D_N} (the drag coefficient of the bluntness in isolation) are to be preferred when attempting to minimise the drag of a complete body having a fixed fineness ratio. However, the drag penalties for increasing V (at fixed fineness ratio) beyond that corresponding to the minimum value of C_D are usually largest for the form of blunting having the highest value of C_{D_N}. Thus, the preference expressed above for high values of C_{D_N} may not be valid for other, albeit less common, optimisation criteria.

The calculated results obtained regarding blunted single cones having the minimum drag for the three forms of blunting described above and three fineness ratios ($f \approx 1$, $f = 2$ and $f = 3$) are summarised in Figs.32, 33 and 34, which use the same form of presentation as Figs.24, 25 and 26. The mean curves through the data points drawn on Figs.24, 25 and 26 have been transferred to Figs.32, 33 and 34 so that the two sets of graphs may be readily compared. It will be seen that, within the limitations of the admittedly approximate correlation of the earlier graphs, a collapse of the data for $(d/D)_{OPT}$ and $(d/D)_{=}$ is achieved, thus further illustrating the usefulness of the parameter $f.C_{D_N}^{\frac{1}{2}}$, particularly since C_{D_N} now varies

between/

between $0.535 \leq C_{D_N} \leq 1.60$.

The drag reduction parameter $(C_D/C_{D_{S.C}})$ is, however, not correlated - indeed many of the data points lie well below the mean curve for spherically blunted cones. This situation is further examined in Fig.35 where $(C_D/C_{D_{SC}})$ is presented as a function of fineness ratio. It is immediately seen that truncated cones perform best at low values of f, but spherical blunting is to be preferred for f = 3. To at least partially explain this effect it is necessary to refer back to section 5.4. There it was pointed out that the use of nose blunting causes two changes to occur in the surface pressures. Firstly, there will be an increase in drag due to high pressures acting on a small area of the body close to the axis of symmetry; but, secondly, this is more than offset due to reduced surface slopes and, hence, lower pressures acting over a larger forward facing area further downstream (and, thus, more remote from the axis of symmetry). It is evident that to minimise the first of these changes C_{D_N} should be small. The blunting will then tend to present comparatively low surface slopes to the oncoming air. Unfortunately, in order to maximise the second (favourable) change, it is necessary that the conical part of the body should commence as little downstream of the stagnation point and as far removed from the axis of symmetry as possible. This, of course, demands that the average surface slope of the blunting should be high and, accordingly implies a high value of C_{D_N}.

Thus, the choice of the best form of blunting is a complex matter requiring close study outside the context of this paper. However, it may be remarked that when the fineness ratio is very low $C_{D_{SC}}$ tends towards C_{D_N} so that the former of the two effects noted above is comparatively unimportant. However, any reduction of nose length (i.e. the streamwise distance from the stagnation point to the bluntness/cone junction) has a marked effect on the apex angle of the conical portion of the body. Thus, the latter effect tends to dominate and high values of C_{D_N} are to be preferred. Conversely, when the fineness ratio is very large $C_{D_{SC}}$ is very small so that the former effect assumes considerable importance. Also, changes in nose length have only a modest effect on the apex angle of the conical part of the body. Thus, the former effect is important and lower values of C_{D_N} are preferred.

It is interesting that unmodified Newtonian theory shows the above trends as exemplified by Figs.36 and 37 where contours of C_D calculated by Newtonian theory for conically blunted cones of varying bluntness ratio and angle are presented. It must be remembered, however, that these figures are a rough guide to the relevant relationships only, since unmodified Newtonian

theory/

theory cannot be held to satisfactorily represent some factors which are favourable to the use of blunting in general, and high values of C_{D_N} in particular.

Sufficient data have, however, been presented to show that the benefits obtained by (spherical) blunting and demonstrated in the main body of the report are only typical of what can be achieved with relative ease. By a proper choice of the type of blunting employed, yet greater benefits can be attained and, presumably, the range over which nose blunting is useful can be extended.

5.8 Alternative optimisation criteria

Hitherto, this analysis has been primarily directed towards the problem of minimising the drag of a forebody subject to the constraint that its fineness ratio is kept constant. This constraint was chosen because, although simple, it closely represents an important and frequently occurring design problem. However, it is certainly not the only optimisation criterion and set of constraints that are of practical interest. For example some practical optimisation problems are summarised in the table below:-

No.	OPTIMUM CONDITION SOUGHT	VARIABLES TO BE KEPT CONSTANT
I	MINIMUM DRAG	FINENESS RATIO
II	MAXIMUM VOLUME	FINENESS RATIO & DRAG
III	MINIMUM STAGNATION-POINT HEAT TRANSFER	FINENESS RATIO & DRAG

As noted above, problem I has been extensively discussed in preceding sections of this report. In this section brief analyses of problems II and III are presented since they represent design situations that can arise in practice even if not as frequently as those represented by problem I.

Taking each in turn, we first consider II in which it is desired to maximise the volume subject to the constraint that C_D and f should be constant.

The topic of increased volume has been touched upon in the earlier discussion of spherically-blunted single cones. There it was shown that even the minimum-drag configurations featured a substantial increase in volume relative to the sharp-nosed cone of the same fineness ratios. However, forebody volume is clearly strongly influenced by the shape of the body downstream of the blunting. Thus, double cones are analysed in this section.

Fig.38/

Fig.38 shows volume as a function of the bluntness diameter D_1 for spherically-blunted cones of $f = 3$ and having given values of C_D (D_2 is, of course, then determined by the need to keep C_D fixed). Because there are cases in which the same value of C_D is generated by two different values of D_2, even when D_1 is fixed, the curves presented in Fig.38 need be neither continuous nor single valued. However, it is clear from this figure that where there are two values of D_2 for the same D_1 and C_D, one configuration has much the higher volume. Both D_1 and D_2 exert a powerful influence upon V. By the correct choice of forebody geometry substantial gains in volume can be achieved. In particular, the volume can considerably exceed that of the minimum drag body for only a modest increase in drag. However, further increases in the premissible drag level purchase diminishing increases in volume. This process is summarised in Fig.39 where the maximum volume attainable for a given C_D is shown as a function of that C_D.

It is interesting to note the substantial gains in volume, relative to that of a sharp-nosed single cone, made by even the forebody shape having the minimum value of C_D. Also, examination of Fig.38 reveals that the use of nose blunting plays an essential part in the attainment of the gains in volume summarised in Fig.39.

Turning now to problem III, it should be recalled that stagnation point heat-transfer rates are, for a given free-stream Mach number, directly proportional to the square-root of the velocity gradient at the stagnation point[16]. This heat-transfer rate is thus dependent upon the geometry of the blunting employed, in a way such that its minimisation tends to favour the use of blunting having a high value of C_{D_N}.

It is, therefore, relevant to enquire whether, in problems involving the minimisation of stagnation point heat-transfer rate, the preferred type of nose blunting is likely to be different from those found in section 5.7. In particular, the question is posed as to whether the relative merits of spherical blunting and truncation are different when tackling problem III than when tackling problem I.

Fortunately, stagnation point velocity gradients have recently been the subject of study and Ref.17 includes observations on shapes pertinent to the present discussion.

Now,
$$\dot{q} = k_1 \left(\frac{\partial U}{\partial s} \right)_s^{\frac{1}{2}}$$

Considering spherically-blunted and truncated bodies (denoted by suffices b, and t respectively).

$$\dot{q}_b = k_1 \left(\frac{\partial U}{\partial s} \right)_{s_b}^{\frac{1}{2}}$$

and/

and

$$\dot{q}_t = k_1 \left(\frac{\partial U}{\partial s} \right)^{\frac{1}{2}}_{s_t}$$

Now, from Ref.17

$$\left(\frac{\partial U}{\partial s} \right)_s = \left(\frac{\partial Me}{\partial (s/s^*)} \right)_s \cdot \left(\frac{a_s}{s^*} \right)$$

where, at M = 3 $\left(\frac{\partial Me}{\partial (s/s^*)} \right)_s \simeq 0.91$ (for a hemisphere)

and $\left(\frac{\partial Me}{\partial (s/s^*)} \right)_s \simeq 0.33$ (for a disc).

Also from geometrical considerations

$$S^* = 0.5\ d \text{ for a truncated cone}$$

$$\text{and } S^* = \theta^* \cdot \frac{d}{2} \sec \varepsilon$$

or, using ref.17, $S^* = 0.386 \cdot d \cdot \sec \varepsilon$ for a spherically-blunted cone having the sonic point located on the spherical portion of the body.

For the purpose of this note the stagnation-point, heat-transfer rates are normalised by dividing them by the stagnation-point, heat-transfer rate of a hemisphere having the same base diameter as the forebody being considered, i.e. for this reference body

$$S^* = 0.386\ D$$

and so:-

$$\left(\frac{\partial U}{\partial s} \right)_{ref} = (0.91 . a_s) / (0.386\ D) = 2.355\ a_s / D$$

or $$\dot{q}_{ref} = 1.535\ k_1 \cdot \left(\frac{a_s}{D} \right)^{\frac{1}{2}}$$

and, denoting quantities such as $\dot{q}_s/\dot{q}_{ref}$ by the symbol Q, we have:-

Q_b/

$$Q_b = \left(\frac{D}{d}\right)_b^{\frac{1}{2}} \cdot \cos^{\frac{1}{2}} \varepsilon \qquad \text{- spherically blunted cone.}$$

and

$$Q_t = 0.529 \left(\frac{D}{d}\right)_t^{\frac{1}{2}} \qquad \text{- truncated cones.}$$

Since from these last two equations, values of $(\frac{d}{D})$ required to produce any desired value of Q may be evaluated and combined with the earlier calculations of drag, the comparison between spherically-blunted and truncated cones may be accomplished.

In fact:-

$$\left(\frac{d}{D}\right)_b = (\cos \varepsilon) / Q_b^2$$

and

$$\left(\frac{d}{D}\right)_t = \frac{0.28}{Q_t^2}$$

Figs.40,41 and 42 show C_D as a function of the normalised stagnation-point heat-transfer rate for blunted single cones of fineness ratios, 1,2 and 3. Also shown are the limiting values of C_D (at $Q \to \infty$) for the sharp cone together with the values of Q for both a disc and a hemisphere. It will be seen that in all cases the minimum value of C_D corresponds also to a fairly modest value of Q. The variation of C_D with Q for values of Q above that corresponding to the minimum C_D is of comparatively little practical interest since no designer is likely deliberately to incur such unnecessary penalties in <u>both</u> C_D and Q. Of much greater interest is the variation of C_D with Q for values of Q below that corresponding to minimum C_D.

In all cases only small decrements of Q below that corresponding to the minimum C_D can be achieved before severe drag penalties are incurred. This is, of course, a direct consequence of the fact that Q varies as $(\frac{D}{d})^{\frac{1}{2}}$ so that reduced values of Q have to be bought at the expense of large increases in (d/D) with accompanying increases in drag if $d/D > (d/D)_{OPT}$.

It is evident that, unless high values of C_D are acceptable (as in certain specialised problems) each type of nose blunting has associated with it a reasonably well defined minimum value of Q. Reductions in Q below this

minimum/

minimum are better accomplished by a change in the type of blunting rather than by a straightforward increase in (d/D). A practical limit to the reduction of Q without excessive C_D is, of course, set by the minimum value of Q attainable with a truncated cone. However, it should be observed that this value is not greatly in excess of 1.0, i.e. $\dot{q}$ does not greatly exceed that for a hemisphere of diameter D and, as such, may well be lower than that required in many practical applications.

These results are summarised in Fig.43 in which typical bounds of stagnation point heat-transfer rate are shown as a function of fineness ratio for two different types of blunting. The upper bound is taken as that corresponding to the minimum value of C_D for each type of blunting and fineness ratio, while the lower bound is taken as that corresponding to C_D equal to that for a sharp cone of the same fineness ratio. It is particularly interesting to note that, as foreshadowed in the earlier discussion, the truncated cone appears to be the most suitable body (in the sense that the maximum reduction in Q can be achieved without increasing C_D beyond that for a sharp cone of the same fineness ratio) throughout the range of fineness ratios considered.

On this basis, it would appear that truncation as a form of blunting has been undeservedly neglected in the past. It must be recognised that straightforward truncation, while reducing the stagnation point heat-transfer rate - and, hence, thermal stress problems in this area[18] - might involve significant thermal stress problems at the downstream end of the blunting due to the rapid changes in heat-transfer rate with streamwise distance that are likely in this region. However, such problems could possibly be alleviated by limited smoothing of the distribution of surface slope over the area affected. Moreover, such detailed worries do not detract from the overall conclusion that, when the aim is to reduce stagnation-point heat-transfer rate without large penalties in C_D, there is considerable scope for the use of forms of blunting having large radii of curvature in the stagnation point region and, hence, usually having large values of C_{D_N}.

5.9 "Off-design" or non-optimum bodies

To consider all aspects of the behaviour of non-optimum bodies would demand a paper in itself and one which would be much longer than the present discussion. Moreover, the preceding sections have already shown that, in most cases, the variation of C_D with the various independent parameters has relatively flat minima which are insensitive to changes in M. One may, therefore, safely make the qualitative statement that the performance of optimum bodies derived as described earlier would not be seriously prejudiced by even substantial changes in Mach number.

However, it is instructive to consider the implications of one additional geometrical constraint. In particular, it is possible that non-aerodynamic considerations might force a designer to fix upon a particular

value/

value for either D_1 or D_2. Unless he is lucky enough to light upon the optimum value for this fixed diameter, a drag penalty will thereby be incurred. Such a penalty in C_D may, however, be minimised by adjustment of the other, disposable diameter.

This point is illustrated in Figs.44,45 and 46. In Figs.44 and 45, the variation of C_D with D_2 for various values of D_1 is contrasted with the variation of C_D with D_2 that occurs when D_1 is chosen so as to minimise C_D for each value of D_2. It will be seen that by varying D_1 in the proper manner, the drag penalties associated with a non-optimum value of D_2 may be greatly reduced, and C_D made to have a very flat minimum. Thus, the drag penalties associated with a fixed non-optimum value of D_2 need not be severe provided that the appropriate value of D_1 is found and D_2 is not too far removed from the optimum value. Likewise, Fig.46 demonstrates that the penalties consequent upon D_1 being fixed at some non-optimum value may be greatly reduced by the proper choice of D_2.

6. Conclusions

From the preceding quantitative discussion certain general principles tend to emerge. In the interests of clarity they are restated here. To facilitate reference to the relevant parts of the discussion the number of the appropriate section in the discussion is quoted in brackets.

When minimising the value of C_D for a body of given fineness ratio, it was found that at a free-stream Mach number of 3.05:-

(5.1)For single cones, nose blunting can be used to decrease the drag at a given fineness ratio, or to increase the volume without any drag penalty, or, at the higher fineness ratios, to reduce the fineness ratio without drag penalty or loss of volume.

(5.2)The above advantages of nose blunting apply equally to both single and double cones. The rudimentary freedom to adjust the shape of the forebody downstream of the blunting (independently of the bluntness ratio), in the case of the double cone does not diminish the utility of nose blunting.

(5.3)A correctly proportioned, blunted double cone can have virtually the same forebody drag as a 3/4 power-law body of the same fineness ratio, thus effecting a marked simplification of the geometry of the forebody without drag penalties.

(5.3)Nose blunting, even when applied in a fairly simple fashion, can achieve improvements in the characteristics of a 3/4 power-law body, notably increased volume. This is of particular interest because 3/4 power-law profiles have often been regarded as optimum for supersonic and hypersonic Mach numbers. In view of this and the previous three conclusions it appears that an investigation of blunted bodies using newly-developed drag-prediction methods together with those powerful numerical optimisation techniques that are currently available should yield optimum bodies that are substantial improvements over those hitherto considered to be optimum.

(5.4)/

(5.4)The physical mechanism underlying the above uses of nose blunting, including the important role of the entropy layer, has been demonstrated. These concepts, which are well understood for single blunted cones, are sufficient to explain optimisation processes for more complex bodies, the underlying physical mechanism being identical in both cases. The use of nose blunting is, thus, a logical extension of earlier optimisation methods.

(5.5)The search for truly optimum forebody shapes is best conducted using a suitable prediction method, such as that used in this report which can itself be validated by a limited number of experimental tests performed specifically for this purpose.

(5.6)The supersonic/hypersonic similarity rules for affinely-related, sharp-nosed bodies may be reinterpreted to give corresponding similarity parameters for blunted bodies. Using these parameters approximate correlations of the characteristics of such blunted bodies may be obtained for wide ranges of Mach number and fineness ratio.

(5.7)Spherical nose blunting, as considered in the main body of the report, is preferable to truncation as a means of reducing the drag of the higher fineness ratio bodies; but it is inferior to truncation at lower fineness ratios. Thus, the drag reductions featured in this report, while typical of those that can be readily achieved, are not necessarily the maximum possible, i.e. when the best form of nose blunting is employed.

(5.8)The blunted forebody shape having the minimum C_D has a substantially greater volume than a sharp cone of the same fineness ratio. Further gains in volume may be made at little cost in C_D.

(5.8)An alleviation of stagnation-point heat-transfer is inherent in the use of nose blunting. In this context blunting which is smaller than that corresponding to minimum drag is of no practical interest since to use such a size of blunting is to incur unnecessary penalties in <u>both</u> heat transfer and drag. Reductions in stagnation-point heat-transfer rate beyond that corresponding to minimum C_D soon cost substantial drag penalties. Thus for each fineness ratio and type of blunting there is only a limited range of normalised stagnation-point heat-transfer rates that can be utilised in practice. Hence any requirement to attain a given stagnation-point heat-transfer rate is best satisfied by the appropriate choice of the type of nose blunting - a possibility which has hitherto received little attention.

(5.9)If a designer is forced to adopt a non-optimum shape for the forebody downstream of the blunting, a drag penalty will necessarily be incurred. This penalty, however, can be considerably alleviated by the proper choice of size for the nose blunting.

References/

References

No.	Author(s)	Title, etc.
1	P. G. Pugh and L. C. Ward	Some notes on the use of bluntness to reduce forebody drag at supersonic speeds. NPL Aero Special Report 011. A.R.C.30 340 (1968)
2	-	Foredrag of spherically blunted cones in supersonic flow. Engineering Sciences Data Unit Date Item 68021 (1968)
3	A. J. Eggers, Jnr. M. M. Resnikoff and D. H. Dennis	Bodies of Revolution having minimum drag at high supersonic airspeeds. NACA Report 1306 (1957)
4	A. Miele	On the theory of optimum aerodynamic shapes. Rice University Astro-Aeronautics Report No.53 (1968)
5	S. L. Brown and D. G. Hall	Axisymmetric bodies of minimum drag in hypersonic flow. Journal of Optimisation Theory and Applications Vol.3 No.1 (1969)
6	P. G. Pugh and L. C. Ward	Drag estimation for simple forebody shapes (1969). NPL Aero Report 1304. A.R.C.31 491 (1969)
7	P. G. Pugh and L. C. Ward	A novel method for the estimation of the zero lift forebody pressure drag of axisymmetric non-slender shapes at supersonic and hypersonic velocities. NPL Aero Special Report 038 (1970)
8	L. C. Ward	Some aspects of the supersonic flow about axisymmetric bodies at zero angle of attack. Lecture to Royal Aero. Soc. (Weybridge Branch) (1969)
9	T. von Karaman	The problem of resistance in compressible fluids. Reale Acad. d'Italia, Fondazine Alessandro Volta, Proc. 5th Volta Congress, Rome 222 - 277 (1935)
10	A. Moore	Private Communication. RAE (1968)

11/

References

No.	Author(s)	Title, etc.
11	-	Engineering Sciences Data Unit. Data Item S.02.03.06 (1958)
12	E. W. Perkins, L. H. Jorgensen and S. C. Sommer	Investigation of the drag of various axially-symmetric nose shapes of fineness ratio 3 for Mach numbers from 1.24 to 7.4 . NACA REPORT 1386 (1958)
13	G. G. Chernyi	Introduction to hypersonic flow. (Translated by R. F. Probstein)Academic Press (1961)
14	L. E. Ericsson	Dynamic stability problems associated with flare stabilisers and flap controls. AIAA Paper 69 - 182 (1969)
15	L. E. Ericsson	Universal scaling laws for nose-bluntness effects on hypersonic unsteady aerodynamics. AIAA Journal Vol.7 No. 12 Dec.1969
16	L. F. Crabtree R. L. Dommett and J. G. Woodley	Estimation of heat transfer to flat plates, cones, and blunt bodies. ARC R & M 3637 (1965)
17	L. L. Trimmer and E. L. Clark	Stagnation point velocity gradients for spherical segments in hypersonic flow. AIAA Journal Vol. 7 No. 10 Oct. 1969
18	M. J. Wooldridge	Aero-Thermo-Structural Optimisation in Radome Design. Aeronautical Journal Vol.74 No.711, March 1970
19	W. A. Murray	Private Communication. NPL (1970)

R 72561/1/503427 K4 12/73 P Produced in England by Her Majesty's Stationery Office, Reprographic Centre, Basildon

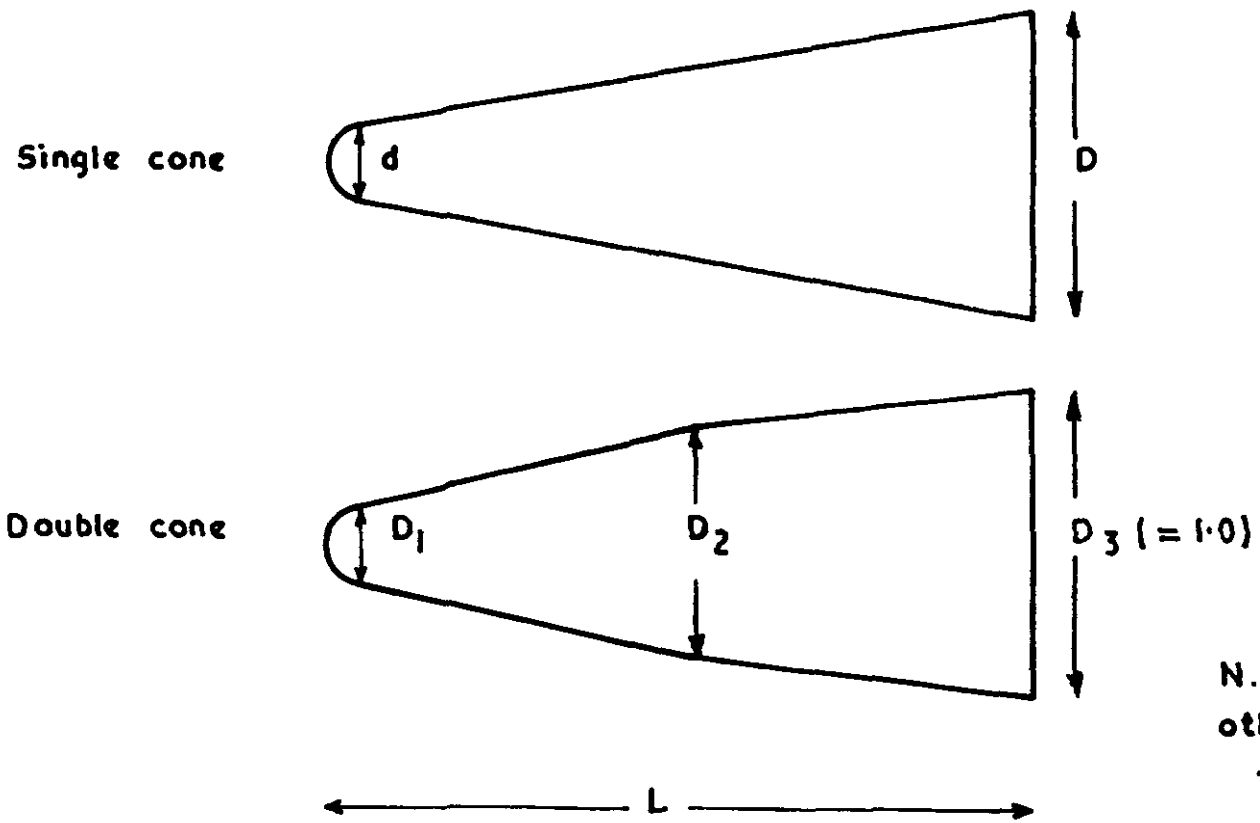

$$f = \frac{L}{D} \text{ or } \frac{L}{D_3}$$

N.B. Unless stated otherwise, D_3 is taken as unity

32284
FIG. 1

Forebodies studied and nomenclature

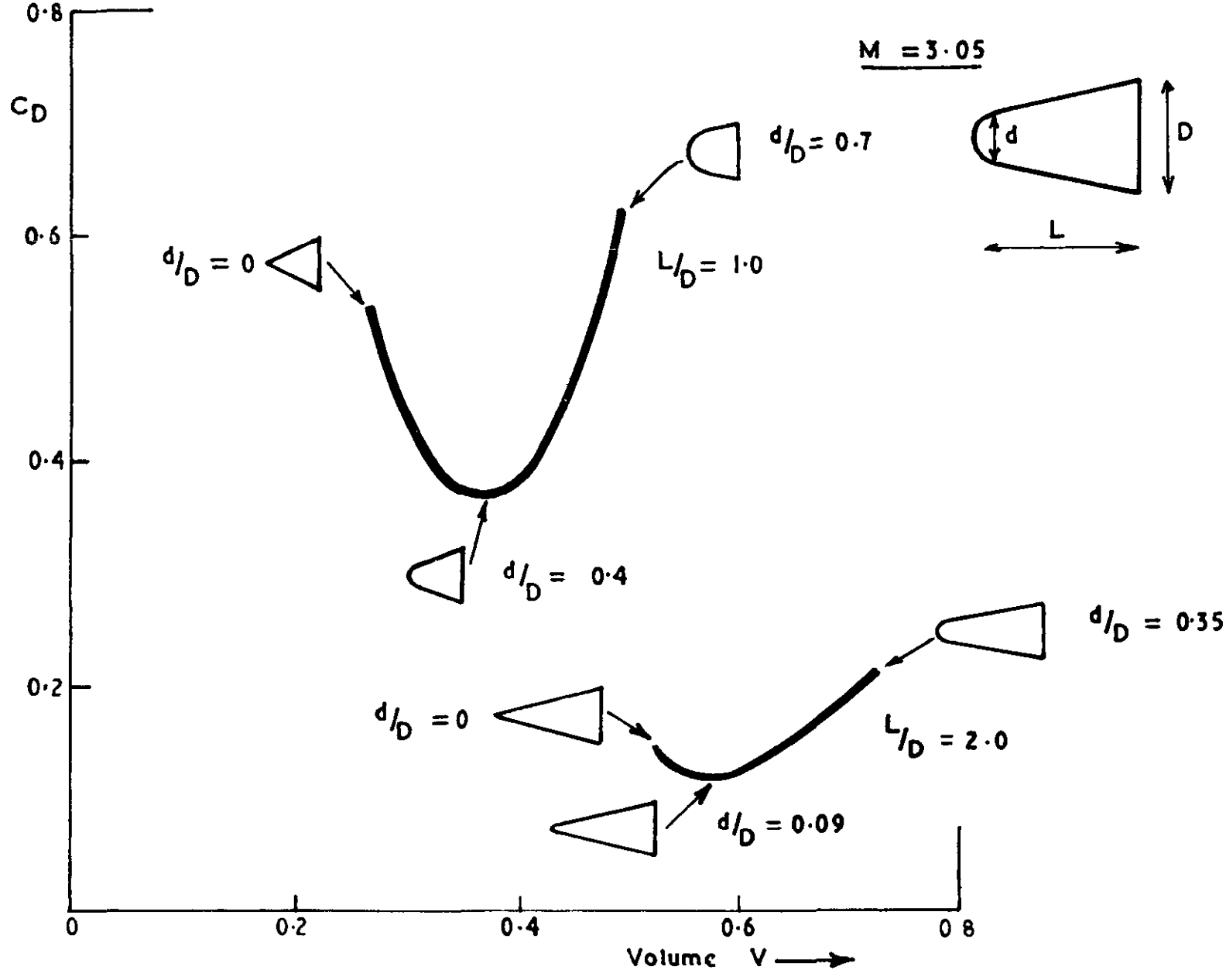

Drag of constant fineness ratio blunt cones

32284
FIG.2

32284
FIG 4

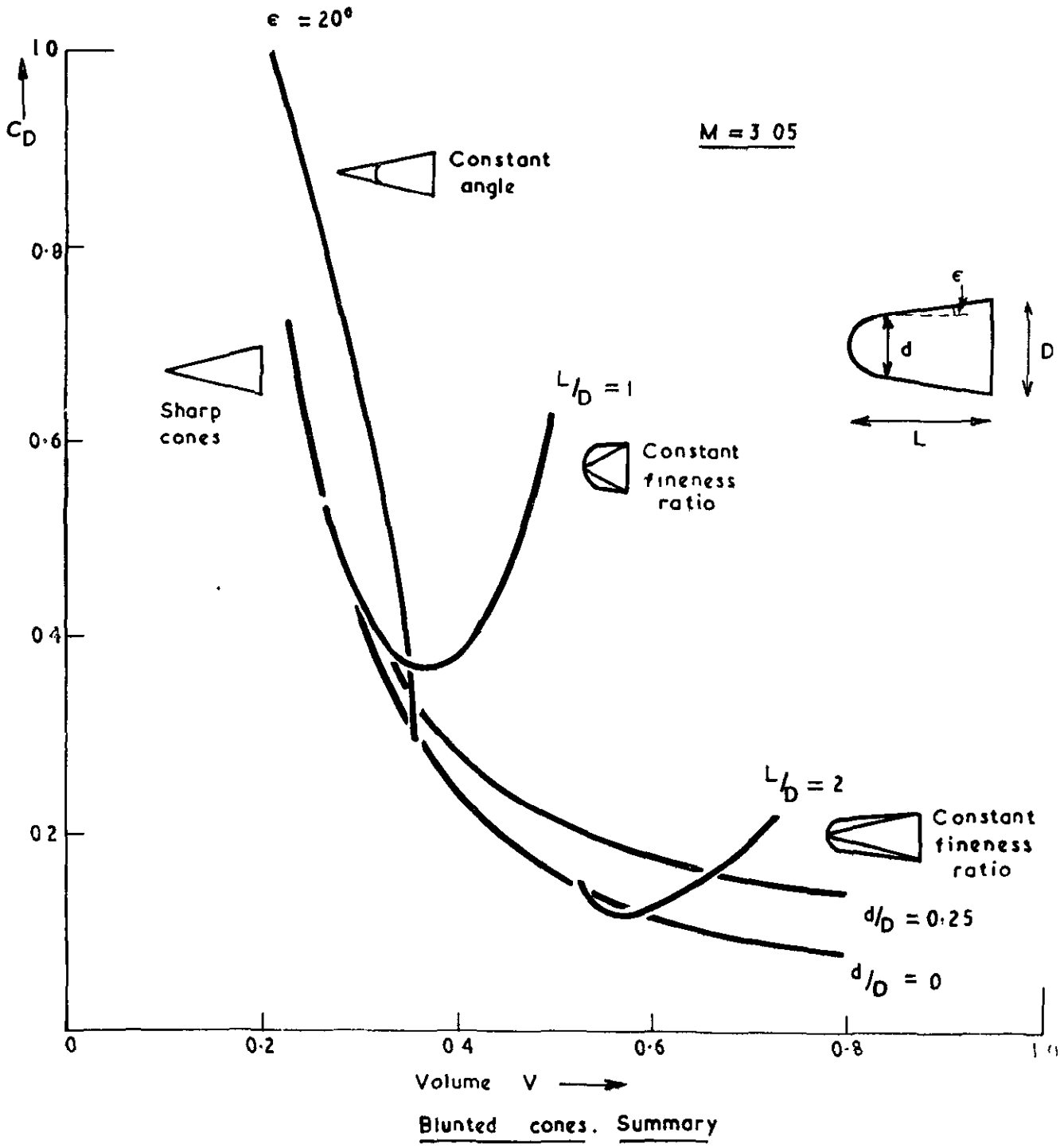

Blunted cones. Summary

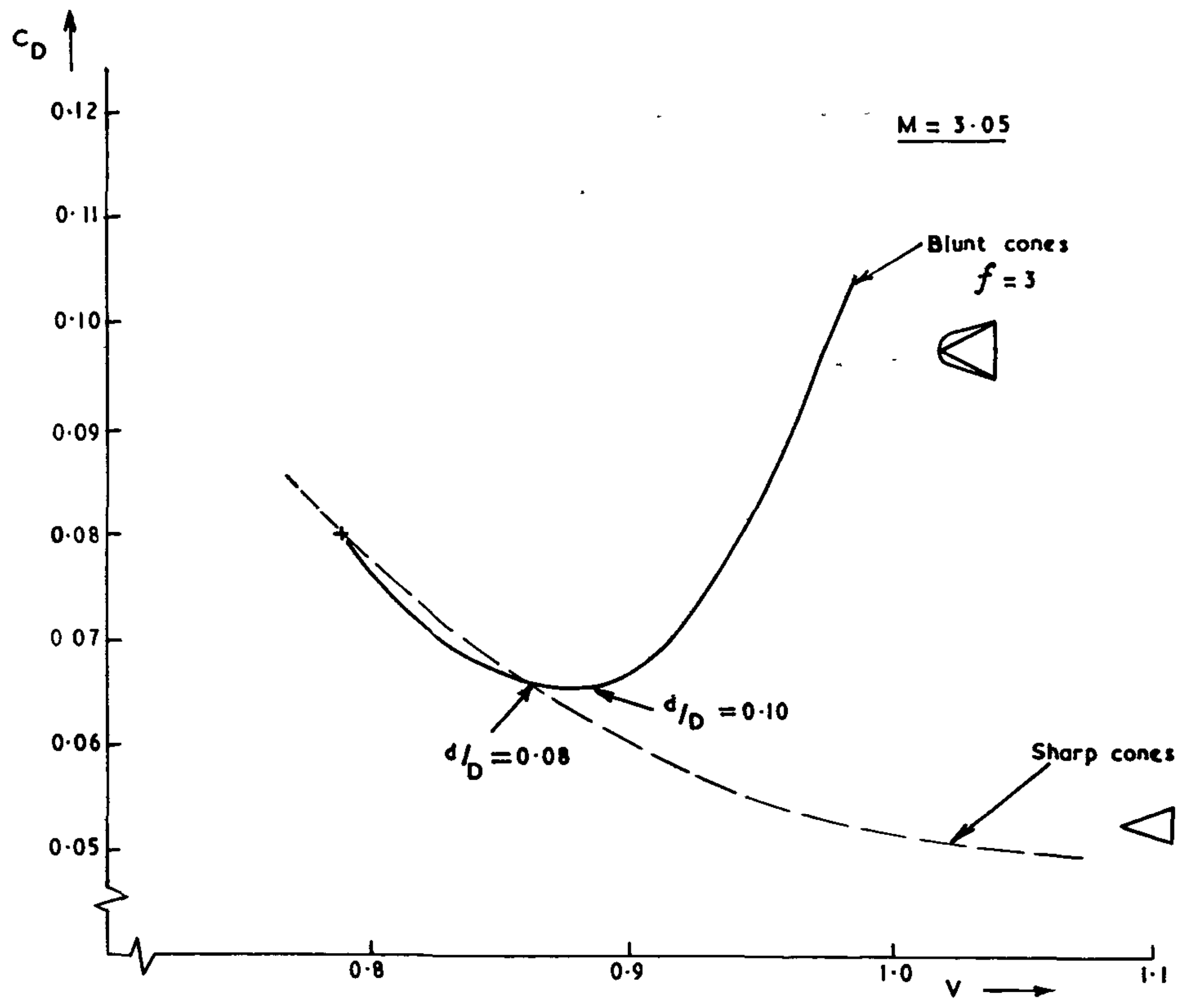

Single cones

32284
FIG. 5

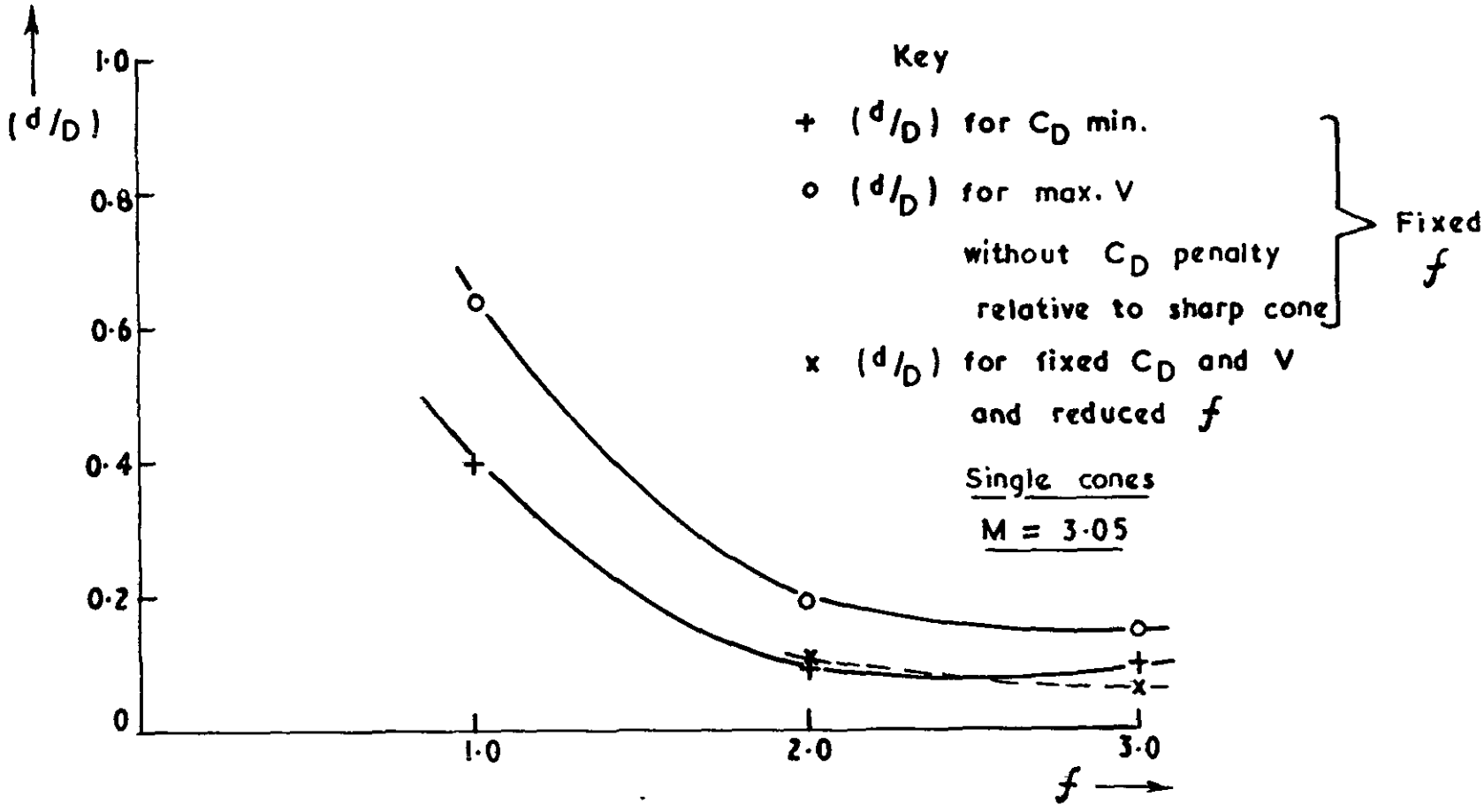

Variation of three significant bluntness ratios with f

32284
FIG.6

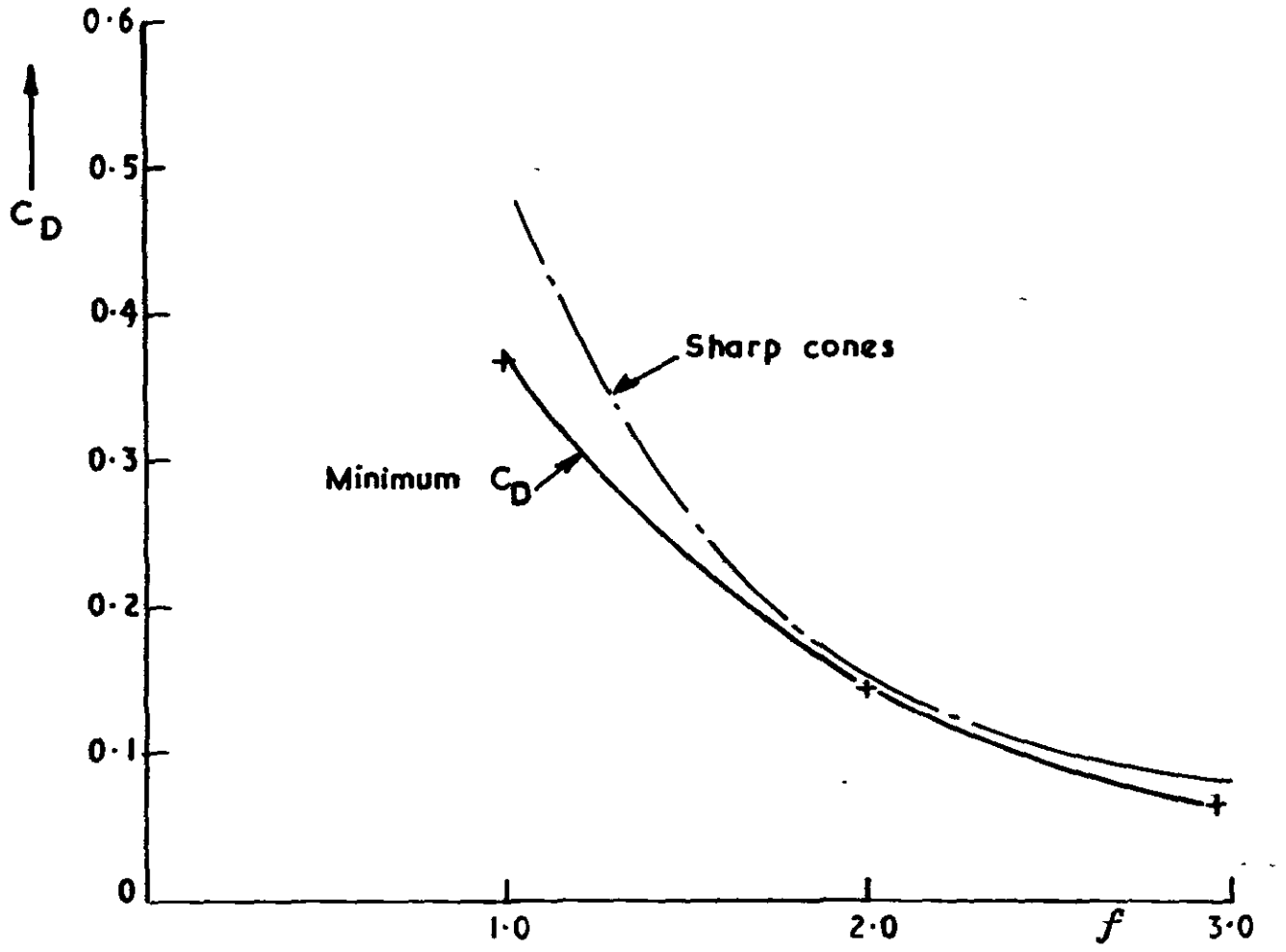

Minimum values of C_D for blunted single cones

3228A
FIG.7

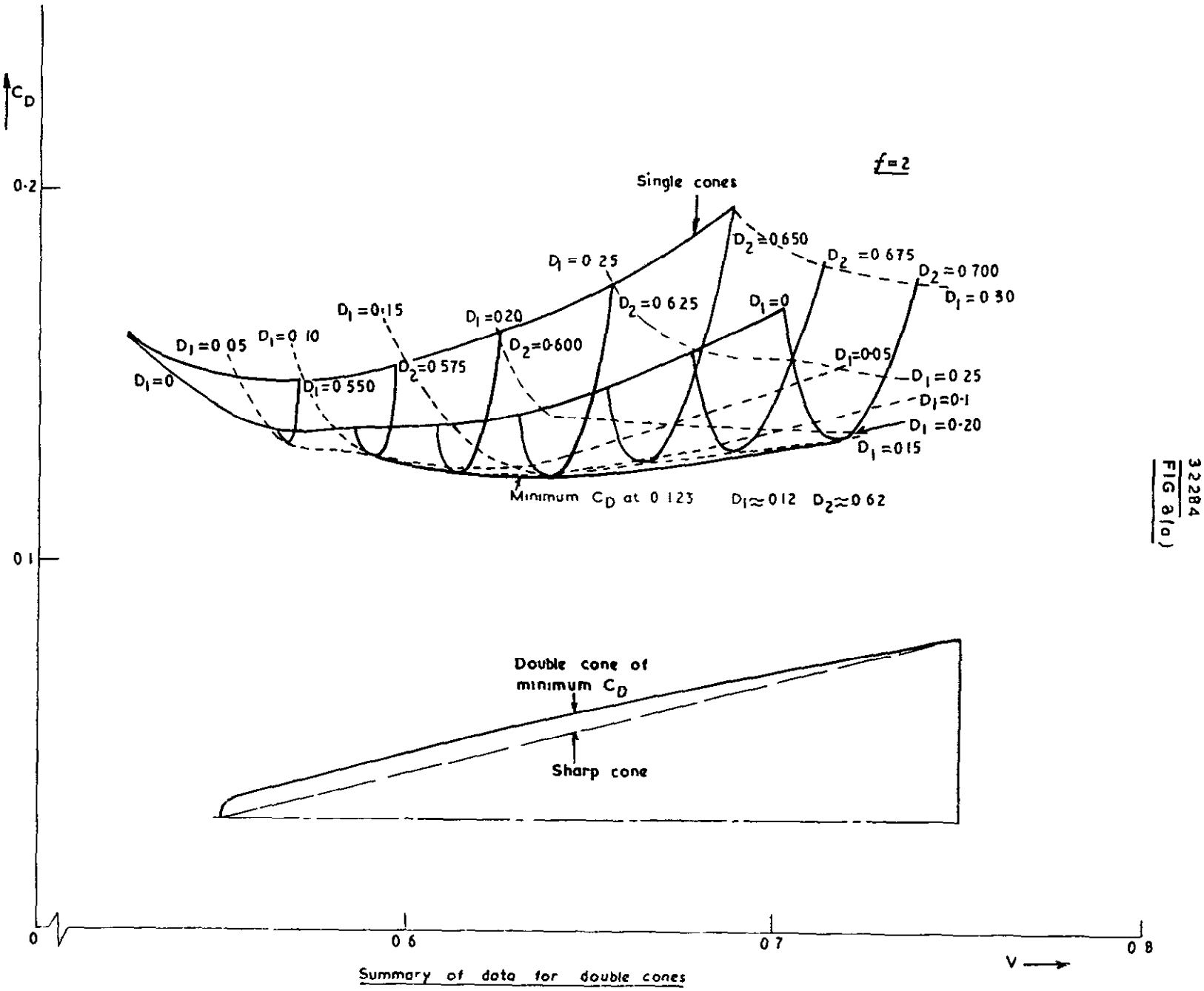

32284
FIG 9(a)

Summary of data for double cones

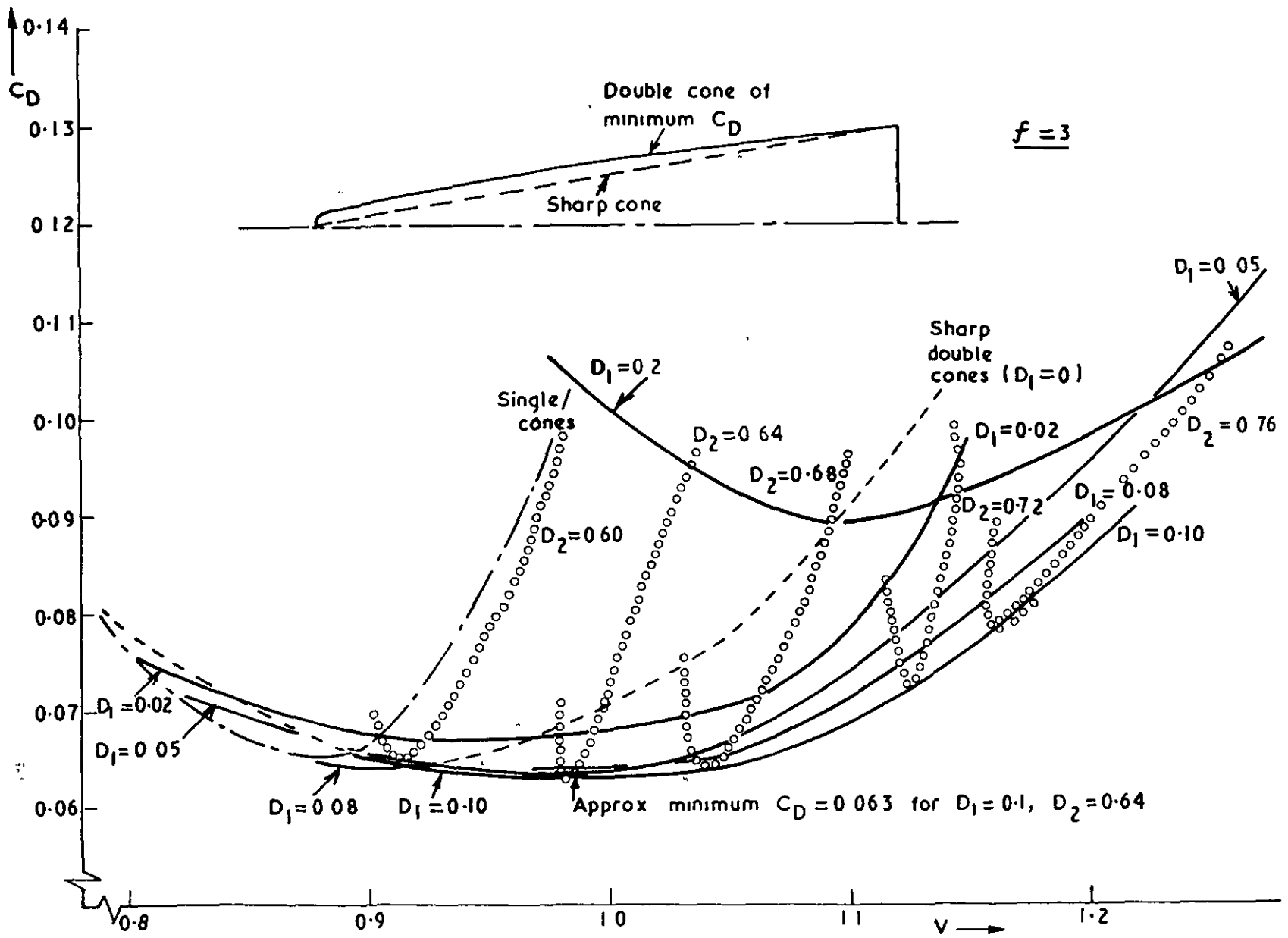

Summary of data for double cones

3 2284
FIG.8 (b)

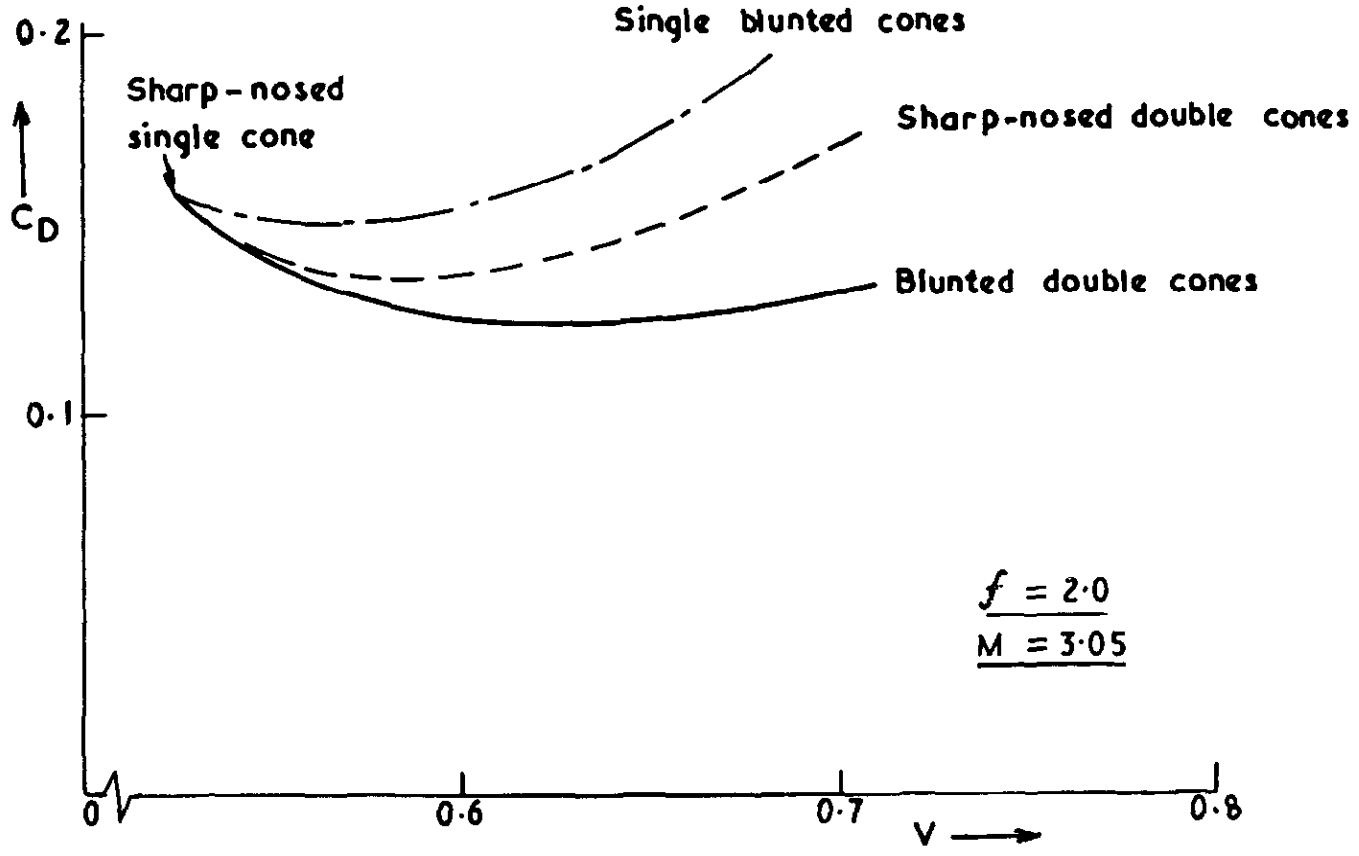

Application of nose blunting to single and double cones

3 2284
FIG. 9

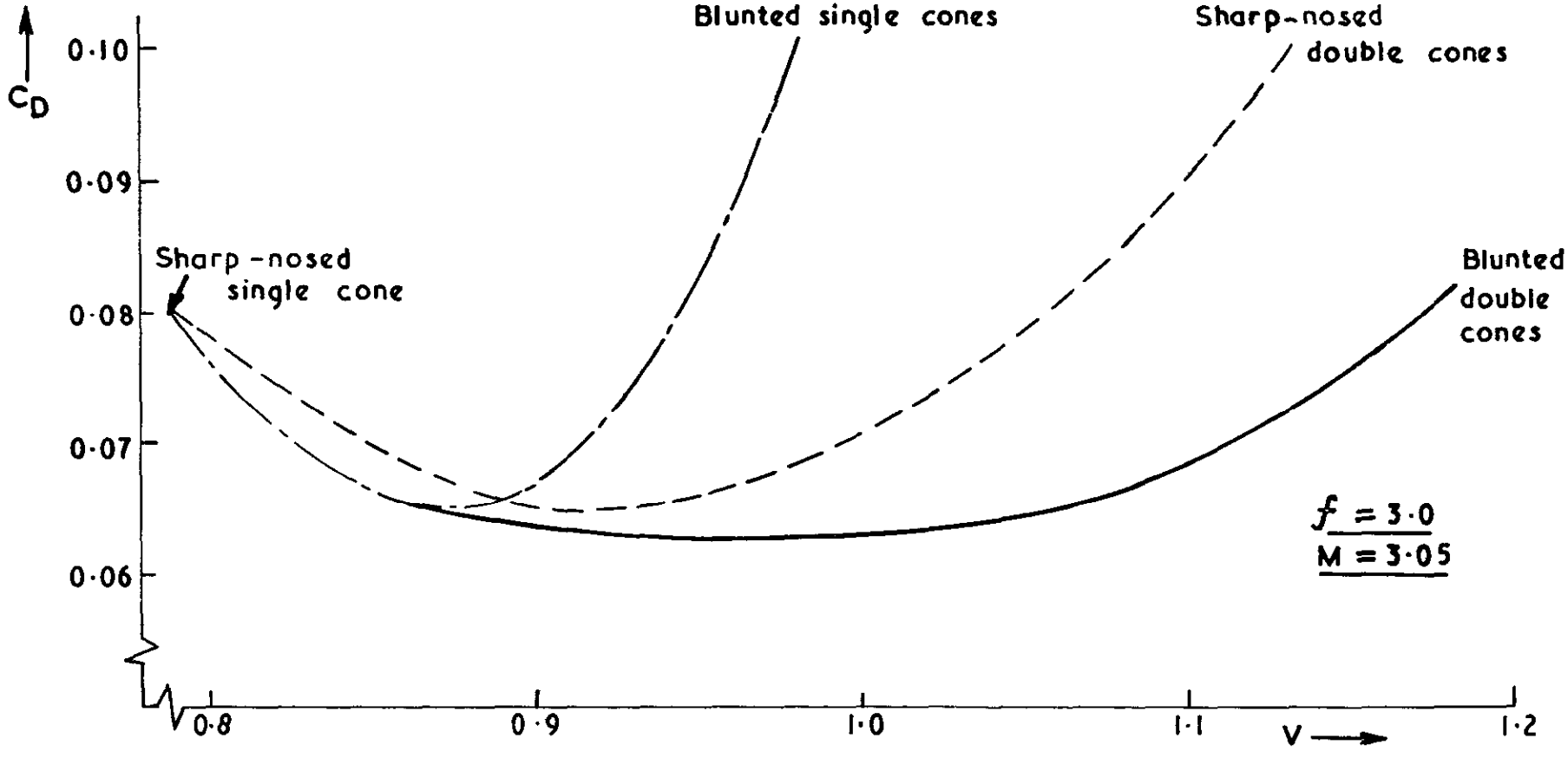

Application of nose blunting to single and double cones

32284
FIG. 10

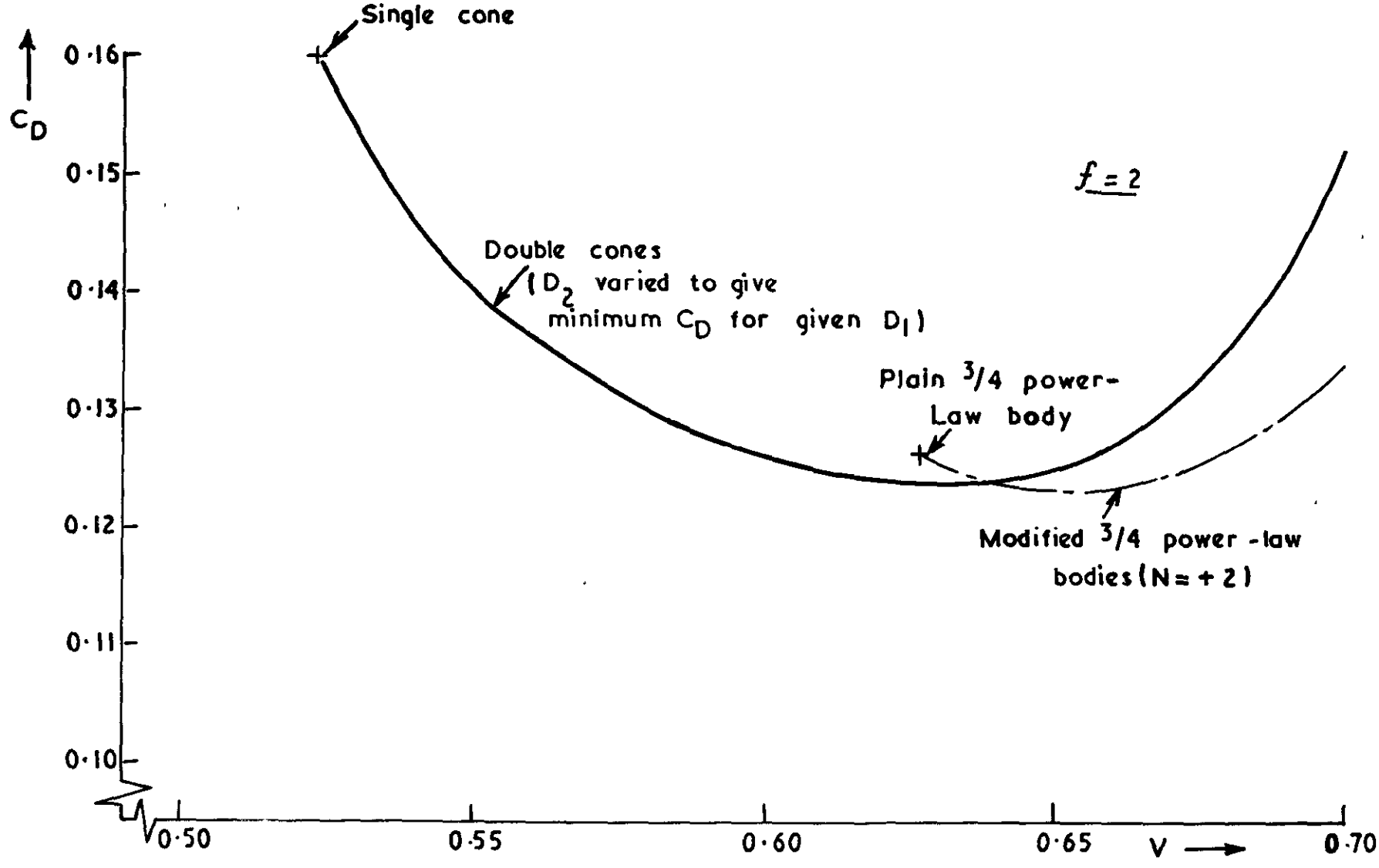

32284
FIG. 11

Comparison of double cones and 3/4 power - law bodies

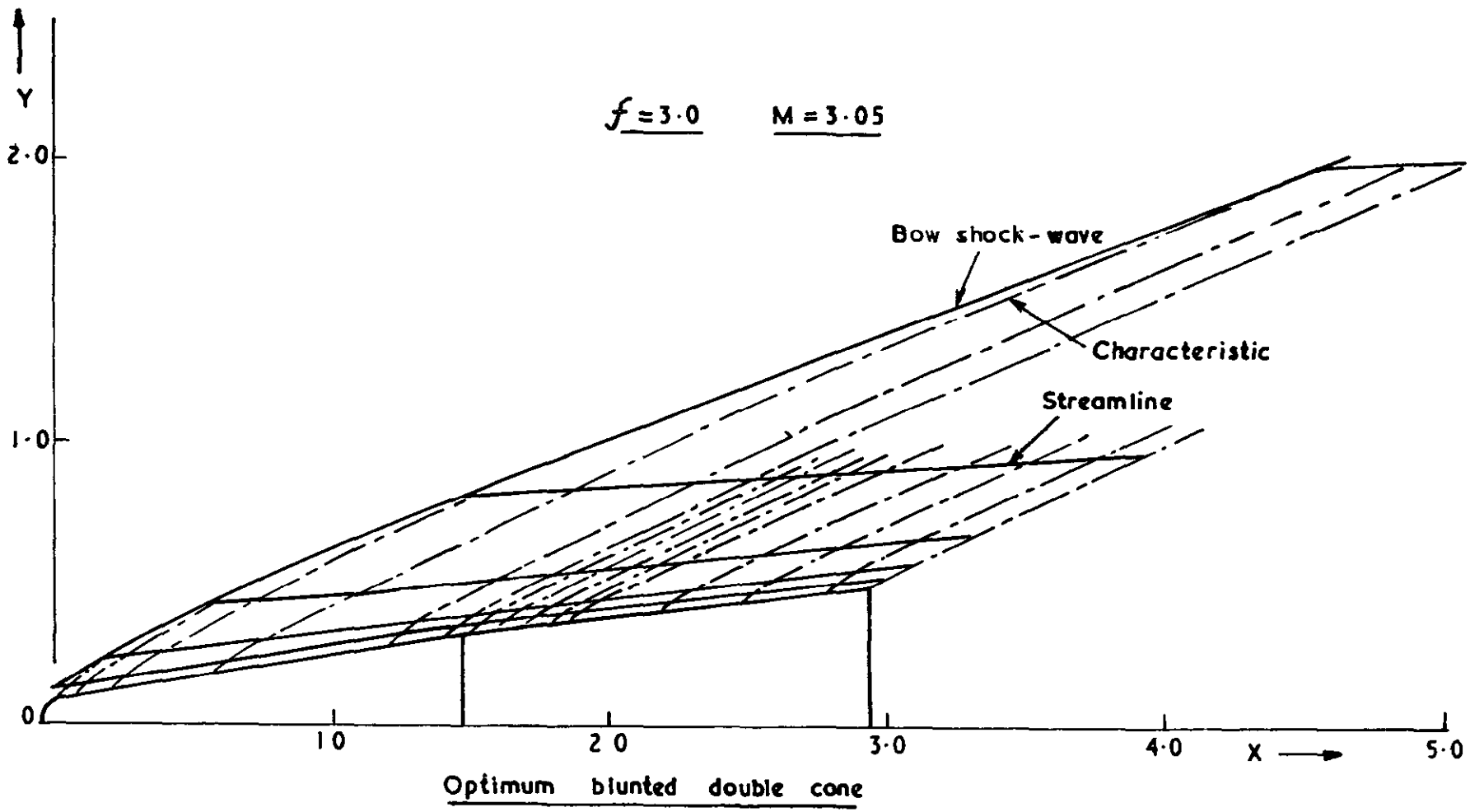
Y
2·0
1·0
0
$f = 3·0$
M = 3·05
Bow shock-wave
Characteristic
Streamline
1·0
2·0
3·0
4·0
X
5·0
Optimum blunted double cone

32284
FIG 12

$f = 3$, M = 3·05

Comparison of estimates of C_D

Body \ Method	Via entropy	Via surface pressures	
Sharp cone	0·0800	0·0767	} Exact solution $C_D = 0·07896$
Optimum double cone	0·0630	0 0618	
C_{Dopt}/C_{Dsc}	0·79	0·81	

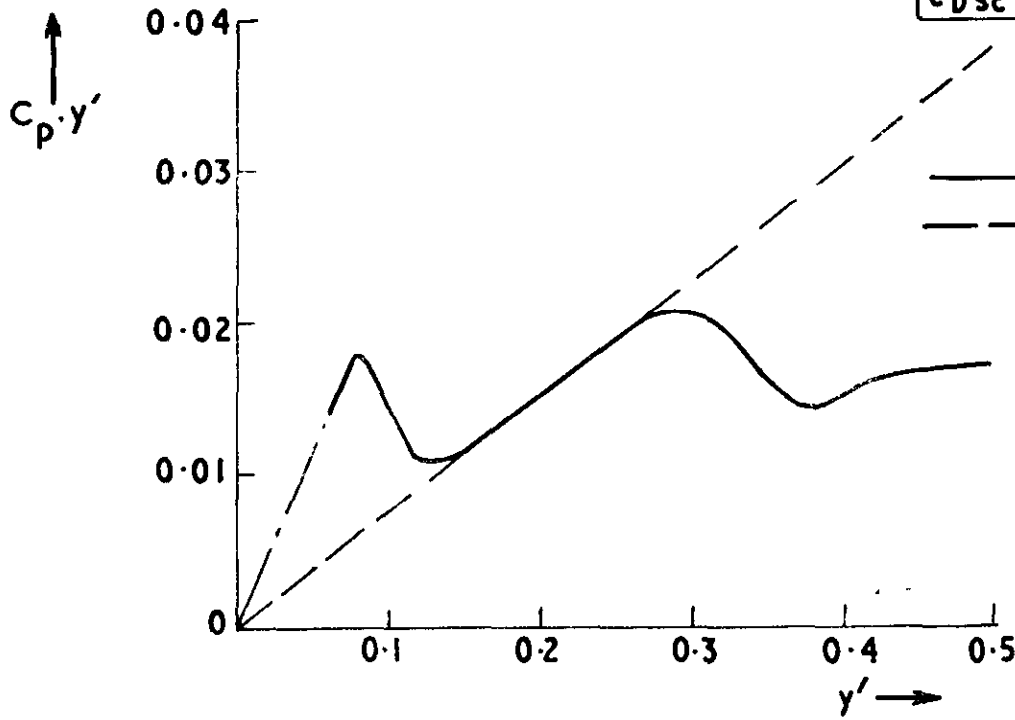

Pressure distributions for two $f = 3$ bodies

3228/4
FIG. 13

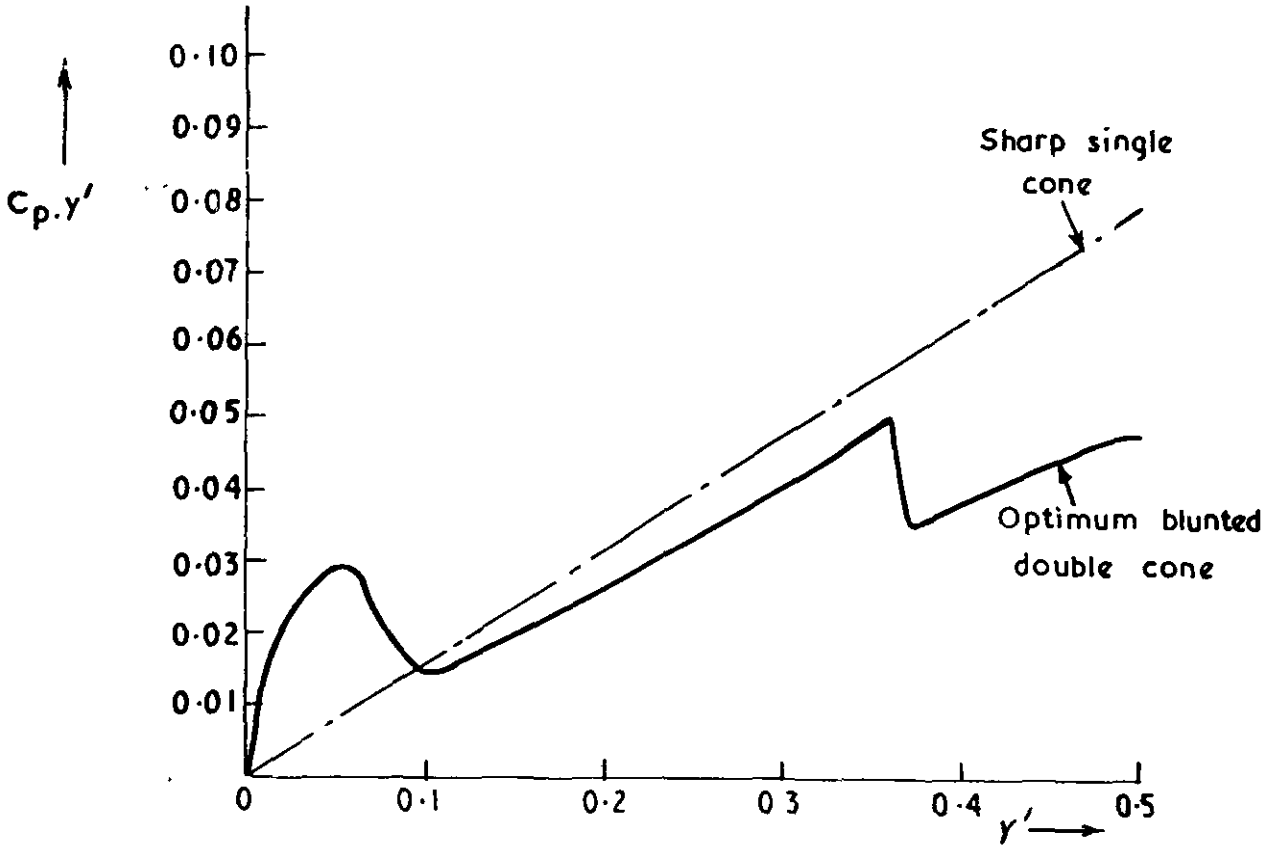

Pressure distributions for two $f = 2$ bodies

Comparison of estimates of C_D

Method / Body	Via entropy	Via surface pressures
Sharp single cone	0·123	0·128
Optimum double cone	0·161	0·158
C_{Dopt}/C_{Dsc}	0·76	0·81

32284
FIG. 14

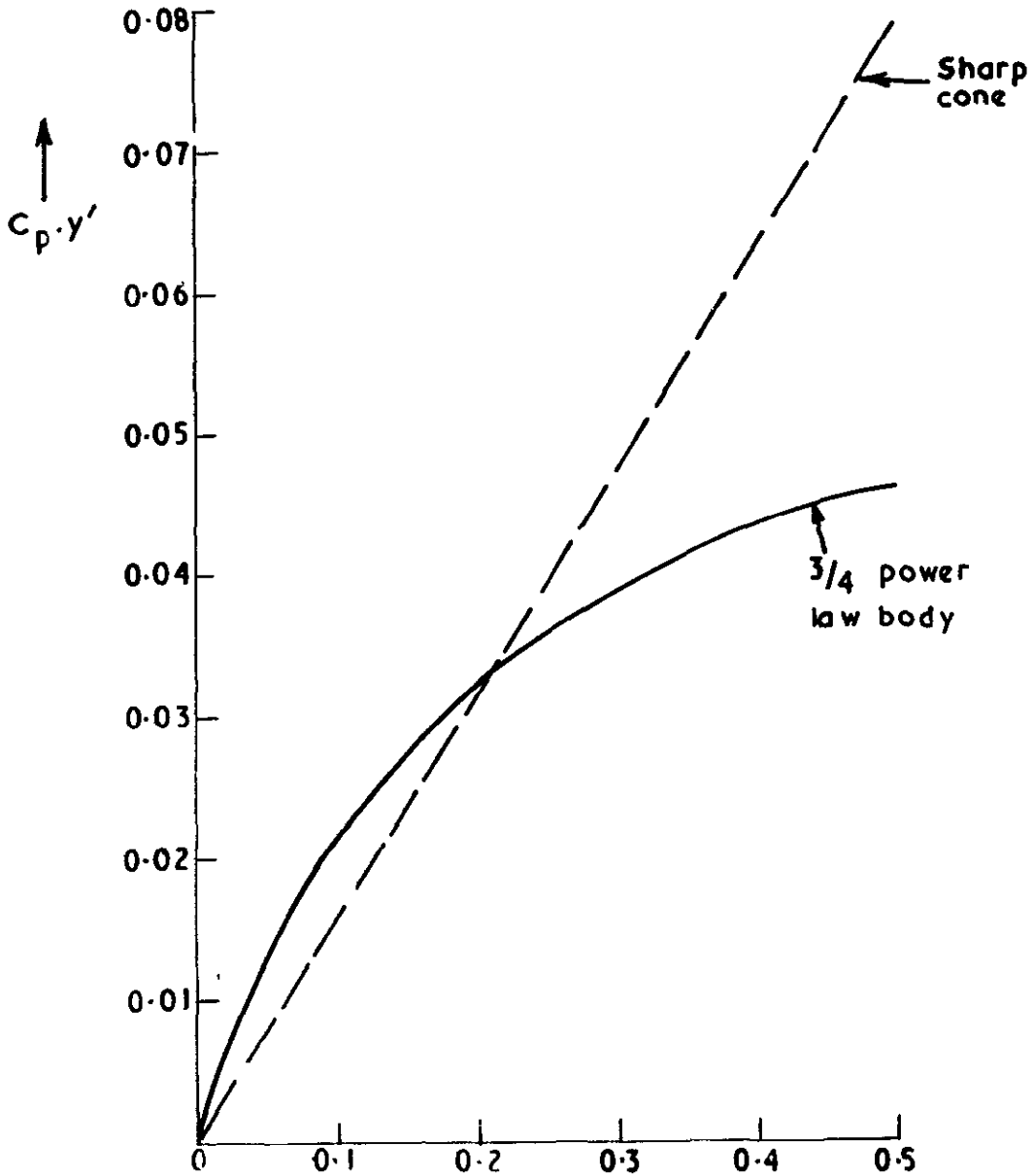

Pressure distribution for $f = 2$, 3/4 power law body

$M = 3 \cdot 05$

Comparison of estimates of C_D

Body \ Method	Via entropy	Via surface pressures
3/4 power law	0·127	0·131
Sharp cone	0·161	0·158
$C_D / C_{D\,sc}$	0·79	0·83

32284
FIG.15

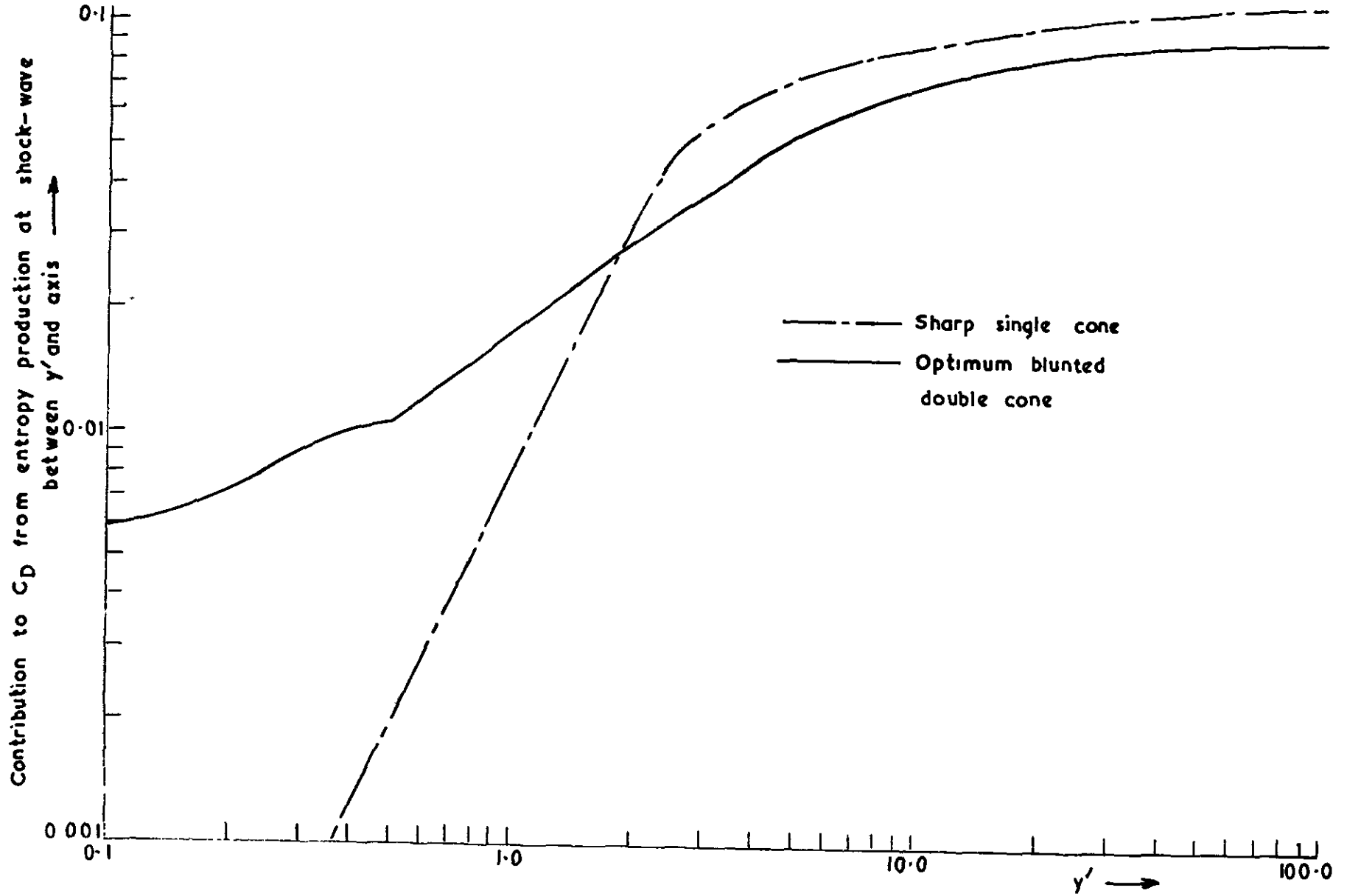

32284
FIG. 16

Analysis of shock shapes for two $f = 2$ bodies

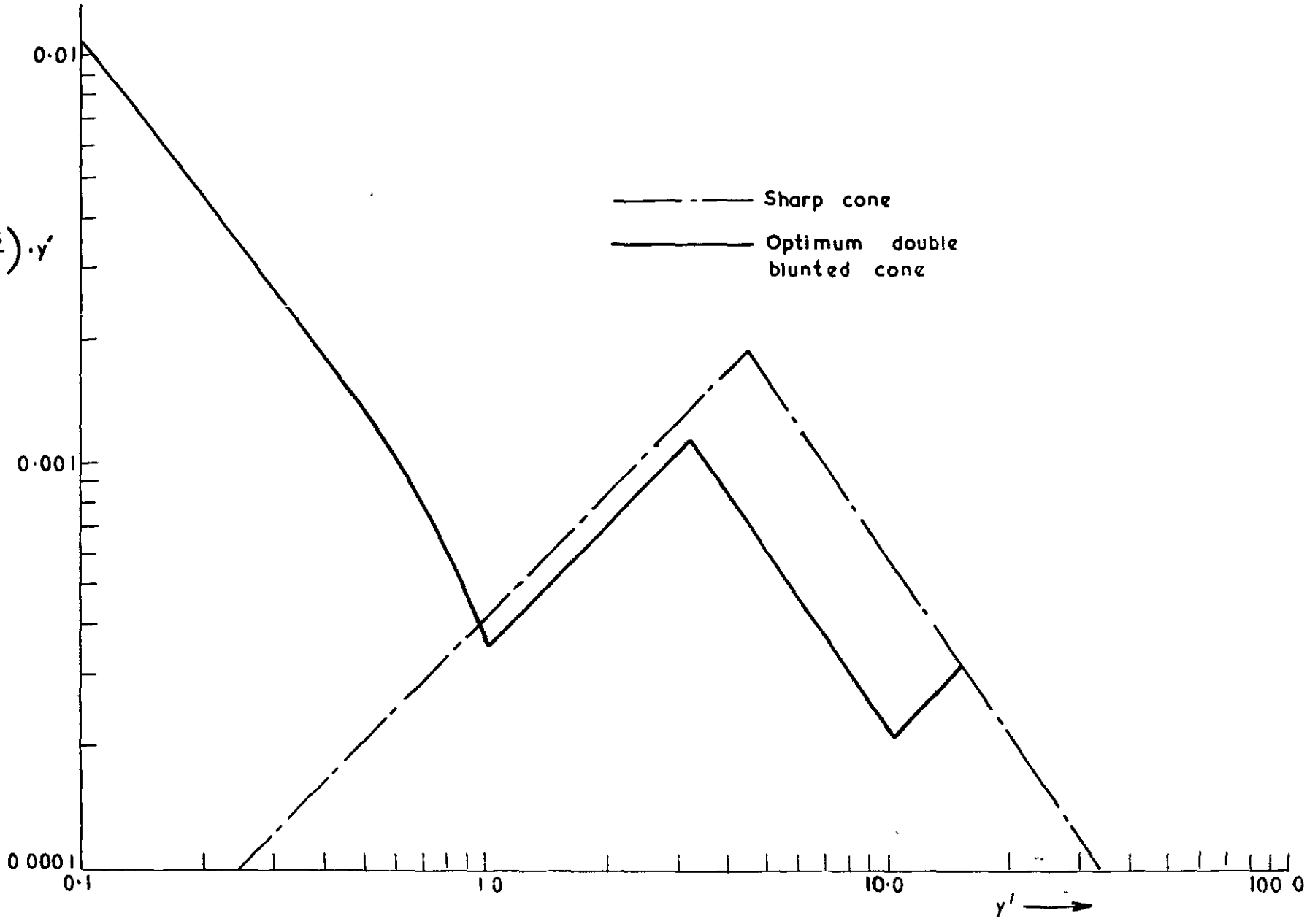

32284
FIG 17

Entropy distributions for two $f = 3$ bodies

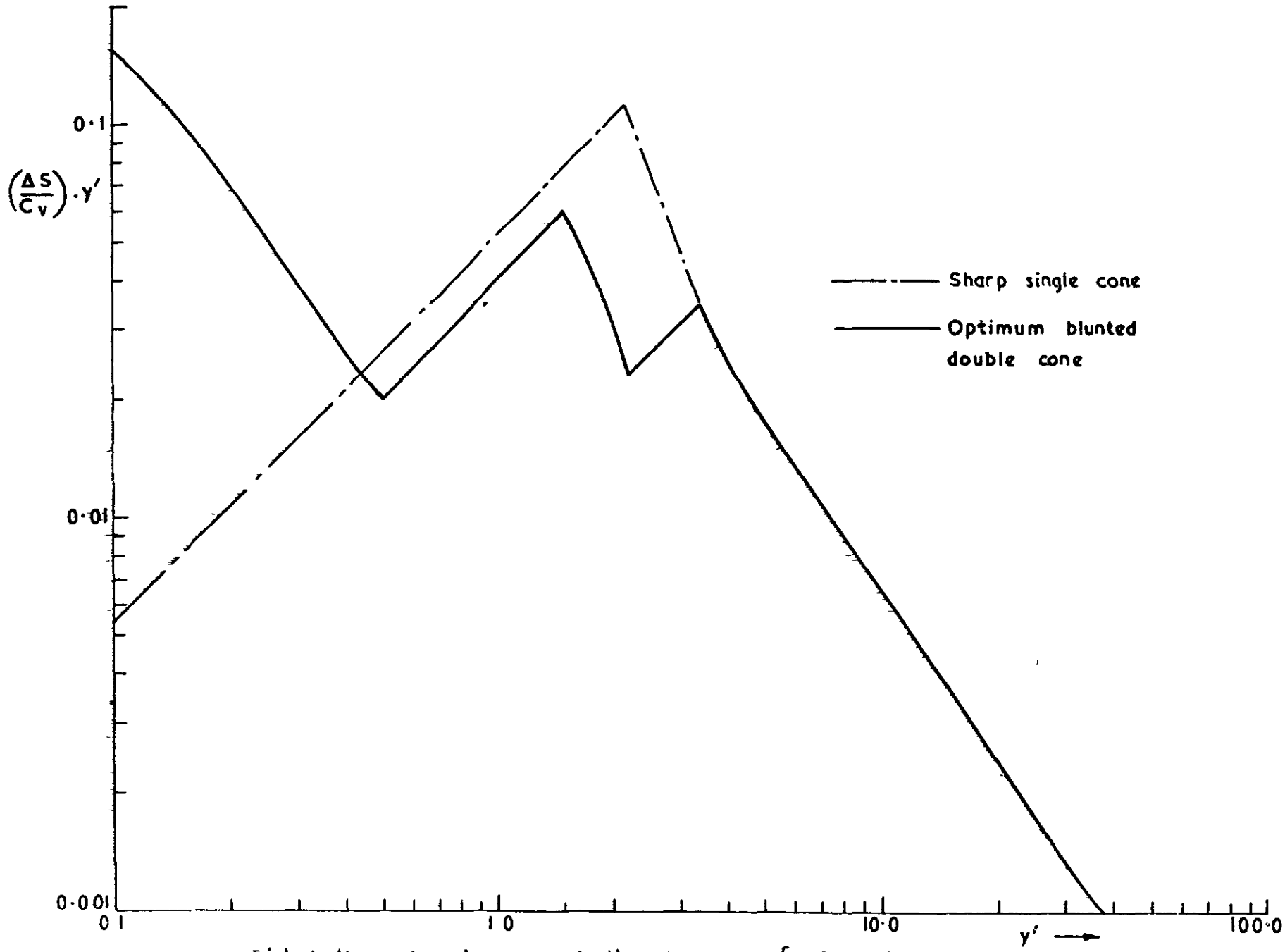

32284
FIG. 19

Distribution of entropy production for two $f = 2$ bodies

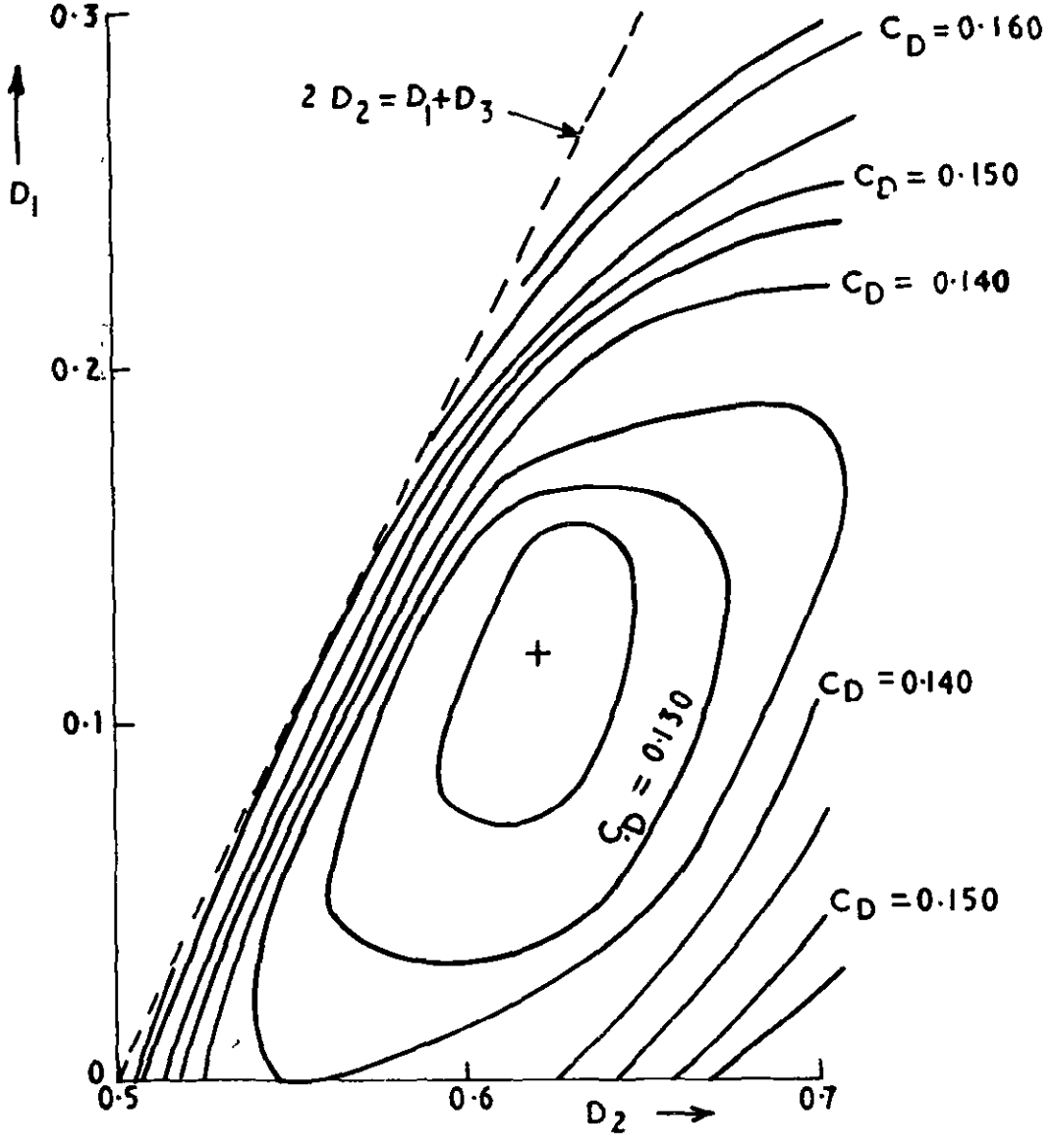

Variation of C_D with D_1 and D_2 for blunted double cones (spherical blunting)

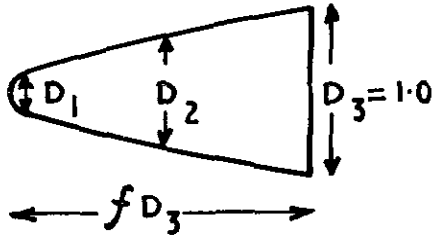

$f = 2$

$M = 3·05$

\+ Denotes optimum body

32284
FIG. 19

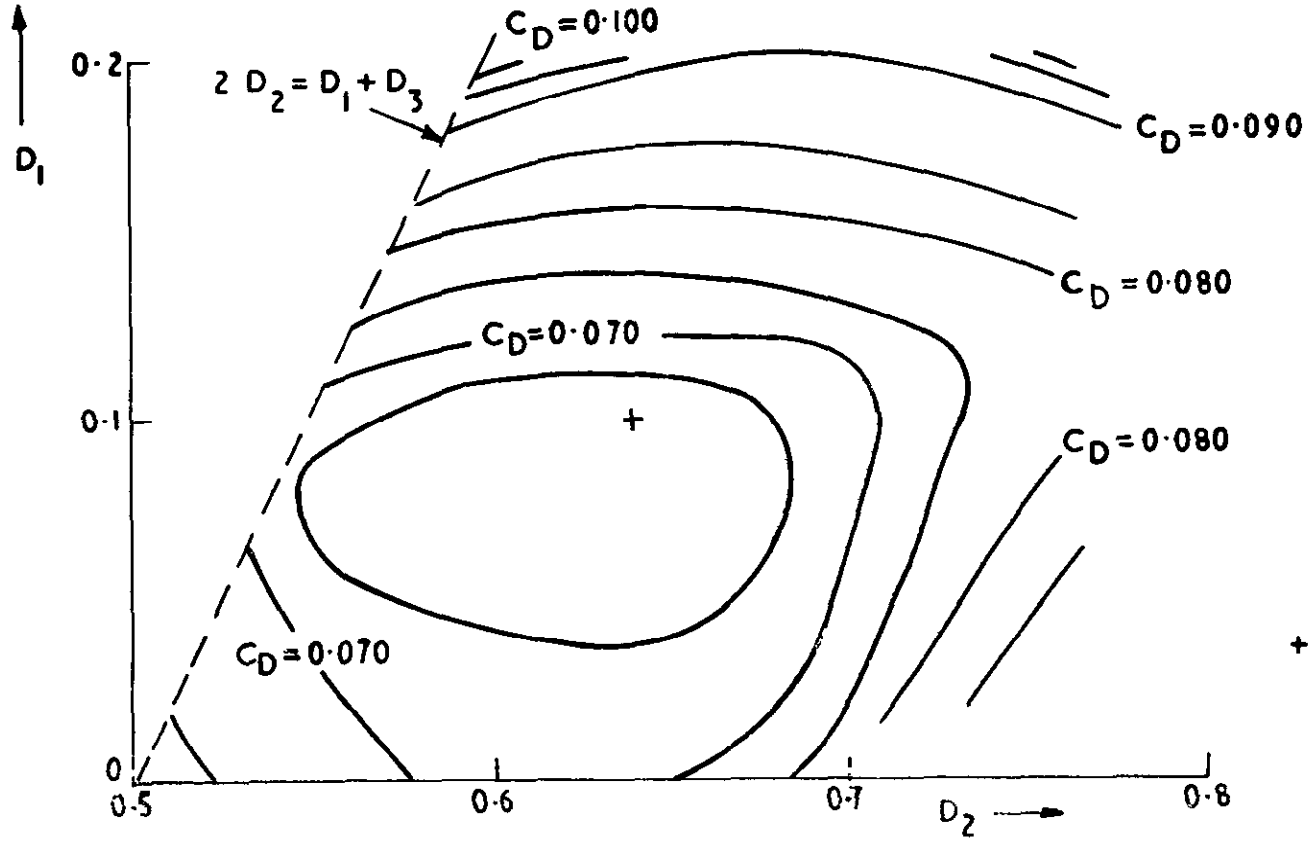

Variation of C_D with D_1 and D_2 for blunted double cones
(spherical blunting)

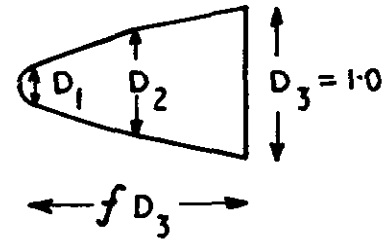

$f = 3$

$M = 3.05$

\+ Denotes optimum body

32284
FIG. 20

3 2284
FIG. 21

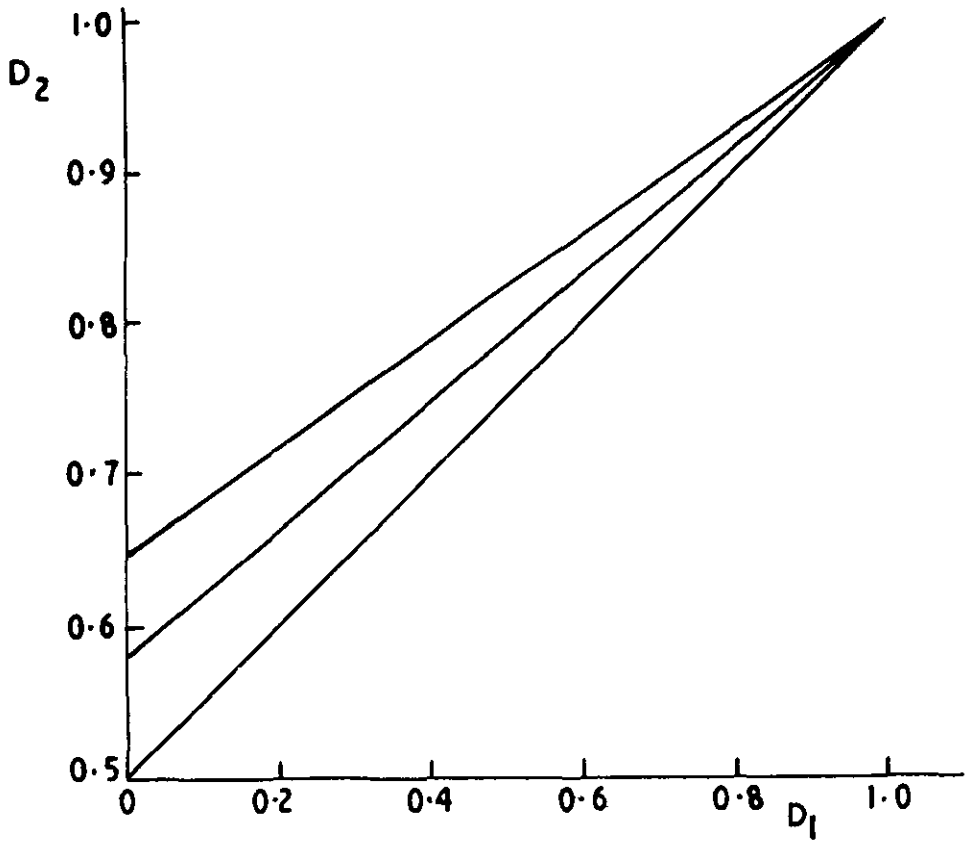

Three "families" of blunted double cones

32284
FIG 22

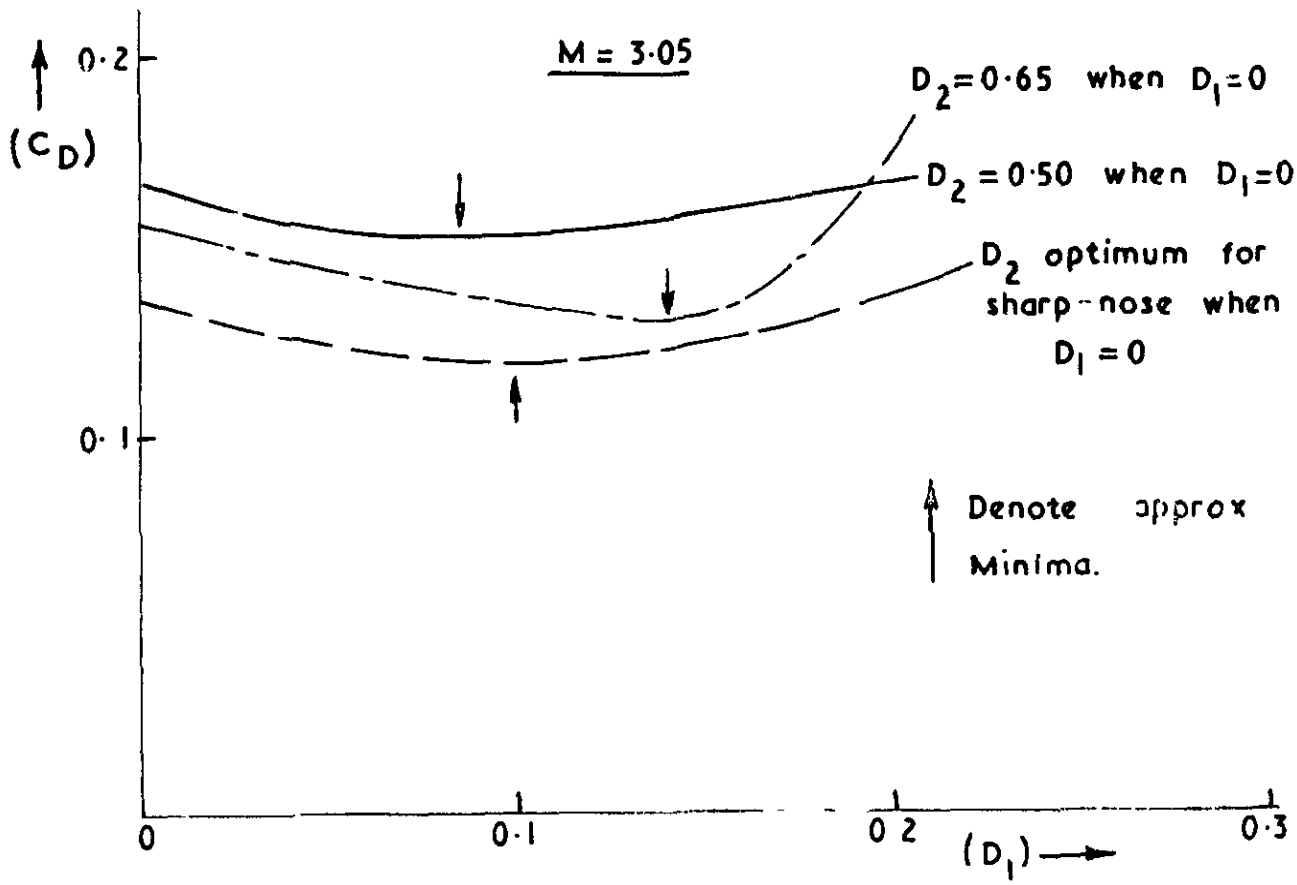

Variation of C_D with D_1 for three families of spherically blunted double cones of fineness ratio = 2

32284
FIG. 23

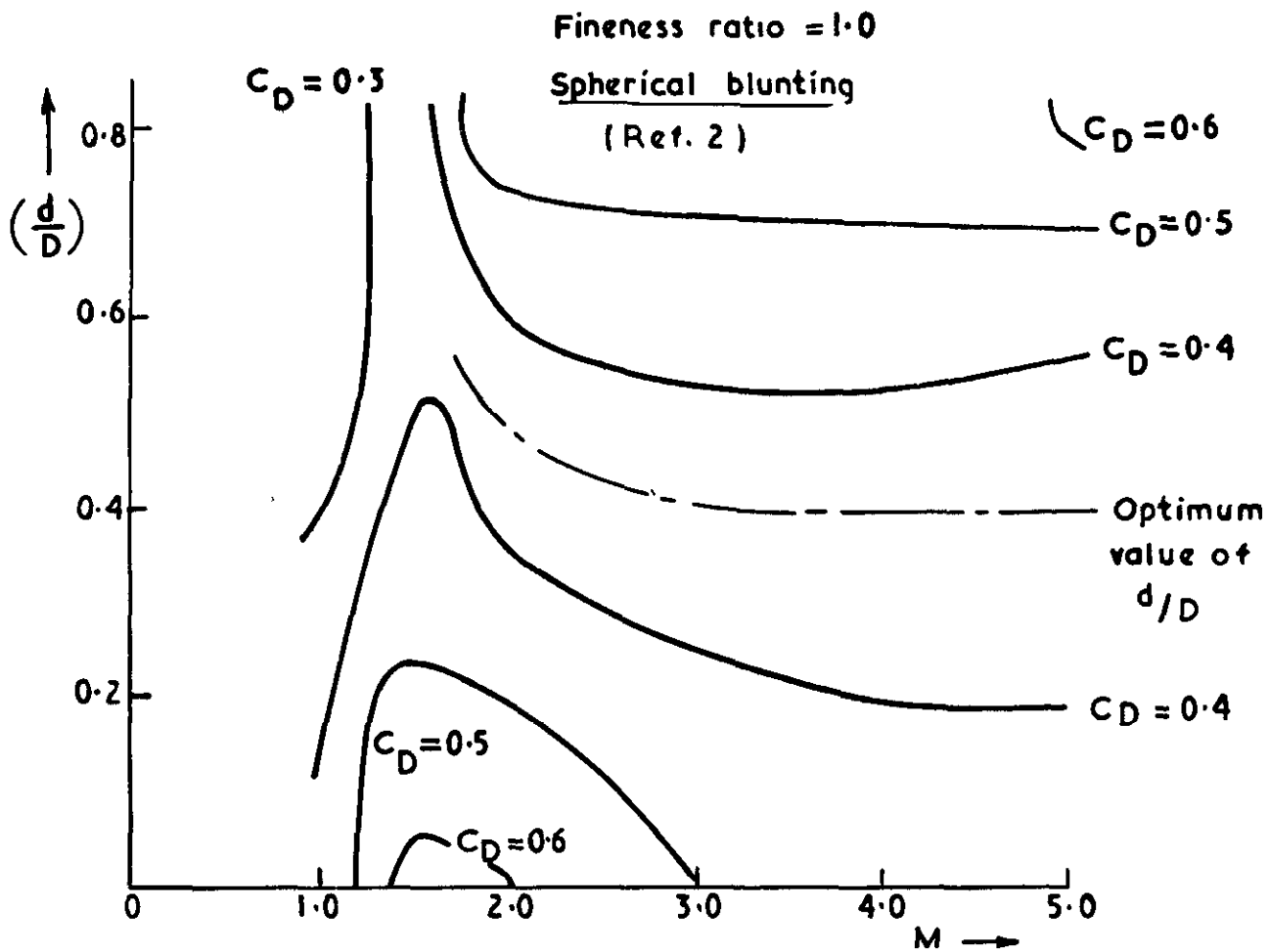

Variation of C_D with bluntness ratio and Mach number

3 2 284
FIG 24

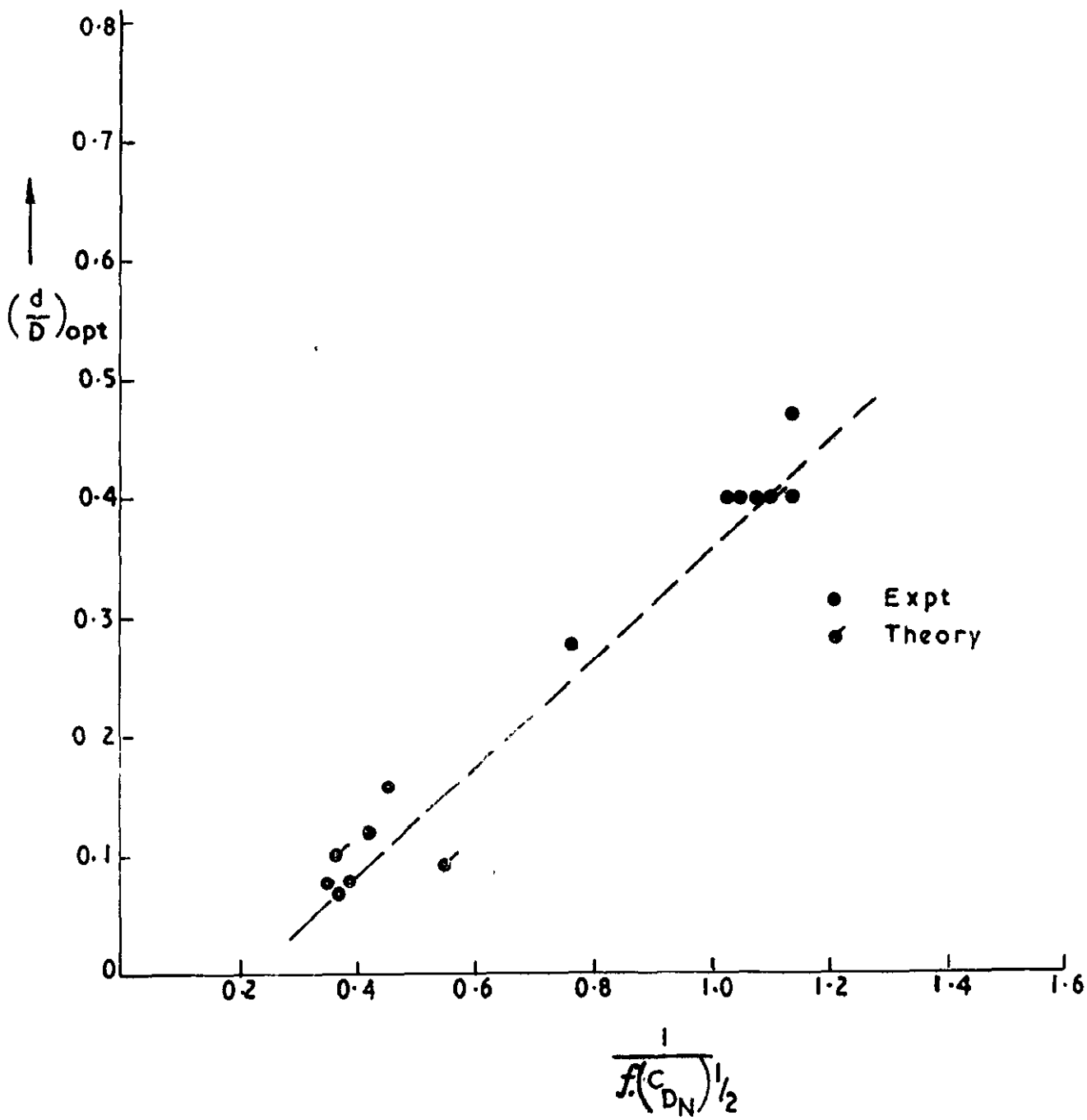

Correlation of optimum nose blunting (spherically blunted single cones)

32284
FIG. 25

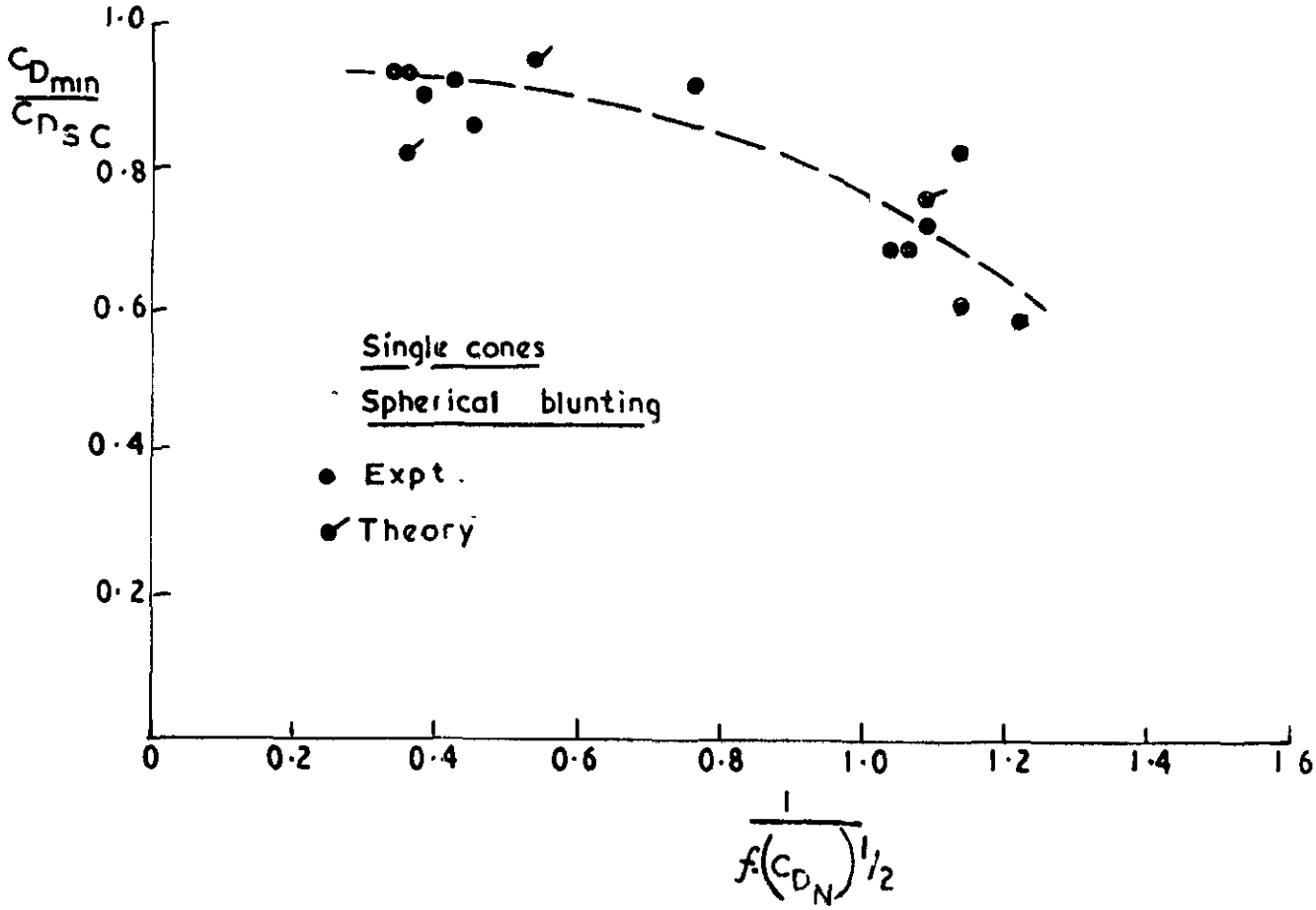

Correlation of maximum drag reduction by spherical nose blunting

32284
FIG 26

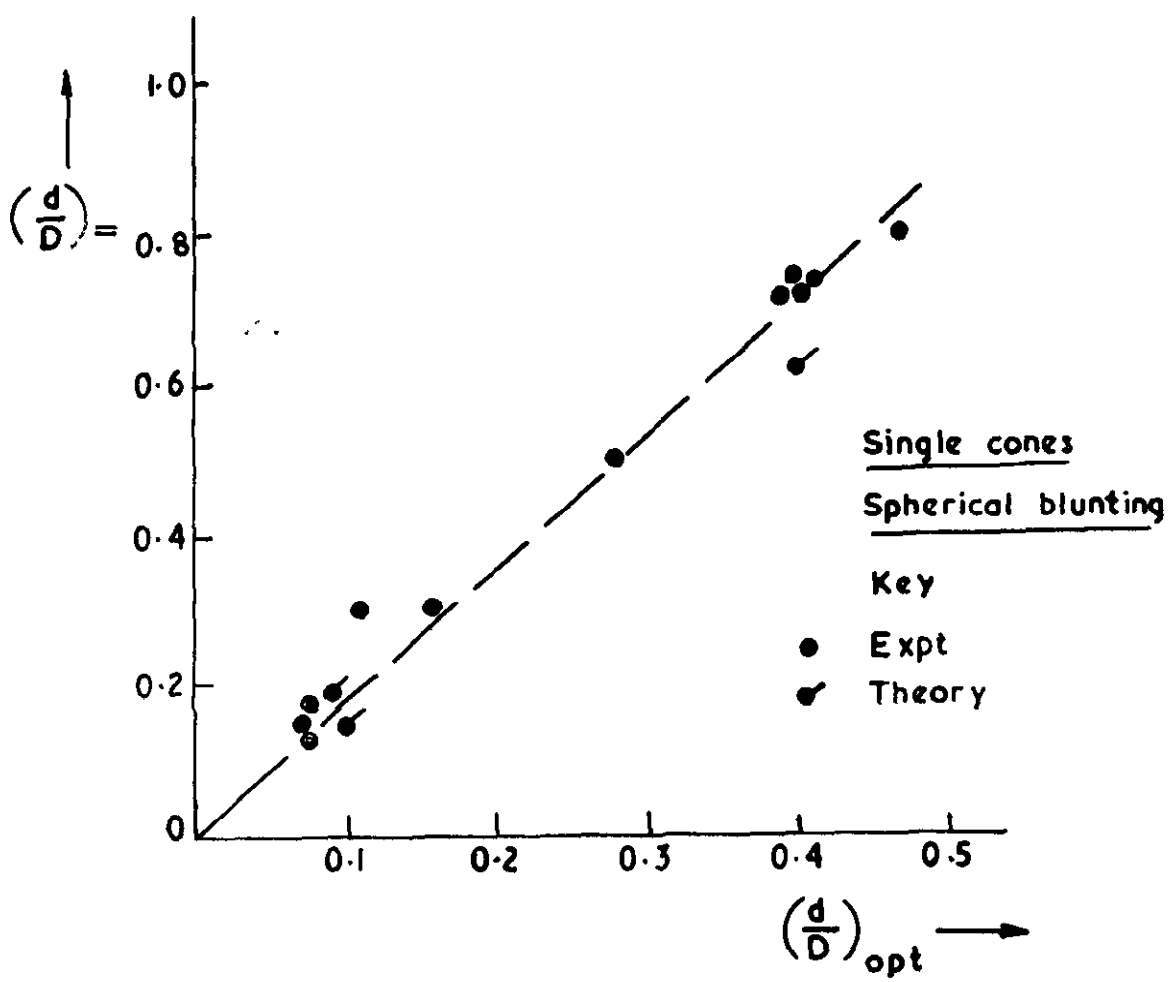

Correlation of two characteristic bluntness ratios

32284
FIG. 27

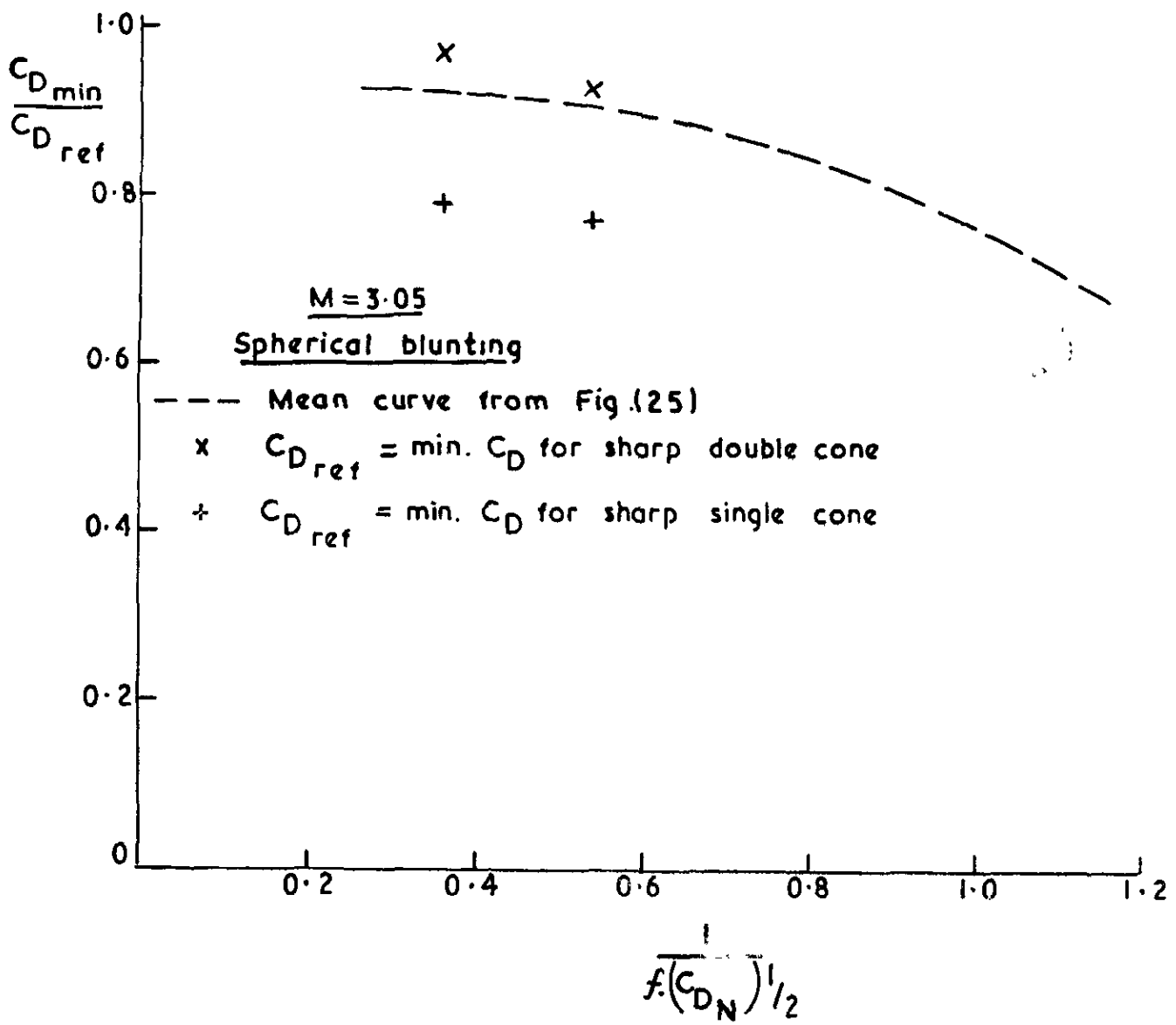

Drag reduction for optimum double cones.

32284

FIG. 28

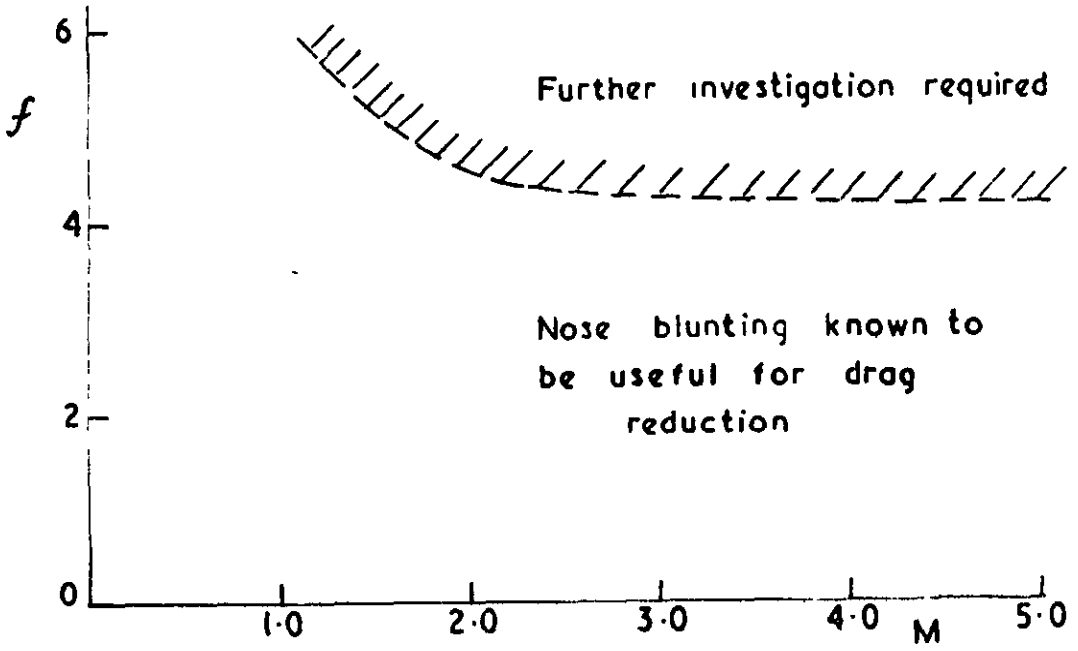

Current bounds of utility of spherical nose blunting for drag reduction

32284
FIG. 29

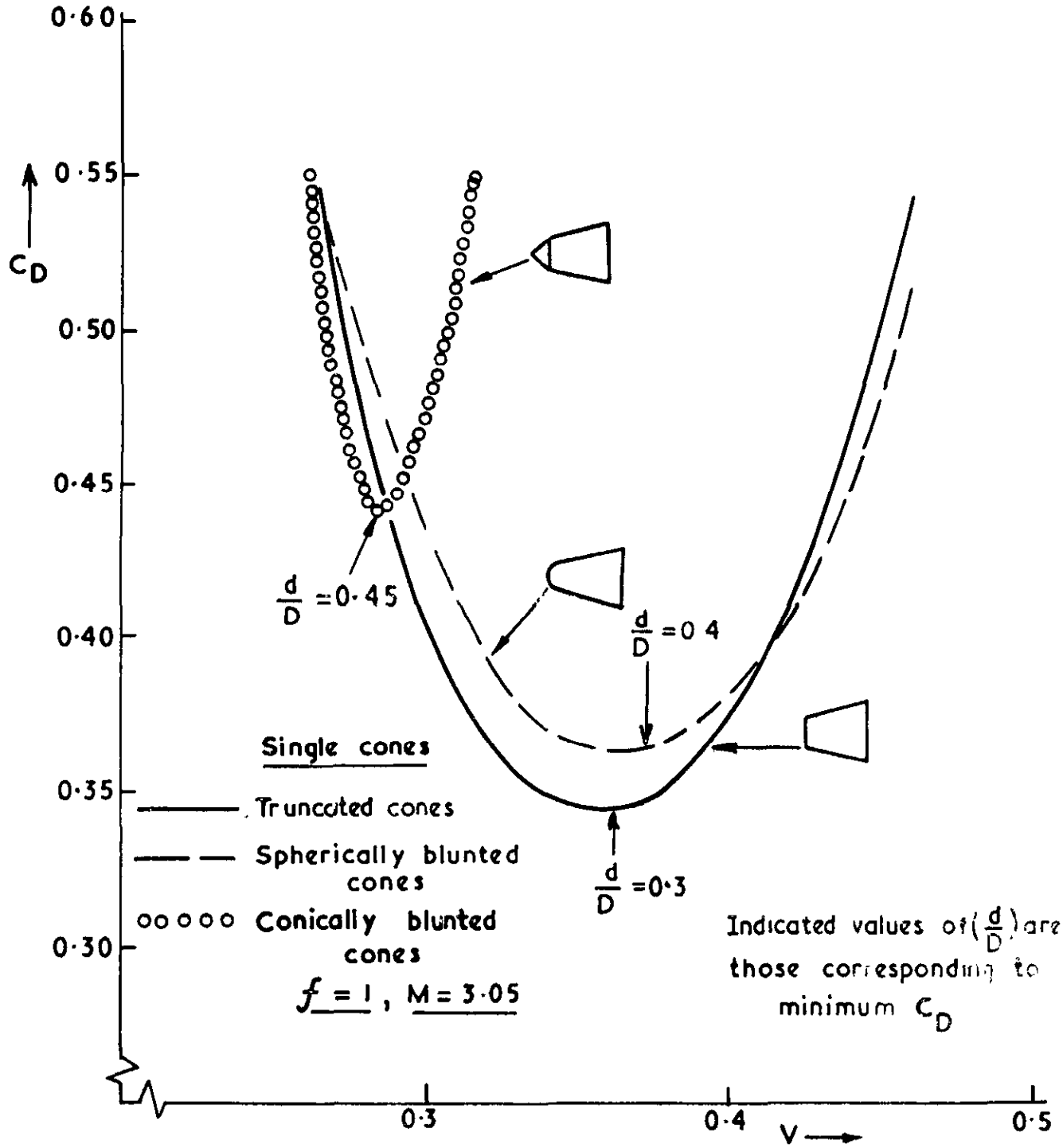
0·60
0·55
0·50
0·45
0·40
0·35
0·30
C_D
$\frac{d}{D}$ =0·45
$\frac{d}{D}$ =0 4
$\frac{d}{D}$ =0·3
Single cones
Truncated cones
Spherically blunted cones
Conically blunted cones
f = 1 , M = 3·05
Indicated values of $(\frac{d}{D})$ are those corresponding to minimum C_D
0·3
0·4
0·5
V

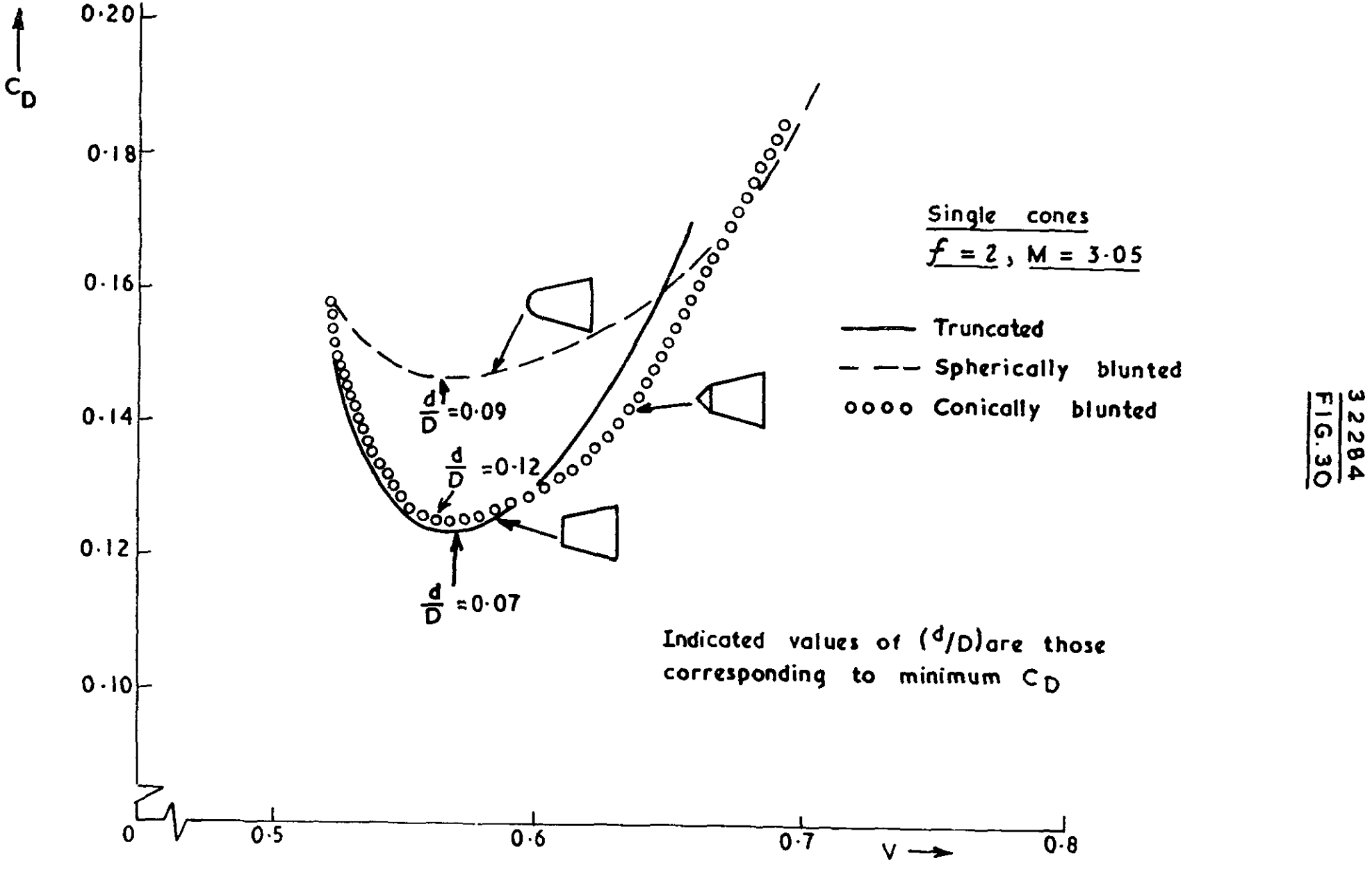
C_D
0·20
0·18
0·16
0·14
0·12
0·10
0
0·5
0·6
0·7
0·8
V →
Single cones
f = 2 , M = 3·05
Truncated
Spherically blunted
Conically blunted
d/D =0·09
d/D =0·12
d/D =0·07
Indicated values of (d/D) are those corresponding to minimum C_D

3·2284
FIG. 30

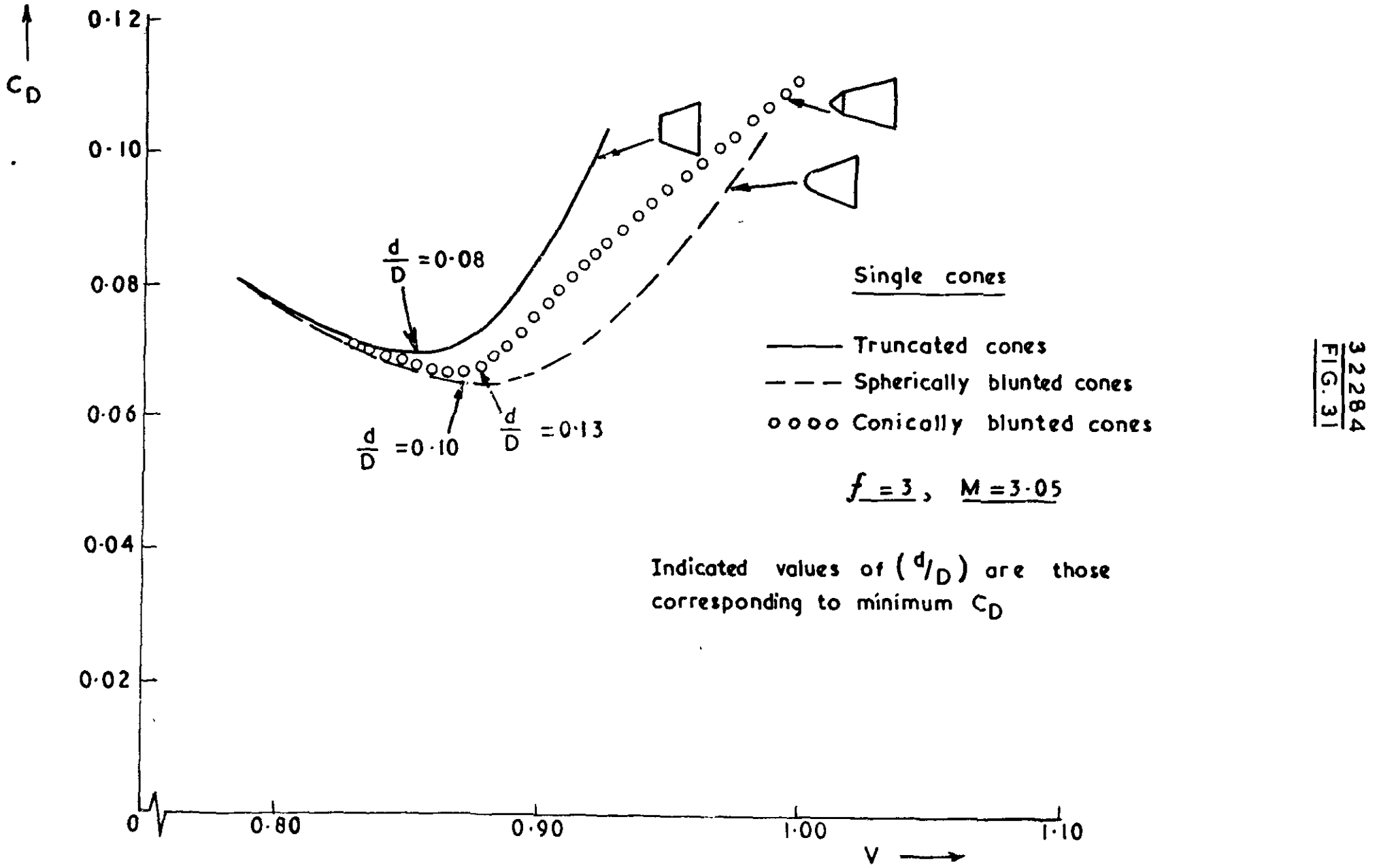
C_D
0·12
0·10
0·08
0·06
0·04
0·02
0
0·80
0·90
1·00
1·10
V
$\frac{d}{D}$ =0·08
$\frac{d}{D}$ =0·10
$\frac{d}{D}$ =0·13
Single cones
Truncated cones
Spherically blunted cones
Conically blunted cones
f = 3, M = 3·05
Indicated values of ($^d/_D$) are those corresponding to minimum C_D

32284
FIG. 31

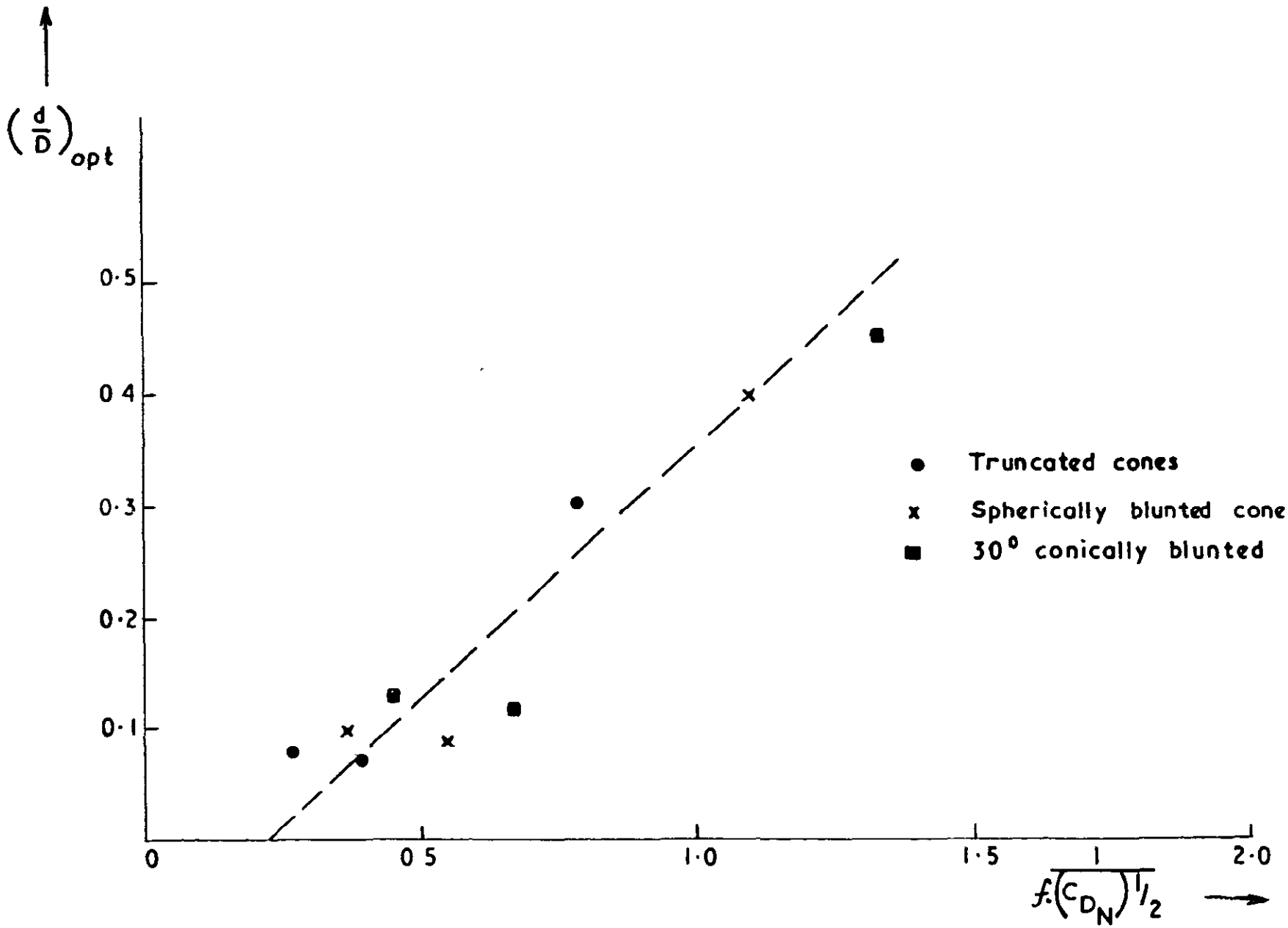

32284
FIG. 32

Correlation of optimum nose blunting

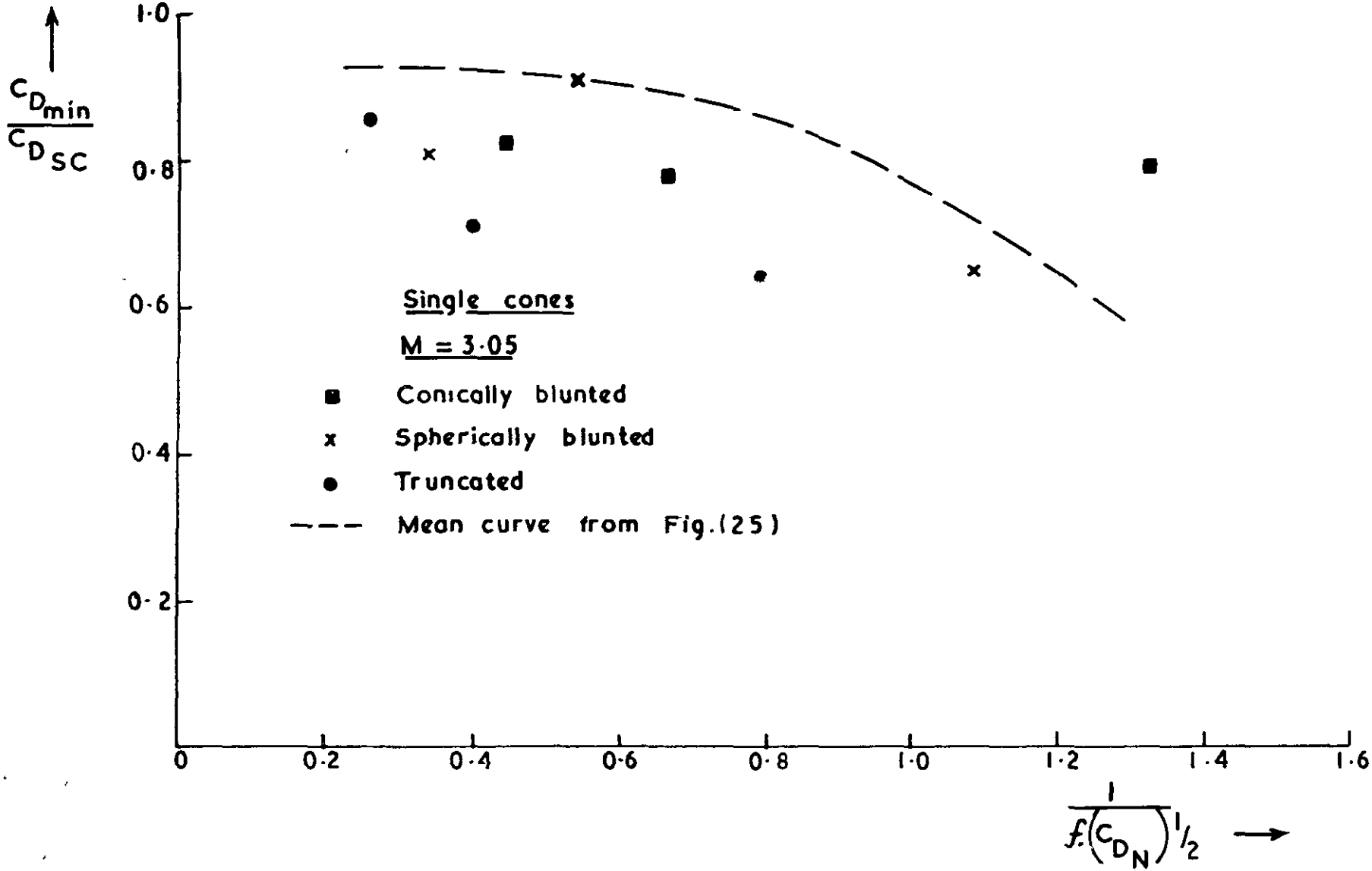

32284
FIG.33

Maximum drag reduction with various forms of blunting

32284
FIG.34

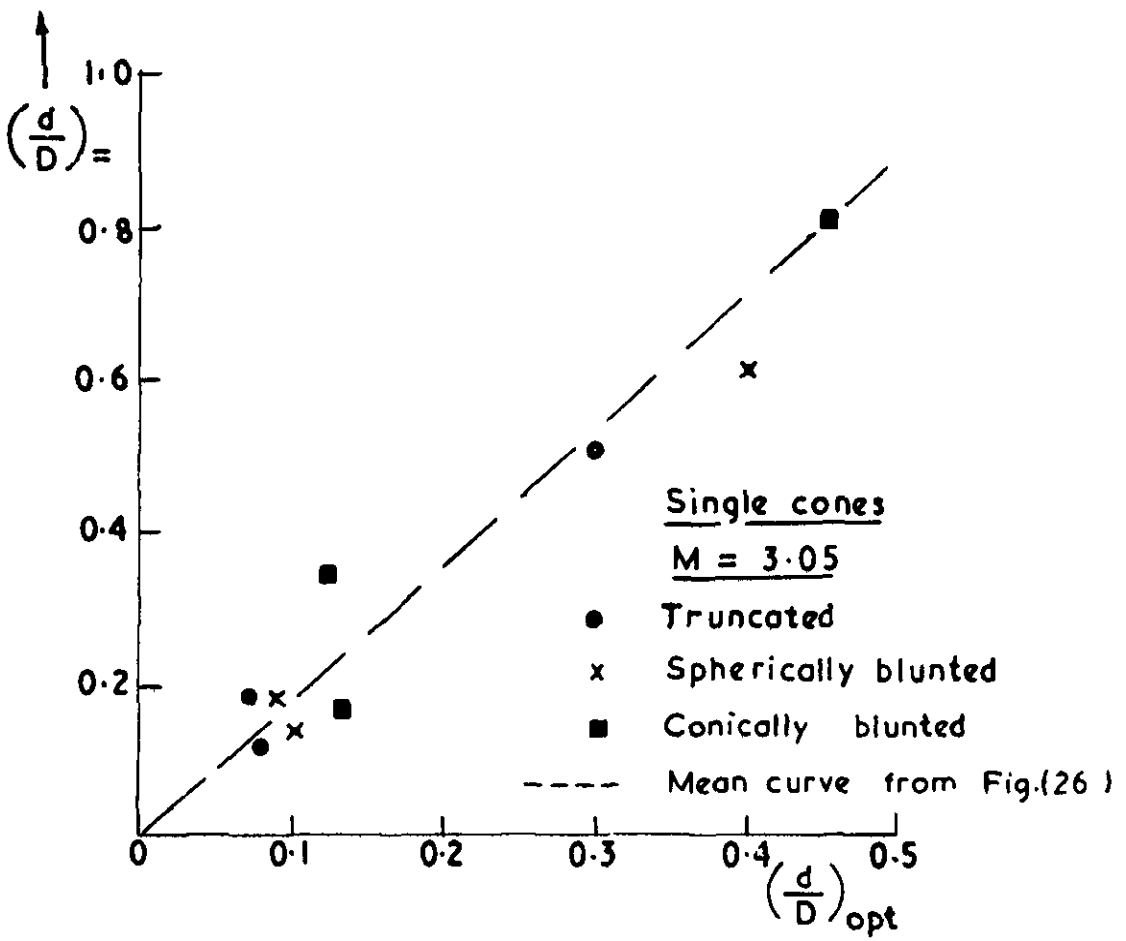

Correlation of two characteristic bluntness ratios

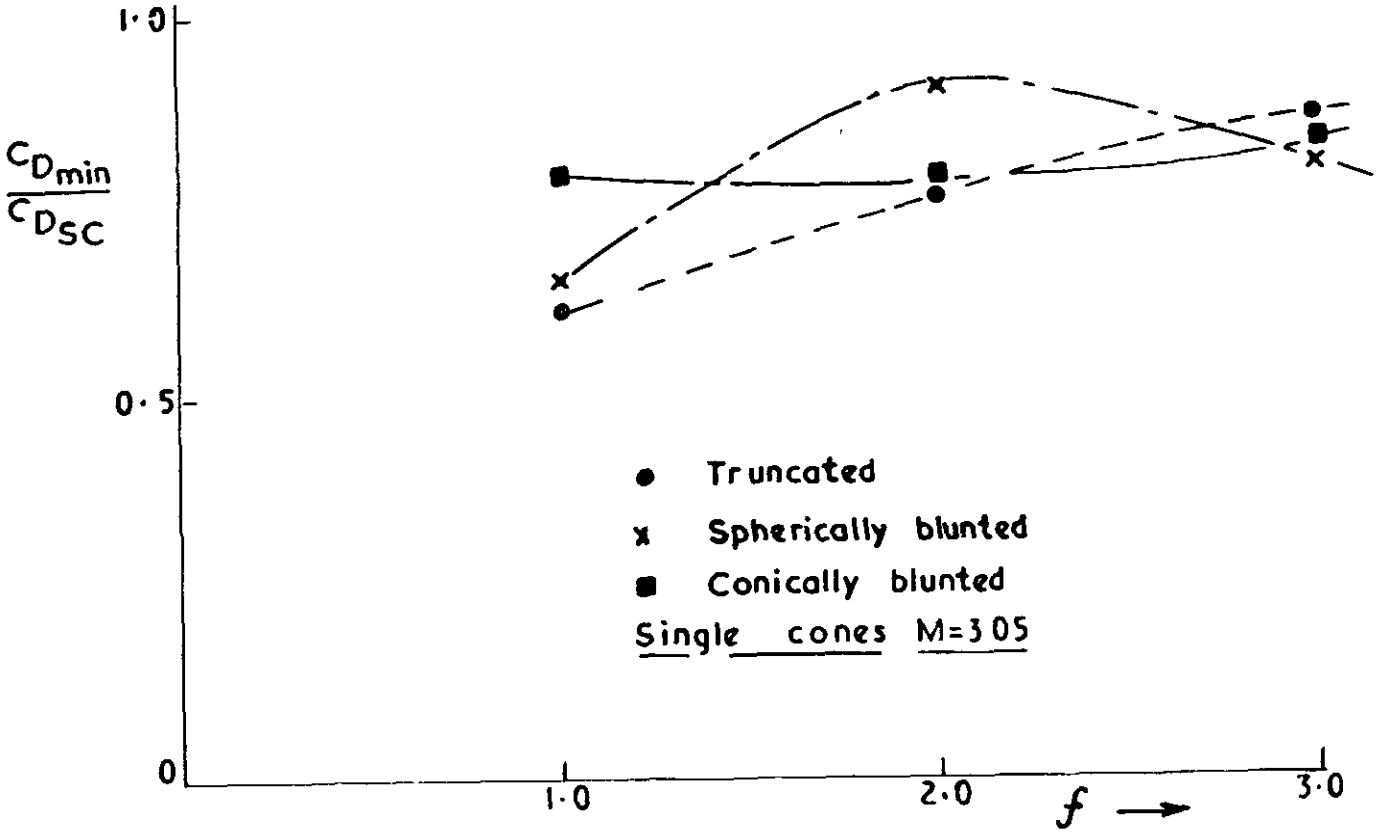

Relative merits of different forms of blunting

32284
FIG. 35

32284
FIG.36

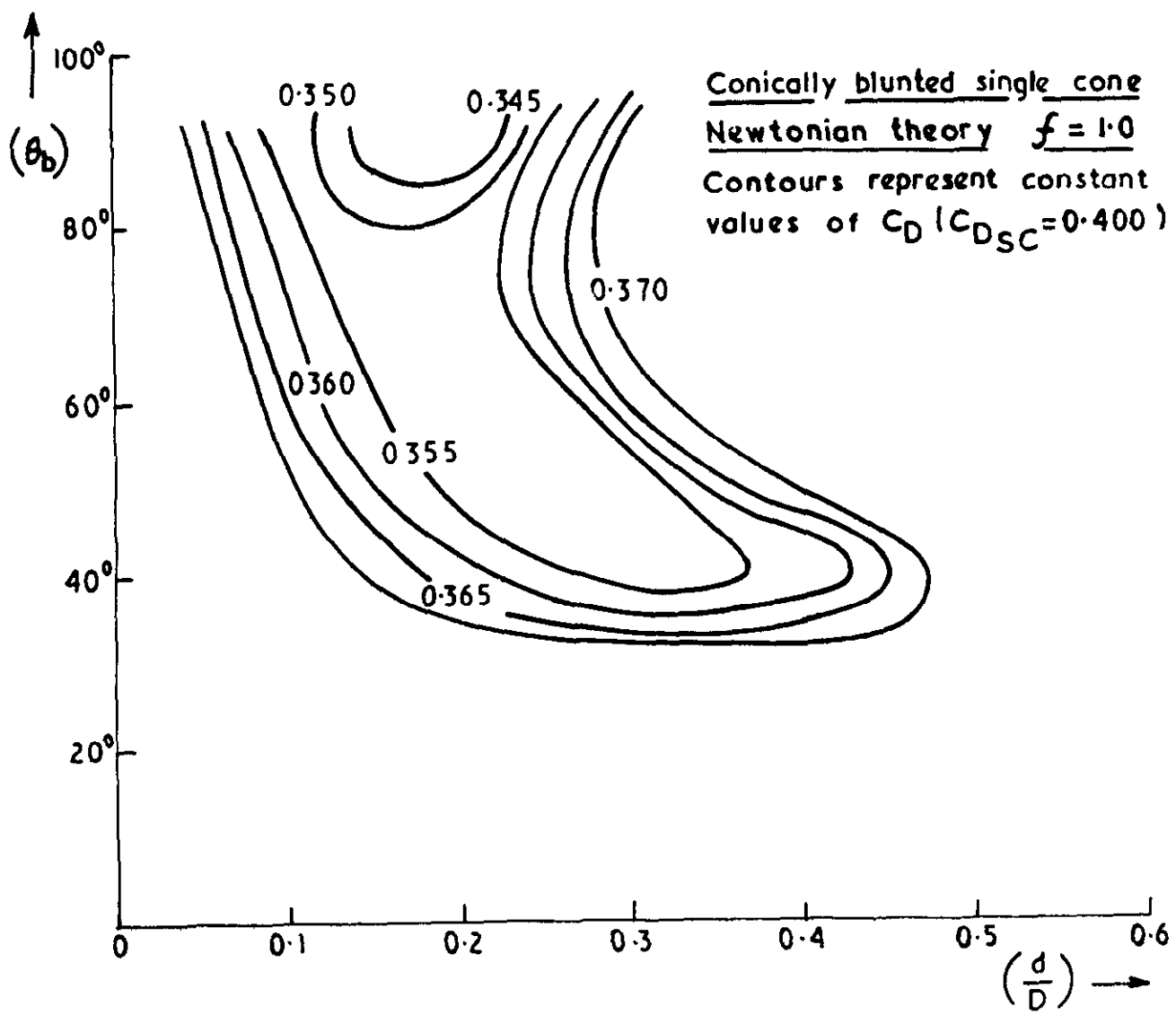
Conically blunted single cone
Newtonian theory $f = 1.0$
Contours represent constant values of C_D ($C_{D_{SC}} = 0.400$)
(θ_b)
100°
80°
60°
40°
20°
0·350
0·345
0·370
0360
0355
0·365
0
0·1
0·2
0·3
0·4
0·5
0·6
$(\frac{d}{D})$ →

32284
FIG. 37

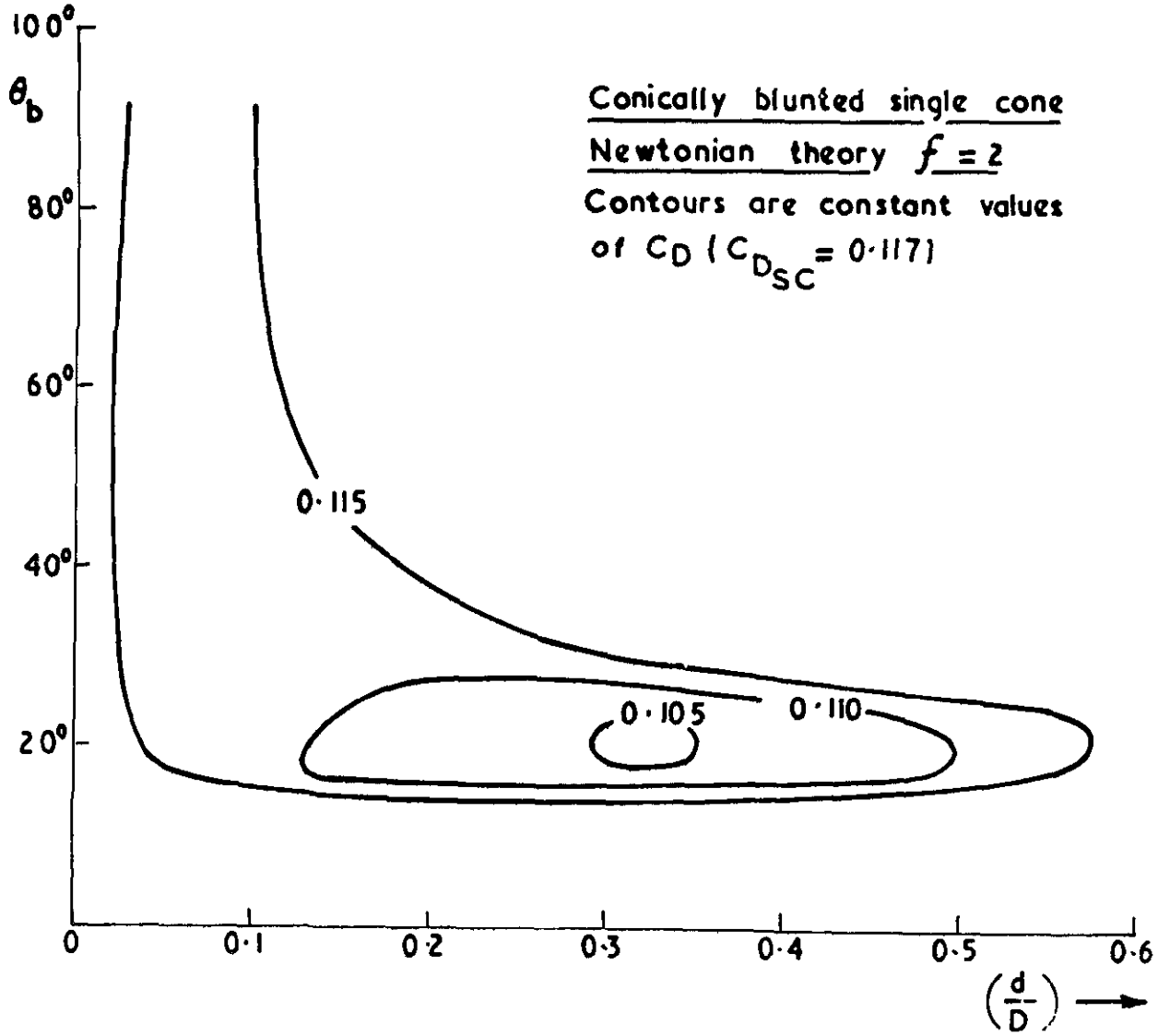
100°
θ_b
80°
60°
40°
20°
0
0·1
0·2
0·3
0·4
0·5
0·6
$\left(\frac{d}{D}\right)$
Conically blunted single cone
Newtonian theory $f = 2$
Contours are constant values
of C_D ($C_{D_{SC}} = 0·1171$)
0·115
0·110
0·105

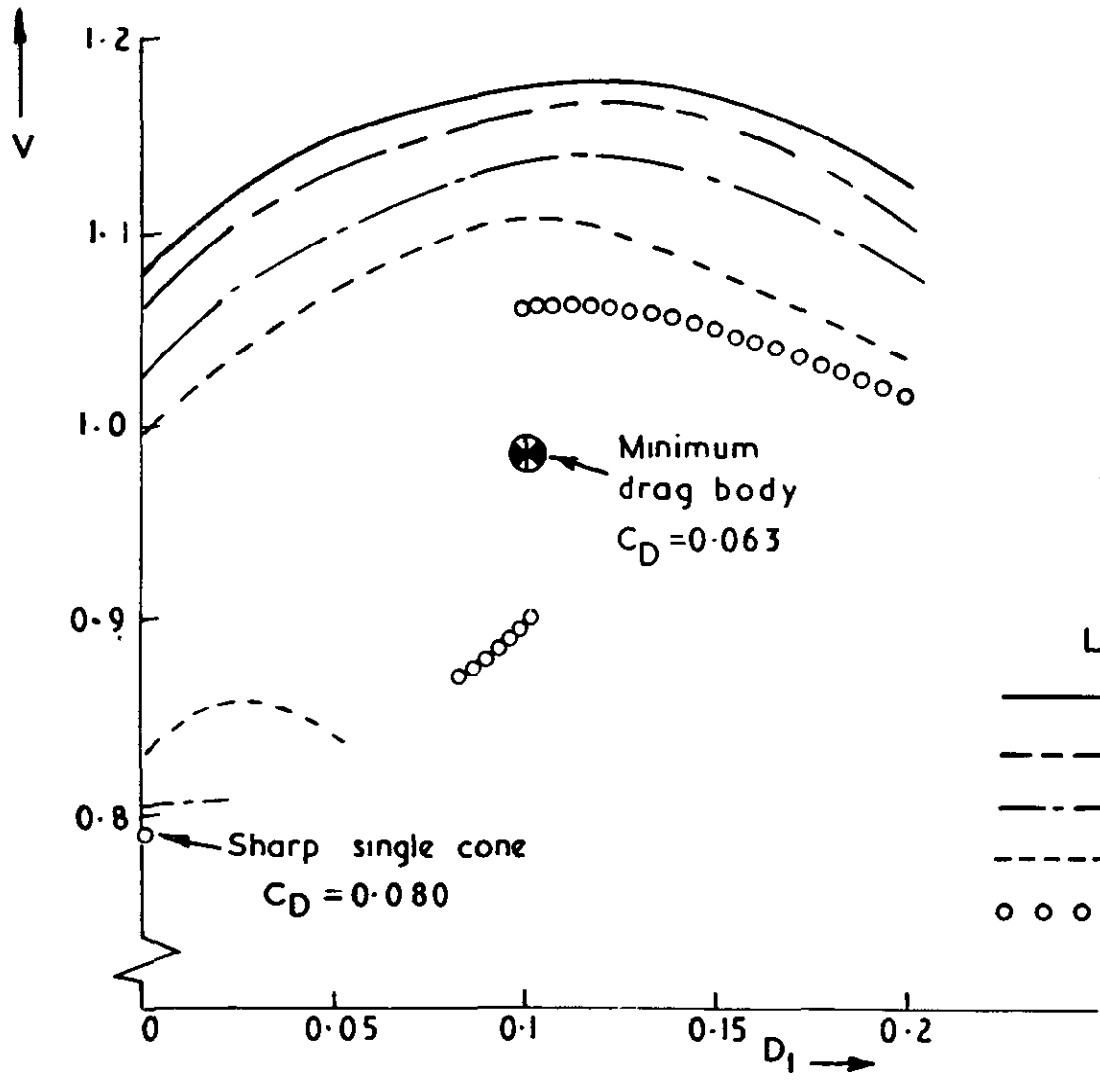

$f = 3$

M = 3·05

N.B. for a sharp cone

V = 0·79

Legend	Value of C_D
———	0·085
– – — – –	0·080
— · — · —	0·075
- - - - - - - -	0·070
o o o o o o	0·065

32284
FIG 38

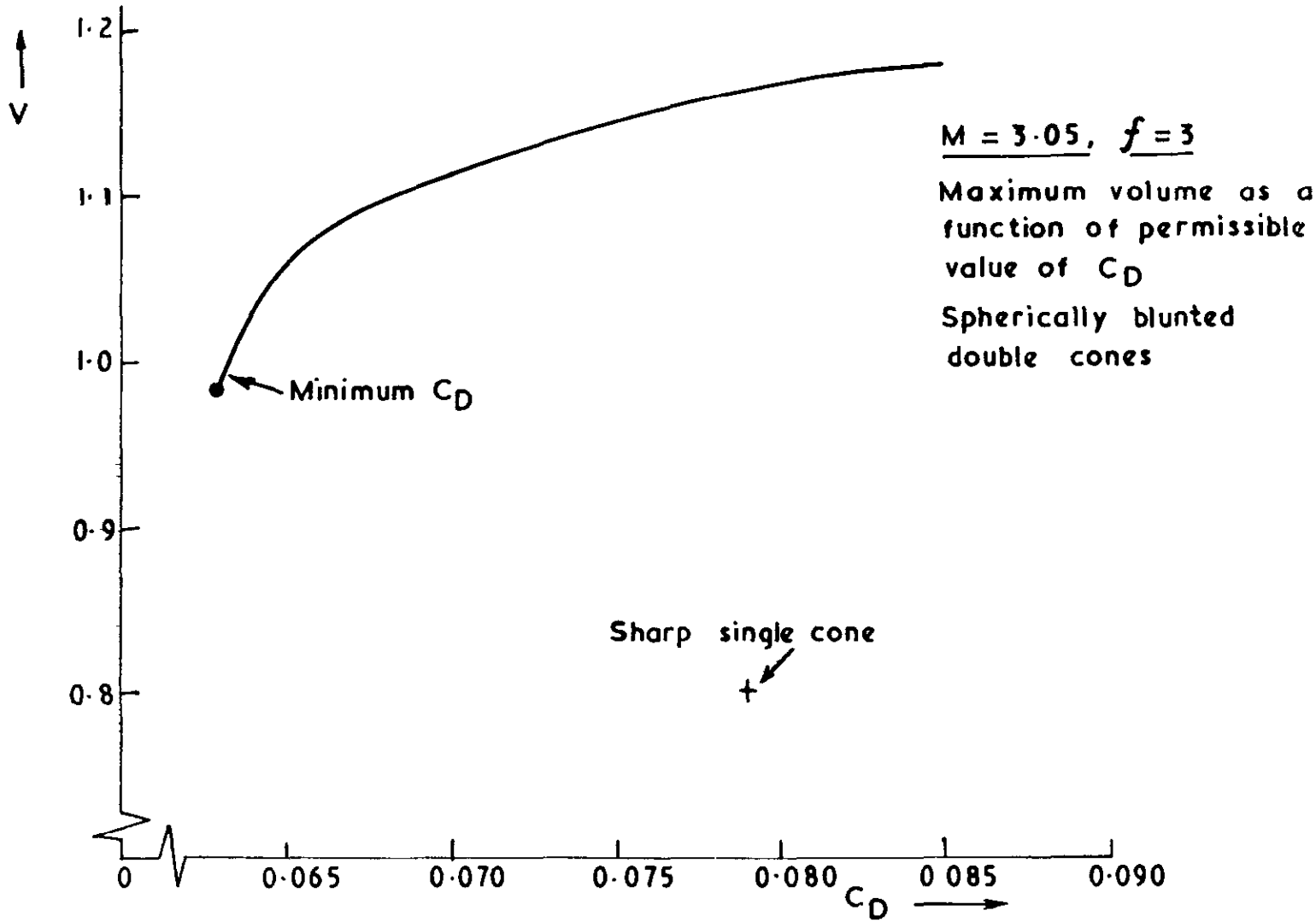
V
1·2
1·1
1·0
0·9
0·8
M = 3·05, f = 3
Maximum volume as a function of permissible value of C_D
Spherically blunted double cones
Minimum C_D
Sharp single cone
0
0·065
0·070
0·075
0·080
0 085
0·090
C_D

32284
FIG. 39

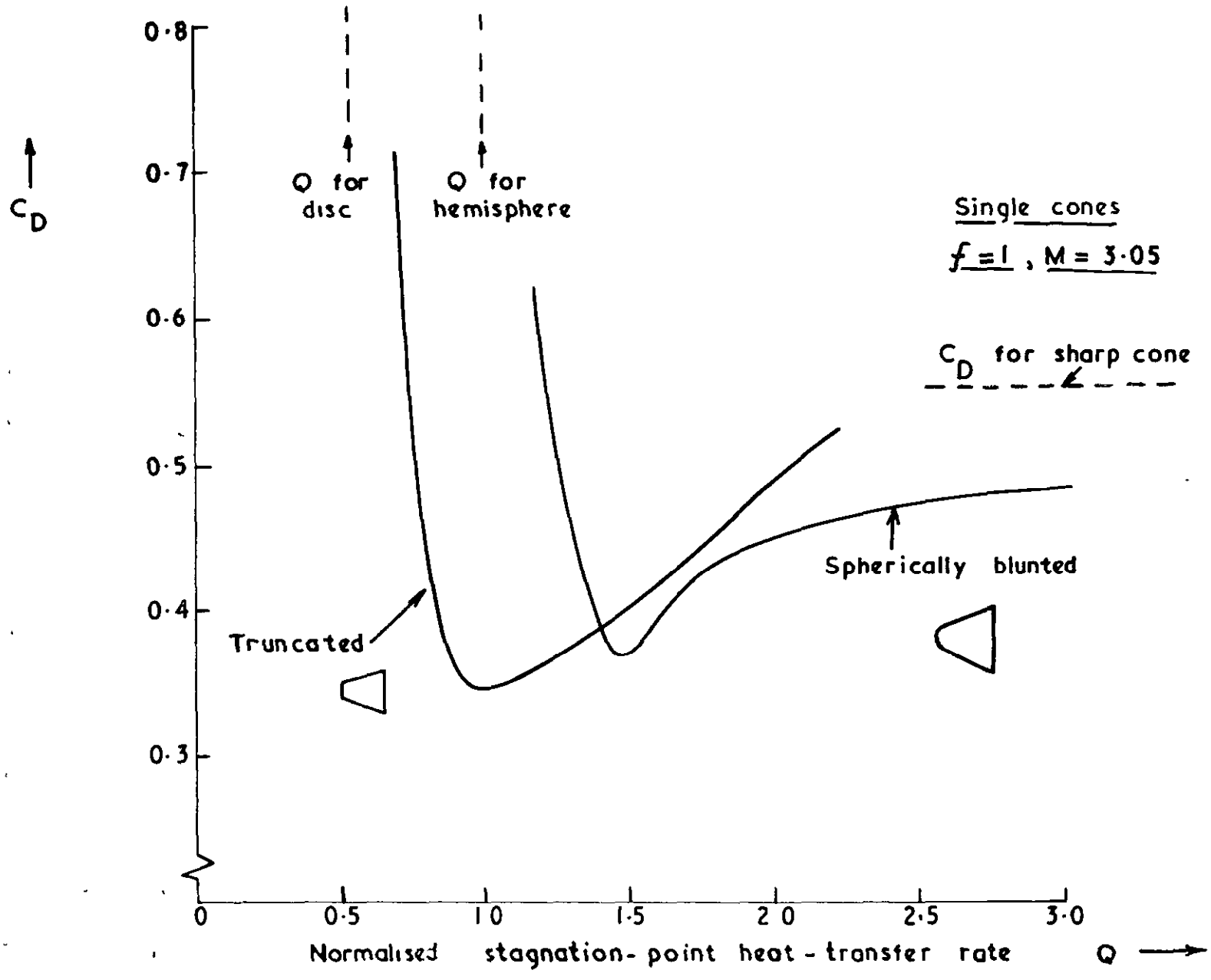

32284
FIG. 40

Variation of drag with stagnation-point heat-transfer rate

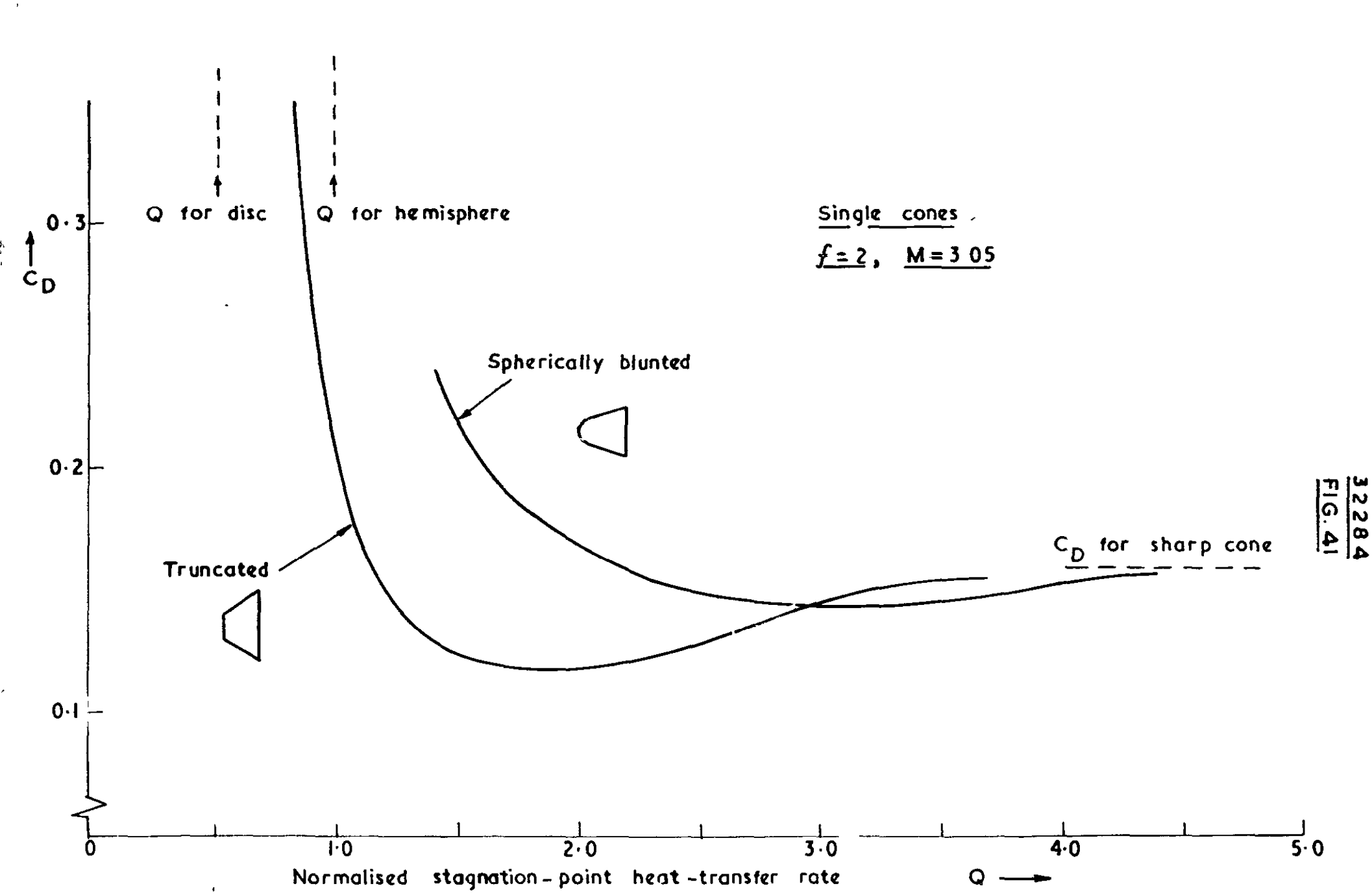

32284
FIG. 41

Variation of drag with stagnation-point heat-transfer rate

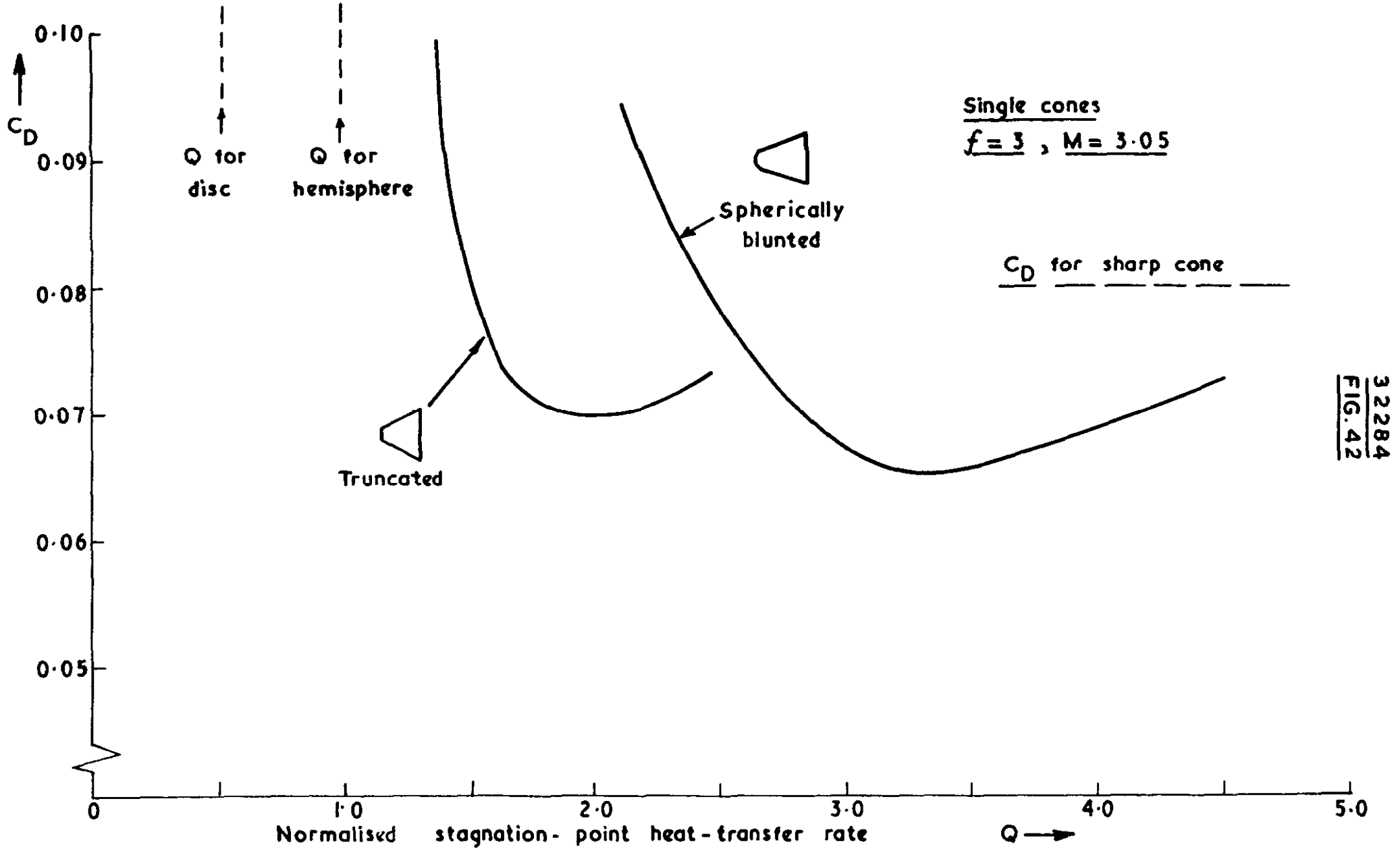

32284
FIG. 42

Variation of drag with stagnation-point heat-transfer rate

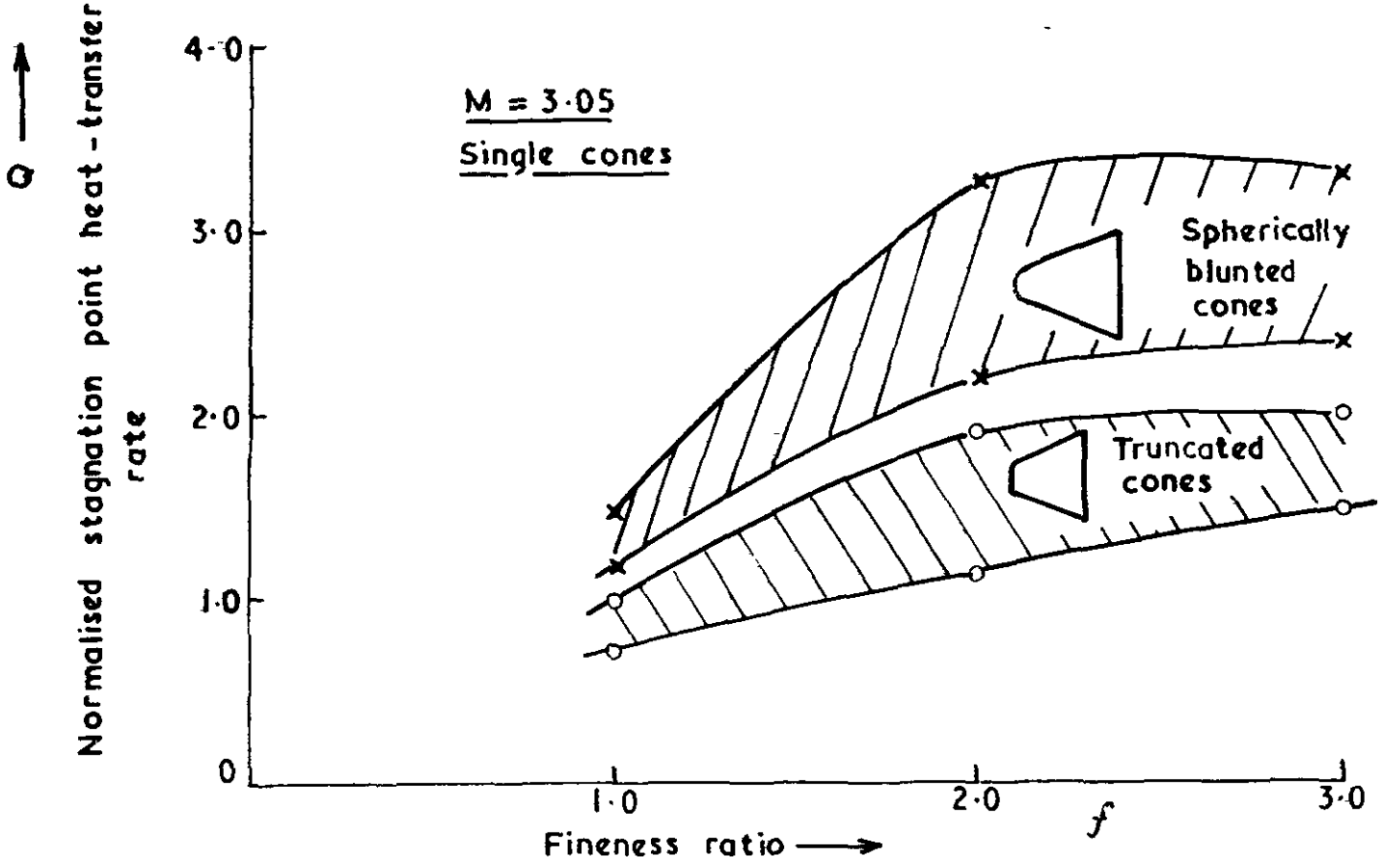

Typical practical bounds to stagnation point heat-transfer rate without excessive drag penalty

32284
FIG. 43

32284
FIG.44

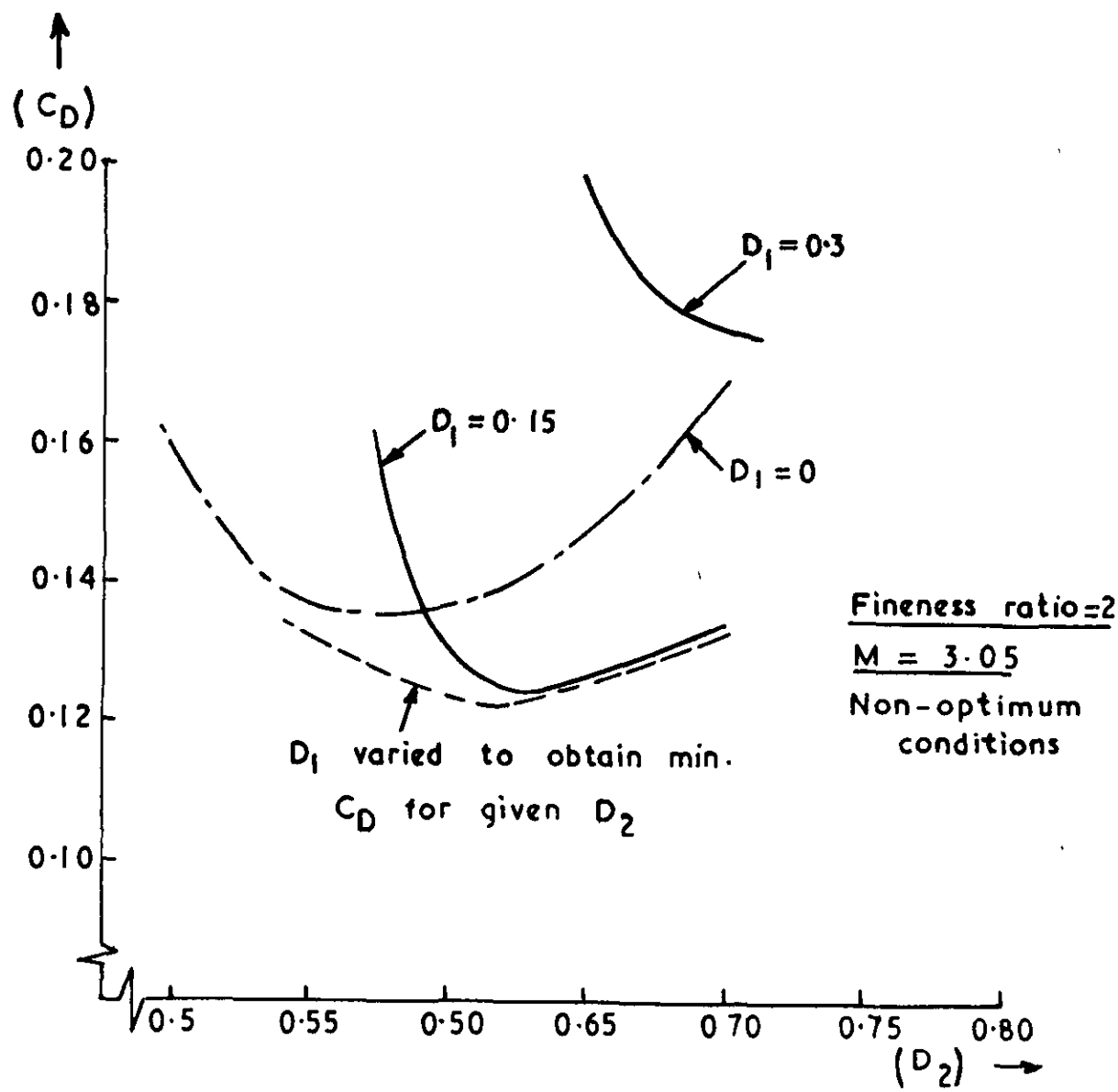

Effect of fixing D_2 at a given value

32284
FIG. 45

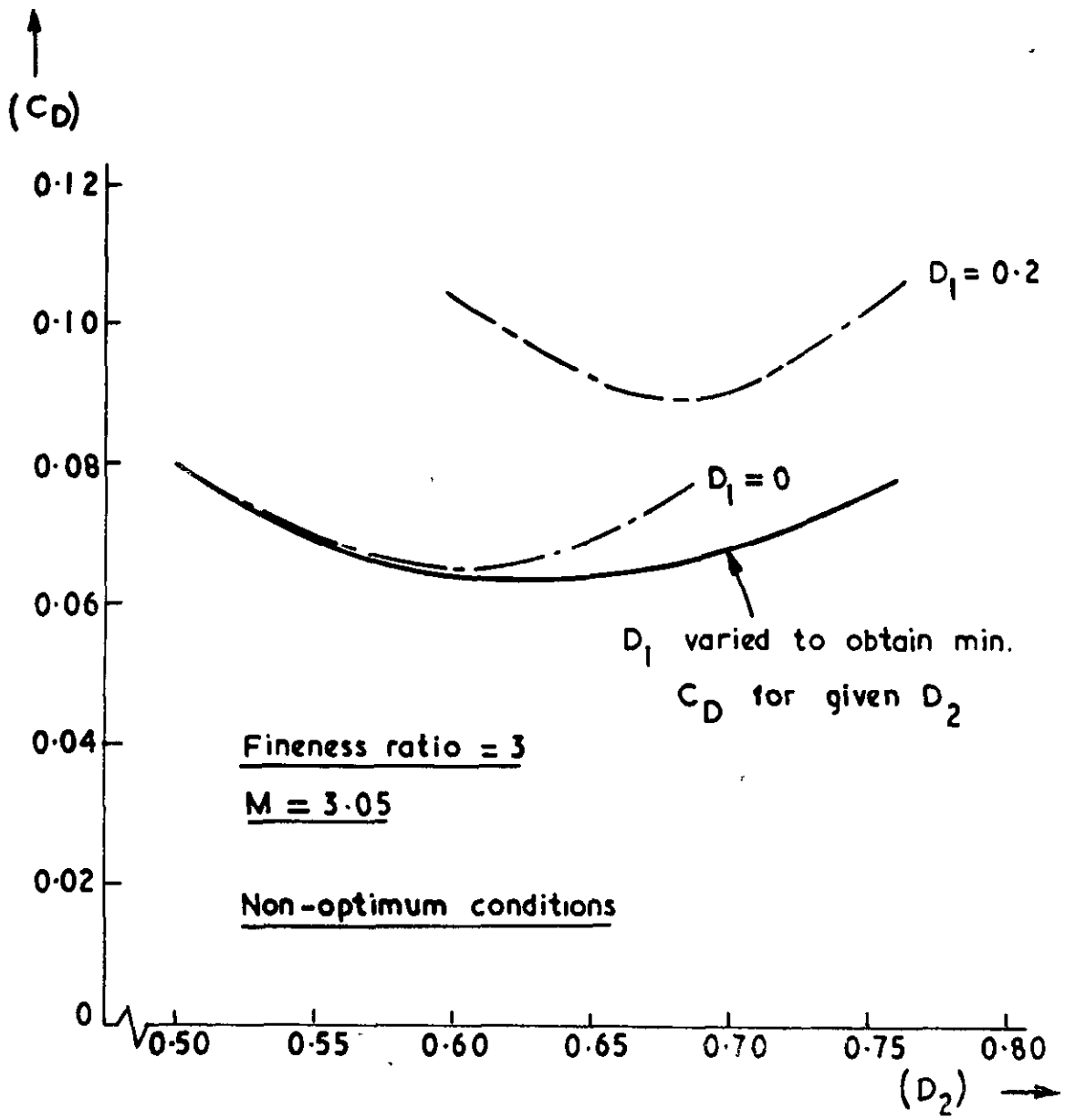

Effect of fixing D_2 at a given value

32284
FIG. 46

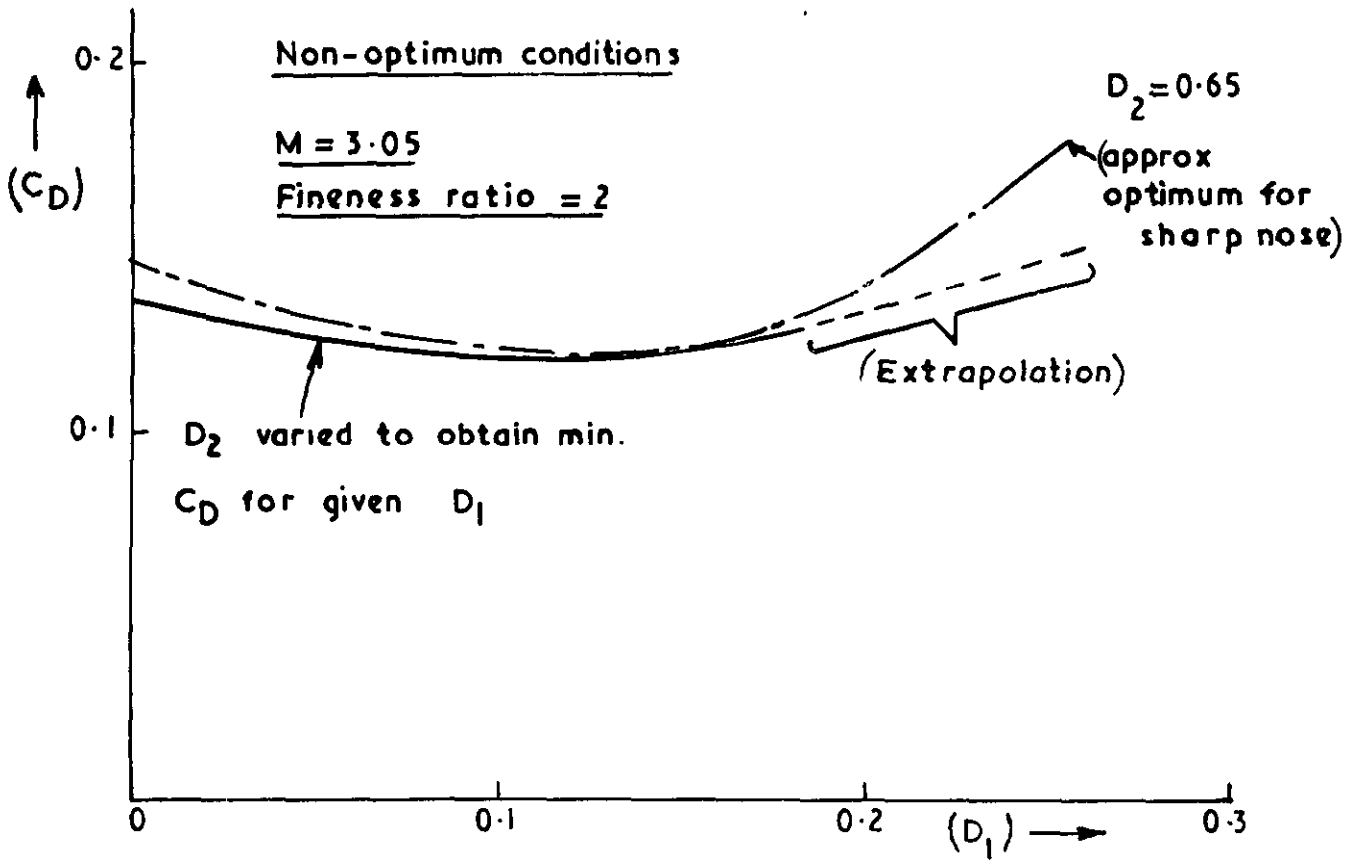

Effect of optimising D_2 at given values of D_1

ARC CP No.1271
August, 1970
Pugh, P. G. and Ward, L. C.

A PARAMETRIC STUDY OF THE USE OF NOSE BLUNTING TO REDUCE THE SUPERSONIC WAVE DRAG OF FOREBODIES

This parametric study examines the application of nose blunting to axisymmetric forebodies at supersonic speeds to reduce pressure drag and stagnation-point heat-transfer rate, and to increase their volume. Sufficient information is given to enable the magnitude of these benefits to be estimated for most practical applications.

ARC CP No.1271
August, 1970
Pugh, P. G. and Ward, L. C.

A PARAMETRIC STUDY OF THE USE OF NOSE BLUNTING TO REDUCE THE SUPERSONIC WAVE DRAG OF FOREBODIES

This parametric study examines the application of nose blunting to axisymmetric forebodies at supersonic speeds to reduce pressure drag and stagnation-point heat-transfer rate, and to increase their volume. Sufficient information is given to enable the magnitude of these benefits to be estimated for most practical applications.

ARC CP No.1271
August, 1970
Pugh, P. G. and Ward, L. C.

A PARAMETRIC STUDY OF THE USE OF NOSE BLUNTING TO REDUCE THE SUPERSONIC WAVE DRAG OF FOREBODIES

This parametric study examines the application of nose blunting to axisymmetric forebodies at supersonic speeds to reduce pressure drag and stagnation-point heat-transfer rate, and to increase their volume. Sufficient information is given to enable the magnitude of these benefits to be estimated for most practical applications.

DETACHABLE ABSTRACT CARDS

HER MAJESTY'S STATIONERY OFFICE

Government Bookshops

49 High Holborn, London WC1V 6HB
13a Castle Street, Edinburgh EH2 3AR
41 The Hayes, Cardiff CF1 1SW
Brazennose Street, Manchester M60 8AS
Southey House, Wine Street, Bristol BS1 2BQ
258 Broad Street, Birmingham B1 2HE
80 Chichester Street, Belfast BT1 4JY

Government publications are also available through booksellers

C.P. No. 1271